physics

Review

Scintillation in Low-Temperature Particle Detectors

Denys Poda

Université Paris-Saclay, CNRS/IN2P3, IJCLab, 91405 Orsay, France; denys.poda@ijclab.in2p3.fr

Abstract: Inorganic crystal scintillators play a crucial role in particle detection for various applications in fundamental physics and applied science. The use of such materials as scintillating bolometers, which operate at temperatures as low as 10 mK and detect both heat (phonon) and scintillation signals, significantly extends detectors performance compared to the conventional scintillation counters. In particular, such low-temperature devices offer a high energy resolution in a wide energy interval thanks to a phonon signal detection, while a simultaneous registration of scintillation emitted provides an efficient particle identification tool. This feature is of great importance for a background identification and rejection. Combined with a large variety of elements of interest, which can be embedded in crystal scintillators, scintillating bolometers represent powerful particle detectors for rare-event searches (e.g., rare alpha and beta decays, double-beta decay, dark matter particles, neutrino detection). Here, we review the features and results of low-temperature scintillation detection achieved over a 30-year history of developments of scintillating bolometers and their use in rare-event search experiments.

Keywords: low-temperature detector; scintillating bolometer; cryogenic scintillator; photodetector; particle identification; rare-event searches; double-beta decay; dark matter; neutrino

Citation: Poda, D. Scintillation in Low-Temperature Particle Detectors. *Physics* **2021**, *3*, 473–535. https://doi.org/10.3390/physics3030032

Received: 31 December 2020
Accepted: 10 June 2021
Published: 1 July 2021

Contents

1. Scintillating Bolometers for Rare-Event Search Experiments

1.1. Bolometers as Viable Detectors of Rare-Event Processes

A unique class of particle detectors is represented by low-temperature calorimeters, often named bolometers, which operate typically at ∼10–100 mK and are instrumented by a temperature sensor to detect a particle interaction with a detector medium as a small temperature rise [1–27]. An operation temperature near absolute zero is exploited to significantly reduce the detector heat capacity, allowing the thermal detection (e.g., ∼0.1 mK temperature rise per 1 MeV deposited energy). Consequently, common detector materials are crystalline insulators and semiconductors, for which the lattice-dominated heat capacity—being proportional to the cube of the ratio of the absolute temperature to a Debye temperature of the material (according to the Debye model) [28]—is very small at low temperatures. The particle energy release in a low-temperature detector (LTD) is converted to phonons (quantized modes of lattice vibrations), which are low-energy elementary excitations and thus their number fluctuations play a minor role on the detector energy resolution. Despite being largely affected by other sources of noise (read-out noise, thermal fluctuations of the detector, vibrational noise), bolometers offer a low detection threshold (in the range of tens eV to a few keV) and a high energy resolution (a few keV in a wide energy interval, from hundreds keV to a few MeV). Thanks to the absence of a dead layer, such instruments can be used for the detection of different types of radiation (α, β, γ, X-ray, neutrons, ...). However, a relatively slow response of thermal detectors (a typical signal duration of macrobolometers is within the ms–s range) imposes a strong constrain on the counting rate of such devices. Thus, taking into account excellent performances of bolometers and a variety of materials suitable for low-temperature applications, such detectors represent a great interest for low-counting experiments to search for rare-event processes (see Table 1).

Table 1. Possible applications of particle detectors containing elements (isotopes) of interest for rare-event searches.

Application	Elements of Interest	Most Promising Isotopes	Ref.
Rare α decay	Ce, Nd, Sm, Eu, Gd, Dy, Ho, Er, Tm, Yb, Lu, Hf, Ta, W, Re, Os, Ir, Pt, Au, Hg, Tl, Pb, Bi, Th, U	^{144}Nd, ^{147,148,149}Sm, ^{151}Eu, ^{152}Gd, ^{174,176}Hf, ^{180}W, ^{184,186,187}Os, ^{190}Pt, ^{209}Bi	[29]
Rare β decay	K, Ca, V, Rb, Zr, Cd, In, Te, La, Lu, Ta, Re	^{50}V, ^{113}Cd, ^{115}In (4-fold-forbidden β decay)	[29–32]
Double-β decay	Ar, Ca, Cr, Fe, Ni, Zn, Ge, Se, Kr, Sr, Zr, Mo, Ru, Pd, Cd, Sn, Te, Xe, Ba, Ce, Nd, Sm, Gd, Dy, Er, Yb, Hf, W, Os, Pt, Hg, Th, U	^{48}Ca, ^{76}Ge, ^{82}Se, ^{96}Zr, ^{100}Mo, ^{110}Pd, ^{116}Cd, ^{124}Sn, ^{130}Te, ^{136}Xe, ^{150}Nd	[33–37]
Dark matter (WIMP [a])	low/high atomic mass (low-/high-mass WIMP)	^{7}Li, ^{11}B, ^{19}F, ^{23}Na, ^{27}Al, ^{73}Ge, ^{111,113}Cd, ^{127}I, ^{155,157}Gd, ^{209}Bi (spin-dependent interactions)	[38–41]
Solar axions	Li, Fe, Kr, Tm (resonant absorption)	^{7}Li, ^{57}Fe, ^{83}Kr, ^{169}Tm	[42–46]
Solar and supernova ν's	Se, Mo, In, Cd, Nd, Gd (charge-current interactions)	^{82}Se, ^{100}Mo, ^{115}In, ^{116}Cd, ^{150}Nd, ^{160}Gd	[3,47–50]
Coherent elastic ν-nucleus scattering	high atomic mass (neutral-current interactions)	isotopically enriched	[51–56]
Neutron detection in rare-event searches	Li, B, Gd/low atomic mass (neutron capture/scattering)	^{6}Li, ^{10}B, ^{155,157}Gd	[57–61]

[a] Weakly interactive massive particles.

A "price" to pay for bolometers—high performance detectors with a large choice of detector materials—is the complication in their operation, in particular the use of cryogenic and vacuum technologies. The required temperature conditions can not be fulfilled with cryogenic liquids as, for example, for semiconductor detectors (the coldest temperature of common cryogenic liquids is 4.2 K for liquid helium). In order to reach millikelvin temperatures, sophisticated and costly cryostats (dilution refrigerators), exploiting the thermodynamic properties of the ^{3}He/^{4}He mixture, are used [62–67]. Despite of the complexity, such instruments are commercially available and provide a stable $\sim$10 mK base temperature and a long duty cycle on a routine basis. There are two distinctive types of dilution refrigerators: the so-called "wet" and "dry" cryostats, that is respectively with and without a liquid helium bath to be refilled periodically with the costly cryoliquid (supplied by a company or recovered using a liquifier). The features of both types of cryostats can be mixed too [68]. Cryogen free dilution refrigerators become more attractive thanks to the use of commercial pulse tubes to pre-cool thermal stages down to 4 K. Modern pulse-tube cryostats also allow a fully automated cool-down process and require a minimal maintenance during the operation (a periodic refill and cleaning of a liquid nitrogen trap) [69]. Depending on the cryostat, the cooling down can last from a day (in the best case) to 1–5 weeks (for large facilities with massive internal shields), inducing a delay in the operation of bolometric detectors. It is important to stress that dilution refrigerators, especially pulse-tube-based ones, are sources of vibrations which can drastically affect the bolometric performance, thus, special interventions are needed to mitigate the noise issue (e.g., see [70–77]). The experimental volume in commercial cryostats, capable of hosting an array of bolometric detectors, is limited to ∼10–100 L. Possibilities to scale up to a 1 m^3 bolometer array and to collect one tonne-year data have been recently demonstrated in the CUORE experiment [77–80]. A cryostat of a similar size will be used in the AMoRE experiment [81]. A four time larger cryostat than that of CUORE is under discussion for the long-term prospects of the CUPID program [82]. Multiplication of cryogenic facilities can also be a (costly) solution to increase the number of individual detector modules. However, a large experimental space is mandatory only for some applications and this review illustrates that many physics results on rare-event searches can be achieved with either small-scale arrays or even with single bolometric modules.

1.2. Particle Identification with Low-Temperature Detectors

Rare-event search experiments face a common challenge in the suppression of different sources of background which can hide or mimic signals searched for. The background sources can be originated to environmental radioactivity, radioactive contaminants of detectors and experimental set-ups, cosmic rays, neutrons, and even neutrinos. (An interested reader can find details in a classical review on low-radioactivity techniques [83], as well as in the recent reviews and original papers on the related topic [24,51,84–99].) Particle identification capability of a detector technology is thus beneficial for rare-event searches as a viable tool for background rejection. Bolometers based on some crystal scintillators show a particle-dependent response exploitable for pulse-shape discrimination (see details in the first original works [100–102] and some updates in the recent review [24]). However, the reproducibility of this method strongly depends on the experimental conditions (e.g., see [24,26] and references therein). It is important to stress that a lack or a poor performance of particle identification limits the application or sensitivity of a bolometric detector in rare-event searches.

A composite device based on a cryogenic scintillator and a photodetector (scintillating bolometer)—originally proposed about 30 years ago [3]—represents one of the most exploitable experimental techniques to identify particles interacting with a bolometric detector. In addition to scintillating bolometers, another types of LTDs with active background rejection are: (a) semiconductor-based (Ge and Si) bolometers with simultaneous measurements of heat and ionization signals [23,68,103–109]; (b) bolometers instrumented with out-of-equilibrium phonon sensors to localize the impact point of a particle [110–115]; (c) metal-film-coated bolometers to tag near surface interactions [116–120]; (d) composite detectors (in a thermal contact) with parallel read-out [115,121–125].

The detection of scintillation light allows particle identification thanks to the dependence of the scintillation light yield on the energy loss mechanism, as described by a semi-empirical relation proposed by Birks [126–128]:

$$\frac{dL}{dr} = S \cdot \frac{dE/dr}{1 + k \cdot B \cdot dE/dr}, \quad (1)$$

where dL/dr is the specific scintillation yield per path length, S is the absolute scintillation efficiency, dE/dr is the particle stopping power in the material, $B \cdot dE/dr$ is the density of excitation centers along the track, and k is a quenching parameter. The product $k \cdot B$ is usually considered a single parameter expressed in g/cm^2/MeV (the so-called Birks' factor) [127], which depends on the detector material, as well as conditions of measurements and data treatment can have a strong impact [128]. At small dE/dr (fast electrons) and at large dE/dr (e.g., α particles) Equation (1) approximates to $dL/dr = S \cdot dE/dr$ and $dL/dr = S/(k \cdot B)$, respectively. The particle-dependent difference in the scintillation light output is often presented as the ratio of a light yield of ions to that of electrons (quenching factor for ions, QF_i), which has the following approximate relation with the Birks' factor and the stopping power:

$$QF_i = \frac{1}{k \cdot B \cdot (dE/dr)_i}. \tag{2}$$

The QF_i value is usually smaller than one [128] and it can be explained by a saturation effect due to the high ionization density that characterizes the interaction of heavy particles in matter. In case of α particles, this parameter is often called the α/β ratio.

Figure 1 illustrates the basic principle of particle identification with scintillating bolometers: particles with energy releases that are different from those of electrons, γ quanta, and muons populate band(s) with lower scintillation. The efficiency of the separation between different particle types increases with energy of the incident radiation (i.e., the amount of detected light).

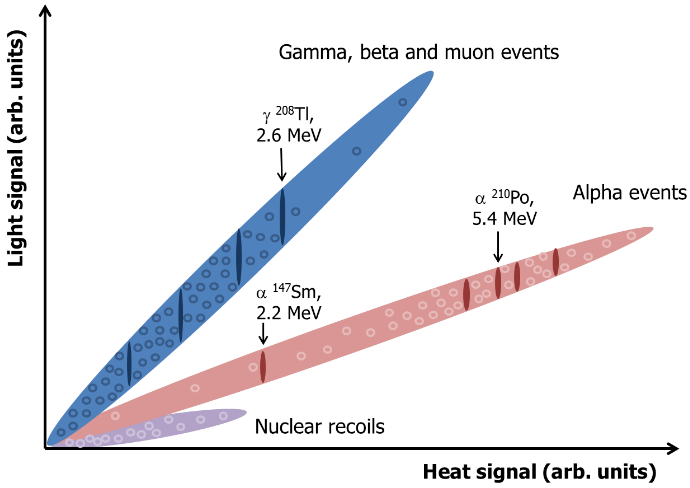

Figure 1. Schematic presentation of particle-dependent distributions of light signals measured by a photodetector in coincidences with the energy releases detected by a crystal scintillator-based bolometer. Circles represent individual events, which can form peaks shown as dark ovals on the β(γ, μ) and α bands. The light output induced by highly ionizing particles (alpha particles, nuclear recoils) impinging the scintillator is suppressed (quenched) with respect to the one induced by electrons (as well as γ quanta, cosmic-ray muons) of the same energy. Therefore, particles with different ionization properties become separated on such light vs. heat scatter-plot. The separation is more profound at higher energies, with increased amount of the detected scintillation light.

1.3. Importance of Scintillation Detection for Bolometric Rare-Event Searches

The necessity of scintillation detection in scintillating bolometers is briefly discussed in this section in view of possible applications of such devices in rare-event searches, as listed in Table 1.

1.3.1. Rare Alpha Decay

A strong impact of the energy releases, Q_α, on the partial half-lives, $T_{1/2}$, of α emitters can be seen from the Geiger-Nuttall law (formulated 110 year ago [129] and still fulfilled [130,131]), expressed by the following relationship:

$$\log_{10} T_{1/2} = \frac{a(Z)}{\sqrt{Q_\alpha}} + b(Z), \tag{3}$$

where charge-dependent coefficients $a(Z)$ and $b(Z)$ are determined by fitting experimental data for each isotopic series. Indeed, the Geiger-Nuttall plots in form of Equation (3) (e.g., see Figure 1 in [130]) show that a change in Q_α of only 10% changes $T_{1/2}$ by about 10^3. Consequently, the naturally occurring α-active nuclides (15 isotopes) have a large spread of half-lives ($\sim 10^9$–10^{21} yr) for a comparatively small range of Q_α-values ($\sim$2–5 MeV) [29,132]. There are also about 70 naturally occurring isotopes which are potentially α-unstable, but the α radioactivity of only 10% from the full list of candidates can possibly be detected ($Q_\alpha \sim 1.6$–2.7 MeV and predicted $T_{1/2} \sim 10^{17}$–10^{22} yr) [29]. The list of isotopes of interest for investigations of rare α decays is given in Table 1.

The region of interest (ROI) in rare α decay searches is dominated by natural γ and β radioactivity, as well as by cosmic rays. The identification of α particles combined with the typically high energy resolution of bolometric detectors allow the realization of a nearly "background-free" experiment even at a surface laboratory, as for example, the first detection of the ^{209}Bi α decay [133], the rarest α decay observed (together with the ^{209}Bi α transition to the first excited level of ^{205}Tl [134]). Often, such experiments are by-products of scintillating bolometer development for dark matter and double-beta decay search programs.

1.3.2. Rare Beta Decay

Taking into account the total angular momentum change, ΔJ, and the parity change, $\Delta\pi$, between the initial and final states, β decays are classified as allowed (ΔJ = 0, 1 and $\Delta\pi$ = no) and nth-forbidden ($\Delta J = n$, $n+1$ and $\Delta\pi$ = no, yes; β transitions with ΔJ = 0 and with parity change also belong to first-forbidden branches) [135,136]. The partial half-lives of β emitters show a strong dependence on the selection rules of ΔJ and $\Delta\pi$, exhibited as significantly longer $T_{1/2}$ of β processes with higher forbiddenness [136]. The rarest β transitions ever observed, 4-fold-forbidden β decays of ^{50}V, ^{113}Cd, and ^{115}In (possible for only these three isotopes), are detected with the half-lives of 10^{14}–10^{16} yr [29].

Studies of highly-forbidden β decays are of particular interest to scrutinize the value of the axial-vector coupling constant, g_A [30,31,137–139]. A possible g_A quenching with respect to the free nucleon value ($\simeq$1.27, see [140] and references therein) would affect the β spectral shape, notably at low energies. The g_A value in this process is expected to be similar to the one involved in the neutrinoless double-beta decay (see Section 1.3.3) [31].

Therefore, a low-threshold bolometer containing isotope of interest for rare β decays (see Table 1) is a viable detector for the study of a β spectrum shape. In spite of the long half-lives of these processes, the induced counting rate and, subsequently, the probability of pile-ups in macrobolometers containing any of these nuclides is rather high (because of the high detection efficiency of the bolometric technique), strongly affecting the precision of the spectrum reconstruction. For that reason, a light-signal-based trigger comparable with a low-energy threshold of the main absorber could be useful to control pile-ups thanks to the much faster response of a photodetector.

1.3.3. Double-Beta Decay

Two-neutrino and neutrinoless double-beta decays (2νDBD and 0νDBD, respectively)—spontaneous nuclear disintegrations with the emission of two electrons accompanied or not by two antineutrinos—are energetically allowed for only 35 isotopes [34]. Here, we consider only DBDs which increase the charge of nuclei by two units. The nuclear charge decreasing DBD processes—namely double-electron capture, electron capture with positron emission and double-positron decay [141–147]—are omitted because of suppressed decay probabilities and experimental issues (see, e.g., ref. [148] and references therein). It is worth underlining that the observation of a 0ν-mode of any of such charge decreasing DBD processes would be extremely important in view of the 0νDBD mechanism determination [141].

The 2νDBD is the rarest process ever observed and it has been detected for a dozen of isotopes with a typical half-life in the range of 10^{18}–10^{24} yr [37,145]. In contrast to 2νDBD, the 0νDBD violates the total lepton number and requires neutrinos to be massive Majorana particles (i.e., particle equal to its antiparticle) [35,36,142,143,149–151]. Therefore, the 0νDBD is forbidden in the Standard Model (SM) of particle physics, but this process is allowed in many SM extensions [142,143,152]. Till today, the 0νDBD has not been detected and the most stringent half-life limits are in the range of 10^{24}–10^{26} yr [36,79,80,153–159].

A 2νDBD study is important for several reasons:

- it provides a valuable nuclear spectroscopy information, such as decay scheme, half-life, summed and/or single electron energy spectra, angular electron correlations (see, e.g., recent topical reviews [33,37,145,160,161] and high precision 2νDBD measurements [154,162–175]);
- it allows us to test theoretical frameworks used also for 0νDBD calculations (e.g., see [31,37,138,171,176–181]);
- it can bring insight on the hypotheses in the 2νDBD calculations, that is a transition through single- vs. high-state dominance of the intermediate nucleus (see details in dedicated theoretical [181–188] and experimental [166,167,169,172,173,189] works);
- it can also be used to test different hypothetical processes, such as Lorentz-violated 2νDBD (Lorentz and CPT (charge-parity-time) symmetry violation) [168,172,190–195], 0νDBD with majoron(s) emission (global $B-L$ symmetry violation) [153,168,172,196,197], admixture of right-handed currents in the weak interactions [198], bosonic neutrinos (Pauli exclusion principle violation) [172,199], sterile neutrinos [200,201], light exotic fermions [201], strong neutrino self-interactions [202].

The interest in the 0νDBD detection is much stronger, because it would unambiguously imply the observation of new physics beyond the SM, the highly successful paradigm nowadays.

The energy spectrum of two electrons in the 2νDBD is a continuum up to the transition energy, $Q_{\beta\beta}$, peaked at $\sim$1/3 of $Q_{\beta\beta}$, while the 0νDBD signature is a peak centered at $Q_{\beta\beta}$ and smeared by the detector energy resolution (e.g., see [33]). The DBD rate strongly depends on the transition energy (with a leading term proportional to $Q_{\beta\beta}^{11}$ and $Q_{\beta\beta}^{5}$ for the 2ν and 0ν modes, respectively), thus an isotope of interest with a high $Q_{\beta\beta}$ is preferred. Only 11 (6) out of 35 potentially DBD-active isotopes have $Q_{\beta\beta}$ values above 2.0 (2.7) MeV [34]; they are listed in Table 1. In case of a $Q_{\beta\beta}$ higher than 2.7 MeV, the contribution of natural $\gamma(\beta)$ radioactivity to the ROI becomes strongly suppressed and the major background contribution comes from surface originated α radioactivity [203]. Therefore, a radiopure detector with embedded high-$Q_{\beta\beta}$-isotope, high energy resolution, and particle identification capability (e.g., a scintillating bolometer) is well suited for DBD searches.

A high energy resolution is of a particular importance to make the 0νDBD ROI narrow (thus reducing the background contribution), as well as to determine background components for the construction of a correct background model. It is worth noting that the energy resolution of a bolometer based on an efficient scintillator is strongly affected by the energy partition between heat, scintillation and energy trapping inside a crystal. Therefore, a correlation between heat and light signals has to be used to improve the detector energy resolution (e.g., see [204]).

Being intrinsically slow, bolometers can suffer from any counting rate higher than a few tens of Hz which can give rise to pile-up issues. Moreover, the 2νDBD event pile-ups can be an unavoidable source of background in the 0νDBD ROI [205,206]. The 2νDBD induced pile-ups are worrisome for ^{100}Mo- and ^{150}Nd-enriched LTDs due to considerably high 2νDBD rates of these isotopes (e.g., $\sim$20 mHz in 1 kg of ^{100}Mo), which are at least an order of magnitude faster than that of other 2νDBD-active nuclides [37]. This issue can largely be mitigated by a pulse-shape analysis of heat signals [205,206], while a further improvement in the pile-up-induced background reduction would be possible by the analysis of the faster scintillation light signals with enhanced signal-to-noise ratio [207].

Scintillating bolometers for 0νDBD searches have been extensively developed over the last decade, particularly in the framework of the following projects/experiments: BoLux R&D (research and development) experiment [208], AMoRE [209], ISOTTA [210], LUCIFER [211] and its follow-up CUPID-0 [212], LUMINEU [213] and its follow-up CUPID-Mo [214], CLYMENE [215], CROSS [216], and CANDLES [217]. Almost 30-year-long development on pure bolometric detectors based on tellurium dioxide, performed within the CUORE project and the predecessors (see [218] and references therein), was also crucial for a fast progress in R&D on scintillating bolometers. Moreover, the CUORE Collaboration has demonstrated the feasibility to realize a tonne-scale bolometric experiment, which is currently ongoing in the Gran Sasso underground laboratory (LNGS, Italy) [77,79,80]. Thus, all these activities play an important role towards the planned realization of CUPID [82,219] and AMoRE [81,209] next-generation large-scale bolometric experiments.

It is worth mentioning that low-temperature scintillation detection can be used not only for DBD detectors, but also for an active veto inside a cryogenic set-up. Such active shield is going to be developed within the BINGO [220] project using crystal scintillators and bolometric photodetectors. In case of the proof of concept, this technology is aiming at the implementation in the CUPID follow-up.

1.3.4. Dark Matter (WIMP)

There are several evidences for the existence in the Universe of a large amount of invisible matter (about five times more than the ordinary matter), the so-called dark matter (DM), which could be constituted by unknown particles, which noticeably interact only gravitationally [40,221,222]. Direct detection of yet unknown DM particles [40,41,223,224] is therefore another hot topic in the searches for beyond-SM physics.

Weakly interactive massive particles (WIMP) are considered one of the most viable candidates for the DM composition [41,224]. The main detection principle of WIMP is based on a registration of a nuclear recoil (a few tens keV or less) induced by the WIMP scattering off a nuclei in a target material [40,41,224]. The WIMP-nucleus interactions are considered to be either spin-independent (with the whole nucleus) or spin-dependent (with nuclei exhibiting non-zero spin). Therefore, the experimental sensitivity to detect a WIMP signal depends not only on detector performance, exposure, and background level, but also on the chemical composition of the detector material (Table 1).

Scintillating bolometers are well placed among DM detection techniques thanks to a low threshold, particle identification capability, and a wide choice of detector (i.e., target) materials containing a variety of elements of interest (see Table 1). Indeed, the detection threshold plays a crucial role taking into account the exponential growth of the WIMP-induced event rate with the decrease of the nuclear recoil energy. The separation between electron and nuclear recoils provides the possibility of searching for a DM signal in an (almost) background-free region [225].

A scintillation-based particle identification at low energies is rather challenging due to the low amount of the expected light and thus it requires the use of efficient scintillators. The improvement in the particle identification at low energies allows us to achieve a lower detection threshold as well [225]. Moreover, taking into account that a spin-independent WIMP-nucleon elastic-scattering cross section is proportional to the square of the mass number of the nucleus, the difference in the light yield for ionizing particles is also crucial for distinguishing nuclear recoils originated from WIMP's scattering off light, mid-weight or heavy nuclei constituting a scintillation target [226]. If a scintillating bolometer has an anisotropic light output (which depends on the particle direction relative the main crystal axes), this feature can be exploited for the search for a diurnal modulation of a DM signal [227–231].

Scintillating bolometers for DM searches have been developed for almost 30 years by ROSEBUD [232] and CRESST [233], together with alternative developments of Ge and/or Si heat-ionization bolometers by CDMS [234] and EDELWEISS [235]. Extensive R&D activities (including those of ROSEBUD and CRESST) were performed to develop different scintillation materials for a potential use in a multi-target tonne-scale array of LTDs of the EURECA DM search project [236–239]. Due to a rapid progress of detector technologies based on liquid noble gases, achieved over the last decade in searches for high-mass WIMP [224], the realization of the EURECA project has become less relevant now. Therefore, the CRESST, CDMS, and EDELWEISS Collaborations are currently focused on the direct detection of low-mass DM particles [108,109,240]. In addition, an R&D on scintillating bolometers for the detection of the annual modulation of the DM signal is currently ongoing within the COSINUS project [241].

1.3.5. Solar Axions

The axion is a hypothetical particle postulated by the Peccei–Quinn theory to solve the "strong CP problem" in quantum chromodynamics [242,243]. The axions are predicted to be neutral, low-mass particles characterized by a low interaction cross section with ordinary matter and thus are considered to be possible DM candidates [222,223,244]. If axions exist, they can be largely produced in the solar core and subsequently detected in a laboratory experiment on Earth exploiting several mechanisms of axion interaction (see, e.g., [244]). The experimental signatures of axions are searched for typically at low energies (few–tens keV), with the exception of a resonant absorption of solar axions which are emitted with the energy of 478 keV (corresponding to the excited level of ^{7}Li) [43]. Moreover, the ROI for axion detection is dominated by irreducible $\gamma(\beta)$ background. Therefore, the detection of scintillation light in a bolometric detector of axions would not provide an essential background rejection.

1.3.6. Solar and Supernova Neutrinos

Some of the most attractive isotopes for 0νDBD search (see Table 1) can also be interesting targets for the detection of solar and supernova neutrinos because of the high neutrino capture cross section expected and detector large mass foreseen in such experiments [3,47–50]. Thus, a primary DBD search experiment with a large-scale array of scintillating bolometers can also be used for the detection in real time of solar and supernova neutrinos. Since the neutrino capture in a DBD detector would result in a continuum energy spectrum peaked at MeV energy (see, e.g., [50,88]), the scintillation-based particle identification can be exploited for the background suppression in the same way as DBD searches with scintillating bolometers.

The coherent elastic neutrino-nucleus scattering [245] (see Section 1.3.7), is another viable channel of neutrino detection [246]. This neutral-current process is characterized by several orders of magnitude higher cross section than that of neutrino-electron scattering. However, a detection signature is a low-energy nuclear recoil and, thus, low-threshold detectors are required. LTDs can therefore be suitable for such application [52,108,109]. At the same time, no scintillation detection can really be exploited as a particle identification tool due to a tiny light signal expected for low-energy release in even efficient scintillators.

1.3.7. Coherent Elastic Neutrino-Nucleus Scattering

The coherent elastic neutrino-nucleus scattering (CENNS)—a process predicted about 45 years ago [245] but detected only recently [247]—is a promising tool to search for effects beyond the SM [53,54]. The CENNS induced by solar neutrinos will be the irreducible background of near future direct DM search experiments because the CENNS signature is exactly the same as WIMP scattering off nuclei [51,52,108,109,224,248]. In turn, it is an opportunity to study this SM process. There is growing interest in precise CENNS investigation using artificial neutrino sources. An experimental approach based on a LTD placed near a nuclear reactor is now considered to be very attractive for such "table-scale" neutrino experiments (e.g., see [54,55] and references therein). Since the expected signal is a very low energy nuclear recoil, a scintillating bolometer approach would not be able to provide particle identification in the ROI (similarly to low-mass WIMP searches). However, this technique can be promising if a low-threshold detector contains a heavy target (as CENNS cross section is proportional to the square number of neutrons) and allows detection of unambiguously neutrons (see Section 1.3.8). R&D on such scintillating bolometers is now ongoing within the BASKET project [249].

It is worth mentioning a recently proposed method for nuclear recoils calibration at the $\sim$100 eV energy scale using a neutron capture reaction to induce recoils by de-excitation

γ quanta (the CRAB project) [250]. The detection of escaped γ quanta in coincidence with nuclear recoils in the CENNS detector can significantly clean up the energy spectrum of recoils suppressing multi-γ-induced background contribution. The feasibility of a γ detector based on a high-Z scintillator with a bolometric light detection, in a similar way as an active shield for bolometric DBD search experiments (BINGO project [220]), is going to be investigated too.

1.3.8. Neutron Detection in Rare-Event Searches

A scintillating bolometer containing ^{6}Li or ^{10}B—isotopes actively used for neutron detection thanks to their high thermal neutron capture cross section (see, e.g., [57,61,251–253])—can be exploited for the in-situ neutron flux monitoring in rare-event search experiments [59,60,74,254,255]. The detection principle is based on the ^{6}Li(n,t)α and ^{10}B(n,α)^{7}Li reactions aiming at detection of the products. The neutron capture on ^{6}Li creates alpha (2052 keV) and triton (2731 keV) particles with a shared energy of 4783 keV. The neutron capture on ^{10}B can lead to the ground state of ^{7}Li (the branching ratio is 6%; the Q-value is 2792 keV), but the transition to the 478 keV excited state of ^{7}Li is dominant (the branching ratio is 94%). The isotopic abundance of ^{6}Li and ^{10}B is 7.5% and 19.8%, respectively, thus detectors with natural isotopic composition of lithium and/or boron can be used for neutron detection too. However, a detector enriched in ^{6}Li and/or ^{10}B would largely increase the detection efficiency. The cross sections of thermal neutron capture on ^{155,157}Gd (15% and 16% in natural Gd, respectively) are much higher than those of ^{6}Li and ^{10}B, however the products are γ quanta (see, e.g., [256]). Therefore, LTDs with ^{6}Li and/or ^{10}B content are preferred, while Gd-containing bolometers can have some specific application (e.g., if the suppression of the contribution induced by thermal neutrons is needed) [59].

Another viable way to detect neutrons with scintillating bolometers is related to the identification of nuclear recoils induced by the elastic neutron scattering off a nucleus in the detector material. Scintillation induced by nuclear recoils is even more quenched than that of α particles and it allows us to discriminate the dominant electron recoil background, as schematically shown in Figure 1. The presence of low atomic mass elements in the detector medium is preferred to get nuclear recoils with higher energies, improving particle identification. A simultaneous use of scintillating bolometers to detect both neutron-induced nuclear recoils and products of neutron captures can also be exploited for the neutron flux measurements [60,257,258].

Li- and/or B-containing scintillating bolometers for neutron detection were actively developed in 1993–2014, particularly for the ROSEBUD DM project. Over the last six years, a significant progress has been achieved in the development of other Li-containing bolometers for DBD (ISOTTA, LUMINEU, CLYMENE, CUPID-Mo, CROSS, CUPID, AMoRE), DM (CRESST) and CENNS (BASKET) oriented projects. The developments of scintillating bolometers for the efficient detection of fast neutron-induced nuclear recoils were and are mainly a subject of DM search programs, but such bolometric detectors developed for other applications can be used for this purpose too.

2. Key Ingredients and Performance of Scintillating Bolometers

Examples of construction elements of a scintillating bolometer and the assembled detector module are shown in Figure 2. The main ingredients of such a device and demands on its performance related to the scintillation detection are briefly discussed in this section.

2.1. Cryogenic Scintillator

At first glance, the term "scintillating bolometer" alludes to a detector material which possesses scintillation properties at low temperatures, but even non-scintillating (transparent) dielectric crystals, acting as Cherenkov radiators, can be suitable too.

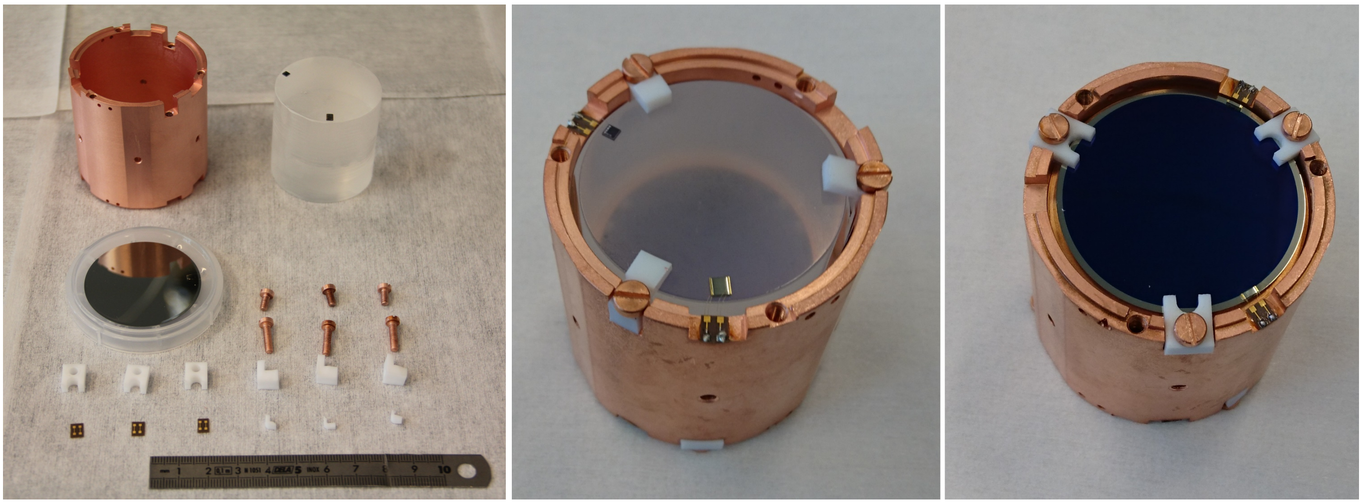

Figure 2. Left panel: A kit of components of a single detector module developed for the CUPID-Mo experiment with 20 scintillating bolometers to search for double-beta decay (DBD) processes in ^{100}Mo [159,259]. Each module is made of a Cu housing, a ^{100}Mo-enriched lithium molybdate crystal scintillator ($\oslash$44 $\times$ 45 mm, $\sim$210 g) and a Ge wafer ($\oslash$44 $\times$ 0.2 mm, $\sim$1.4 g) with glued small sensors, the Cu screws, the PTFE (polytetrafluoroethylene) spacers and fixing elements, and the Kapton® film with Au pads. **Middle panlel:** The assembled CUPID-Mo module, view from the top on the semi-transparent crystal surface with a Neutron-Transmutation-Doped Ge thermistor (3.0 $\times$ 3.0 $\times$ 1.0 mm) and a P-doped Si heater. A reflective film (Vikiuti$^{\text{TM}}$) has been put around the lateral side of the crystal. **Right panel:** The CUPID-Mo module, view from the bottom on the Ge disk equipped with the smaller thermistor (3.0 $\times$ 0.8 $\times$ 1.0 mm). The wafer is coated with a $\sim$70 nm SiO layer (dark blue internal circle); the 2 mm on the edge of the wafer (17% of the area) remain uncoated. All photos are reprinted with permission from [259]. Creative Commons License CC BY 4.0.

There is definitely an advantage in the use of scintillation materials in such devices. Moreover, different crystal scintillators at low temperatures have an increased light output compared to room temperature, as observed in tungstates, molybdates, and some other oxide compounds, as well as in selenides and alkali halides [260–265]. Such a feature opens the possibility to use also those materials that scintillate little at room temperature (e.g., lithium molybdate [266]). Some crystal scintillators exhibit the suppression of the scintillation at low temperatures (e.g., Tl-doped sodium iodide [263]), but the amount of the emitted light remains well detectable. It is also worth noting the temperature dependent scintillation kinetics of materials, which can result to a rather long fluorescence decay time at low temperatures (e.g., hundred(s) µs [261]), to be taken into account for a proper integration of photons by a light-sensitive device.

Some materials can remain be poorly- or non-scintillating even at low temperatures (e.g., tellurium dioxide [267–269]). In such occasion, the detection of a $\gamma(\beta)$-induced Cherenkov radiation can open a window to particle identification, because no emission is expected for α's due to a significantly higher energy threshold of the Cherenkov light production (e.g., 400 MeV for α's compared to 0.05 MeV for β's in tellurium dioxide) [270]. However, this approach is challenging due to a low radiation expected [270], requiring photodetectors with a low threshold (below 60 eV). For instance, the 2615 keV γ interaction with the full energy release in a tellurium dioxide crystal produces $\sim$300 Cherenkov photons [271].

In addition to the impact of temperature conditions, the light output depends on many other parameters such as the scintillation efficiency and optical properties of the detector material (chemical composition), the crystal chemical purity (the purity of starting materials) and quality (the crystal growth process), the thermal treatment (if needed), the sample shape and the roughness of the crystal surface (see, e.g., [272–274]). The choice of the detector material is crucial, but it depends on the physics goals and availability of crystal producers, starting materials (and their purification if required), and developed crystal growth process. The optimization of a proper crystal shape and/or surface treatment may drastically improve the light output [271,272,274–277], if there are no restrictions (e.g., related to the crystal size and/or radiopurity). In its turn, the measured light signal additionally depends on the light collection efficiency and the photodetector sensitivity (as briefly discussed in Sections 2.2 and 2.4). Different scintillation materials used in scintillating bolometers and the results of scintillation detection are detailed in Section 3.

2.2. Reflector

By default, a reflector is present around a crystal to enhance the light collection efficiency; it is particularly crucial for scintillators with low light output. Widely used materials with a high reflection efficiency are reflective films from 3M (VM2000, VM2002, Vikiuti™) and TORAY (Lumirror®), an aluminum foil, a PTFE (Teflon®) tape, and an Ag-coated detector housing [74,272,274,276,278–280] (some other reflectors can be found, for example, in [279]). Another reason for the use of a reflector is related to possible scintillation properties of this material, which can be exploited for the identification of the following surface-induced backgrounds: (a) nuclear recoils in direct DM searches [281]; (b) α events degraded in energy in 0νDBD searches with poorly- or non-scintillating bolometers [282]. At the same time, the scintillating properties of a reflective film can spoil the particle identification of 0νDBD bolometric detectors with (reasonably) good scintillation [74]. The removal of the reflective film can also be driven by radiopurity considerations and/or improvement of coincidences in detector array [74,283].

2.3. Temperature Sensor

A particle interaction in a cryogenic scintillator is detected via a phonon signal collected by a special sensor. The sensor technology exploits the following working principles [17,284]:

- temperature-dependent resistivity of highly doped semiconductors (neutron-transmutation-doped, NTD);
- superconducting transition (transition-edge sensor, TES);
- temperature-dependent magnetization of paramagnetic materials (metallic magnetic calorimeter, MMC);
- kinetic inductance in superconducting materials (kinetic inductance detector, KID).

Up to now, sensor technologies based on NTD Ge (heavily doped germanium thermistor) and TES W (thin tungsten superconducting film) are the dominant choices for a phonon readout in scintillating bolometers. However, most of the scintillation materials were tested using NTD Ge thermistors and only some crystal compounds were studied with TES W phonon sensors (mainly within the CRESST and COSINUS programs). The use of MMC sensors in scintillating bolometers (mainly in the AMoRE project), began a decade ago [285] and is slowly increasing. A first operation of a cryogenic scintillator with a KID-based phonon sensor has been realized only recently [286].

2.4. Photodetector

In a scintillating bolometer, a photodetector working at millikelvin temperatures needs to be coupled to a cryogenic scintillator. The first proof of concept of scintillating bolometers was demonstrated with Eu-doped calcium fluoride scintillators and PIN silicon photodiodes [287,288] (further developments are reported in [289]). The use of an auxiliary bolometer as a photodetector in a scintillating bolometer was realized for the first time in [290,291], where a composite detector was constructed with the scintillator itself and a Bi-coated sapphire disk. A conception of a scintillation read-out using a low-temperature photomultiplier tube, coupled to a scintillator-based (calcium tungstate or calcium molybdate) bolometer, has been recently demonstrated too [292].

The use of thin ($\sim$0.05–1 mm) bolometric light detectors (LDs) in scintillating bolometers is dominant thanks to high radiopurity, high sensitivity to a wide range of photons emitted and more compact and simplified detector module structure. Moreover, being slow response photodetectors (a signal rise time is in the µs–ms range), LDs are also well suitable for slow scintillators. Thus, we focus here only on bolometric photodetectors. As for the energy absorber of such devices, the most frequently used materials are originally dark semiconductors (Ge or Si), but also transparent dielectric crystals (sapphire) coated typically with a Si thin layer.

In addition to the use of a reflective film, light collection in a scintillating bolometer can be enhanced by the optimization of the LD design, in particular following one or several actions:

- The detection area of a photodetector and the crystal-side surface facing it are made comparable [24,74,272,274]. In an extreme case, an LD can cover a significant part of the cryogenic scintillator surface. For example, a beaker-shaped LD allows us to drastically improve (by a factor of 3) the detected light signal [293–295].
- A special LD coating is required to reduce the light reflection. The widely used coating materials are silicon dioxide and oxide, SiO_2 and SiO (e.g., see [75,272,296–299]). For instance, the detection of $\sim$600 nm light signal by a Ge LD coated with a 70 nm SiO (SiO_2) layer is improved by approximately 30% (20%) [298]. Several other materials together with SiO_2 have been recently investigated aiming at the optimization of the antireflective coating [300].
- The distance between scintillator and photodetector is minimized, typically to a few millimeters. A method for putting an LD in direct contact with a crystal has been proposed recently [301].

The energy scale of scintillating bolometers is mostly determined with sources of γ quanta, but it does not allow calibration of LDs due to their small sizes. In principle, the calibration of LDs is not mandatory for particle identification. However, the knowledge of the LD energy scale provides a valuable information about the device performance, as well as the measurement of the detected scintillation light energy. The LD calibration can be realized in several ways [302,303], for example, using:

- an X-ray source facing an LD (the most popular method; for example, ^{55}Fe with 5.9 and 6.5 keV doublet);
- an external high-activity γ source to induce X-ray fluorescence near an LD (e.g., it can be useful for the calibration of LDs in low-background experiments, where the presence of an X-ray source near an LD is prohibited);
- the energy distribution of cosmic-ray muons passing through an LD (not valid for deep underground measurements);
- photon statistics (e.g., LED injected photons).

A low-threshold detection of scintillation light is of special importance for scintillating bolometers taking into account that only a small part of the particle energy release is converted into scintillation photons and detected by an LD (typically, $\sim$(0.1–1)% of the measured heat energy is detected in form of scintillation with the light collection efficiency of $\sim$(10–30)%). Certainly, the fluctuation of the LD noise determines the device threshold. Even if the threshold can be lowered by exploiting coincidences between phonon and scintillation signals (e.g., [304]), a primary goal of an LD technology is to achieve as low noise as possible. At the same time, the demand on the LD threshold is mainly determined by the scintillation efficiency of the chosen cryogenic scintillator and its application to rare-event searches (briefly discussed in Section 2.5). The state-of-the-art of bolometric LD technologies is summarized in Table 2.

Table 2. Technologies of bolometric photodetectors and representative baseline noise resolution (RMS). The Neganov-Trofimov-Luke (NTL) gain of a signal-to-noise ratio is given only for technologies exploiting the signal amplification based on the NTL effect [305,306]. The transition-edge sensor (TES) technology-based QETs stands for quasiparticle-trap-assisted electrothermal feedback transition-edge sensors (each QET consists of a W TES and an Al fin.). NTD, KID, and MMC stand for neutron-transmutation-doped semiconductors, kinetic inductance detector, and metallic magnetic calorimeter, respectively.

Sensor	Absorber	Area (cm^2)	Noise (eV RMS)	NTL Gain	Ref. (Project)
NTD Ge	Ge	2	31–130		[275,307,308] (LUCIFER)
	Ge	5	9–10		[74,309] (ROSEBUD)
	Ge	10	n/a		[310]
	Ge	13	18–34		[74,309,311] (ROSEBUD)
	Ge	15	32–70		[75,312] (LUCIFER, CUPID-0)
	Ge	15	30–85		[74,259,308,313,314] (LUMINEU, CUPID-Mo)
	Ge	15	20		[301] (CUPID R&D)
	Ge	15	8–17	10–11	[303,308,313,315] (LUMINEU)
	Ge	20	37–120		[308,316–318] (LUCIFER)
	Ge	34	97		[310,319]
	Si	4	$\sim$5	$\sim$100	[320,321]
TES W	Al_2O_3+Si	4	6–27		[272,322,323] (CRESST)
	Al_2O_3+Si	13	4–23		[324–326] (CRESST)
	Al_2O_3+Si	16	11		[272] (CRESST)
	Si	4	8–14		[327] (CRESST)
	Si	9	14–15		[327,328] (CRESST)
	Si (beaker)	63	6–8		[293,326] (CRESST)
QETs W	Si	1	3		[329]
	Si	46	4		[330] (CPD)
TES IrAu	Si	4	4–8	6–9	[225,302,331–334] (CRESST)
TES IrPt	Si	20	70		[335] (CUPID R&D)
KID Al	Si	4	82		[336] (CALDER)
KID AlTiAl	Si	4	26		[337] (CALDER)
	Si	25	34		[338] (CALDER)
MMC AuEr	Ge	20	n/a		[339] (AMoRE)
	Si	2	n/a	4	[340] (AMoRE)
MMC ErAg	Si	20	n/a		[341] (LUMINEU)

2.5. Demands on Particle Identification Efficiency

A commonly used particle identification parameter of scintillating bolometers is the ratio between a scintillation light signal measured by an LD (in keV) to an energy release in the cryogenic scintillator detected as a heat (in MeV), the so-called light-to-heat ratio, L/H. (This parameter is often called as "light yield", but such term can be confused with the absolute scintillation yield.) An illustration of the L/H parameter versus the particle energy extracted from the scintillating bolometer data [74] is shown in Figure 3 (left panel). As one can see, the $\gamma(\beta)$ events are clearly separated from α's, exhibiting a factor of 5 difference in the scintillation light signal associated to these particles. Figure 3 (left panel) illustrates the application of scintillating bolometers to 0νDBD searches, showing a ROI at 3 MeV in the $\gamma(\beta)$ band, which is free from α particles degraded in energy due to the decays at the surface of the detector materials (mimic using an α source).

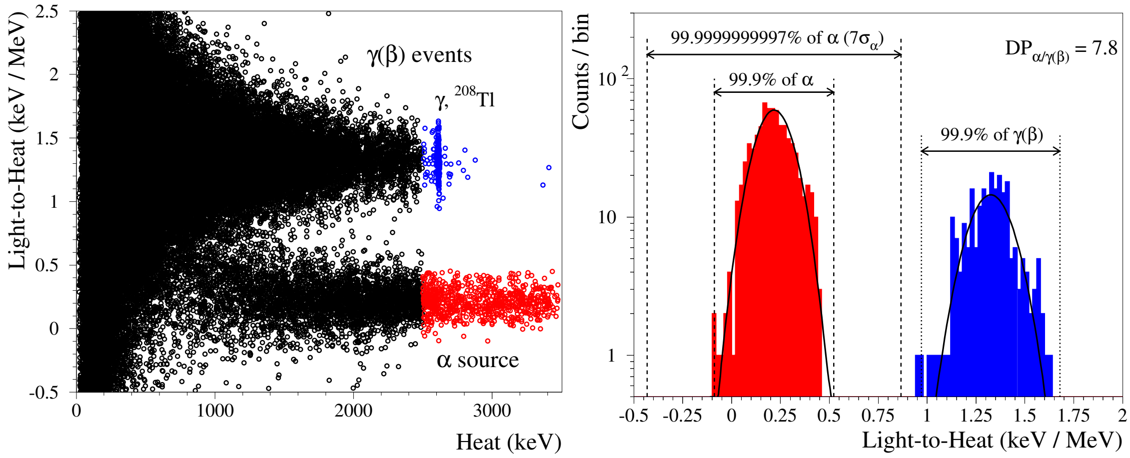

Figure 3. Left panel: Heat energy distribution of the light-to-heat parameter, L/H, of nuclear events detected by a scintillating bolometer based on a 379 g ^{100}Mo-enriched zinc molybdate crystal (enrZMO-t in [74]) and a thin Ge bolometric light detectors (LDs). first The detector was operated deep underground over 78 h of γ calibration and 593 h of background measurements. The crystal has been also irradiated by a ^{238}U/^{234}U α source, emitting α particles degraded in energy. The 2.5–3.5 MeV events, marked in blue and red, are used to illustrate the discrimination power parameter (see text). **Right panel**: Distributions of the L/H parameter of events selected from the data (shown in the left panel) in the 2.5–3.5 MeV energy interval [74]. Both distributions are fitted by Gaussian functions shown by solid lines. The intervals containing 99.9% of both event types and $\pm 7\sigma$ range of the α band are indicated. The discrimination power is evaluated as $DP_{\alpha/\gamma(\beta)}$ = 7.8 (see text for details). Right panel is reprinted with permission from [74]. Creative Commons License CC BY 4.0.

Some events present in Figure 3 (left panel), mostly at low heat energies, exhibit the negative values of light signals and consequently the negative L/H values. This situation is common for low efficient scintillators and is caused by the search for low-energy scintillation signals in the LD noise. In order to increase the signal-to-noise ratio, bolometric data are processed with a digital filter (e.g., the optimum filter [342,343]). Then, the light signal amplitudes (i.e., energies) are estimated at a certain time shift with respect to the heat events trigger positions (e.g., as proposed in [304]), taking into account the difference in the time response of the channels. It may happen that the filtered waveform contains a light signal completely hidden in the LD noise fluctuation, and the optimum filter can thus return a negative signal amplitude. If light signals are searched in a comparatively large time interval (i.e., tens of the sampled channels), positive values of the noise fluctuations are then represent amplitudes of low-energy scintillation signals (e.g., see Figure 4 in [74]).

The separation between α and $\gamma(\beta)$ events is often expressed by a discrimination power parameter [101,344]:

$$DP_{\alpha/\gamma(\beta)}(E) = \left|\mu_{\gamma(\beta)}(E) - \mu_\alpha(E)\right| / \sqrt{\sigma^2_{\gamma(\beta)}(E) + \sigma^2_\alpha(E)}, \quad (4)$$

where μ (σ) denotes the mean value (width) of the corresponding L/H distributions of $\gamma(\beta)$ and α events with energy E. The meaning of the $DP_{\alpha/\gamma(\beta)}$ parameter is illustrated in Figure 3 (right panel), where the L/H distributions are shown for events detected around the ^{100}Mo 0νDBD ROI (3 MeV). As it is seen in Figure 3 (right panel), the $DP_{\alpha/\gamma(\beta)}$ can be roughly interpreted as the α events rejection efficiency expressed in numbers of σ_α.

The widths of the L/H bands are determined (in an ideal case) by the fluctuations of the LD baseline noise and the detected photons (that should follow the Poisson distribution). Taking that into account, Figure 4 illustrates the expected discrimination power depending on the noise conditions and the L/H parameter of the detector. The L/H of $\gamma(\beta)$'s is varied from 0 keV/MeV (a non-scintillating material) to 1 keV/MeV (a scintillator with a low light output).

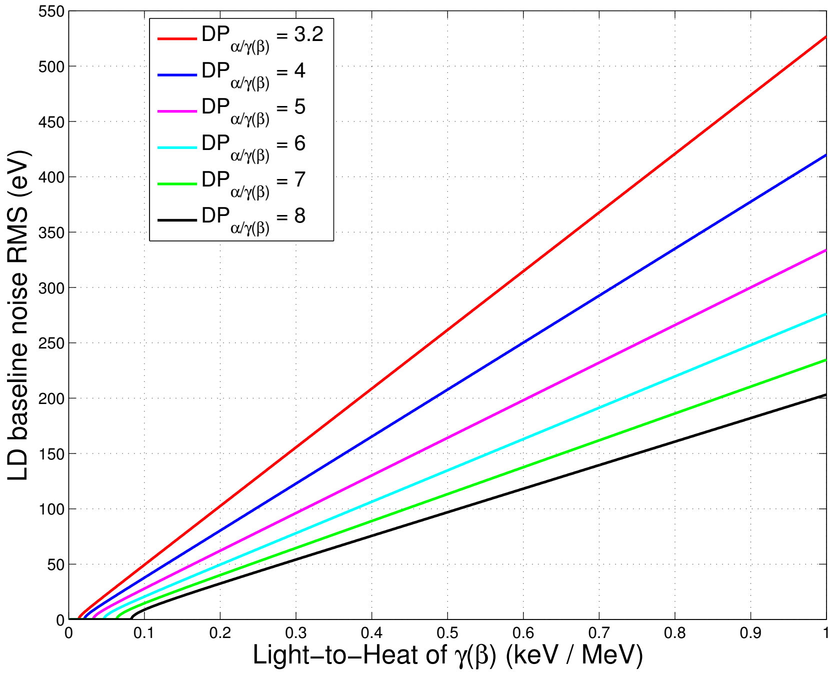

Figure 4. Discrimination power $DP_{\alpha/\gamma(\beta)}$ expected at 3 MeV (^{100}Mo 0νDBD region-of-interest (ROI)) as a function of the LD noise resolution and the relative scintillation signal of a scintillating bolometer expressed by the $L/H_{\gamma(\beta)}$ parameter. The used quenching factor for alpha particles (0.2) and an average photon energy (2.07 eV) are taken as for lithium molybdate scintillating bolometers.

The smallest $DP_{\alpha/\gamma(\beta)}$ value present in Figure 4 corresponds to the minimal $\alpha/\gamma(\beta)$ separation required for a scintillating bolometer technology to be used in 0νDBD searches. Indeed, with a $DP_{\alpha/\gamma(\beta)}$ equal to 3.2, a rejection better than 99.9% of α events with a high acceptance of $\gamma(\beta)$'s (more than 90%) can be achieved. Consequently, the importance of highly performing LDs for scintillating bolometers with a low scintillation efficiency is evident in Figure 4.

The discrimination power parameter is typically used to characterize the particle identification capability of scintillating bolometers developed and/or used in searches for 0νDBD. Certainly, such a parameter can also be calculated for other particle types to be used instead of α's. An example of such particles is shown in Figure 5, where the detection of neutrons by a Li-containing scintillating bolometer and neutron-induced nuclear recoils in materials with different scintillation efficiency are illustrated. A significantly improved particle identification, especially at low energies, is evident for a scintillating bolometer based on an efficient scintillator (Figure 5). Following the same approach as in Figure 4, we can illustrate the needs of LD performance and L/H for the separation between low energy nuclear recoils (DM search ROI) and $\gamma(\beta)$ events, shown in Figure 6. As it was provisioned above (Section 1.3.4), an efficient particle identification for DM search scintillating bolometers requires both an ultra-low LD threshold and a scintillation material with a high light output.

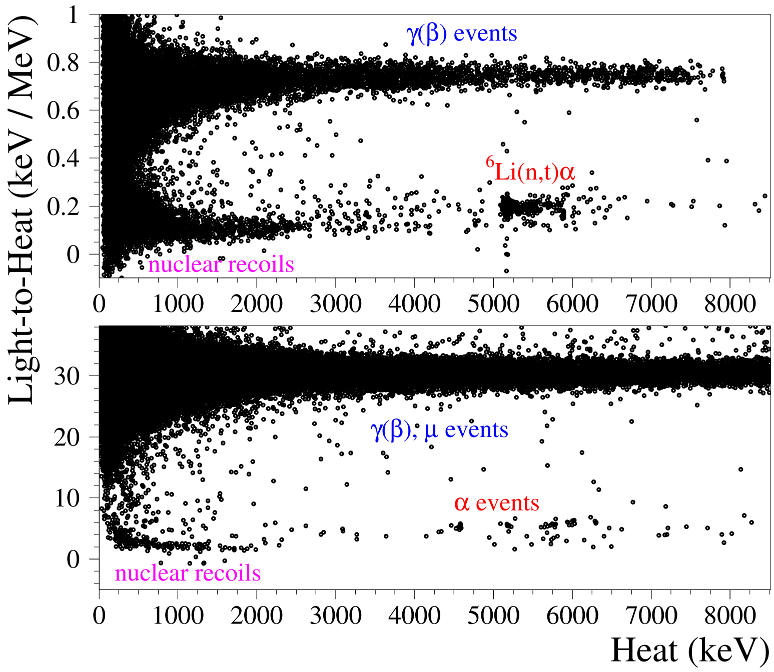

Figure 5. Energy distribution of the L/H parameter of nuclear events detected by scintillating bolometers based on a 213 g ^{100}Mo-enriched lithium molybdate (top panel; enrLMO-3 in [345]) and a 35 g ^{116}Cd-enriched cadmium tungstate (bottom panel; [346]), and both accompanied by a Ge LD. The data were acquired over 290 h of AmBe neutron calibration in an underground set-up (top panel) [345] and over 250 h of measurements (190 h of background and 60 h of γ calibration with a ^{232}Th source) in an aboveground laboratory (bottom panel) [346]. Bottom panel is reprinted with permission from [346]. Creative Commons License CC BY 4.0.

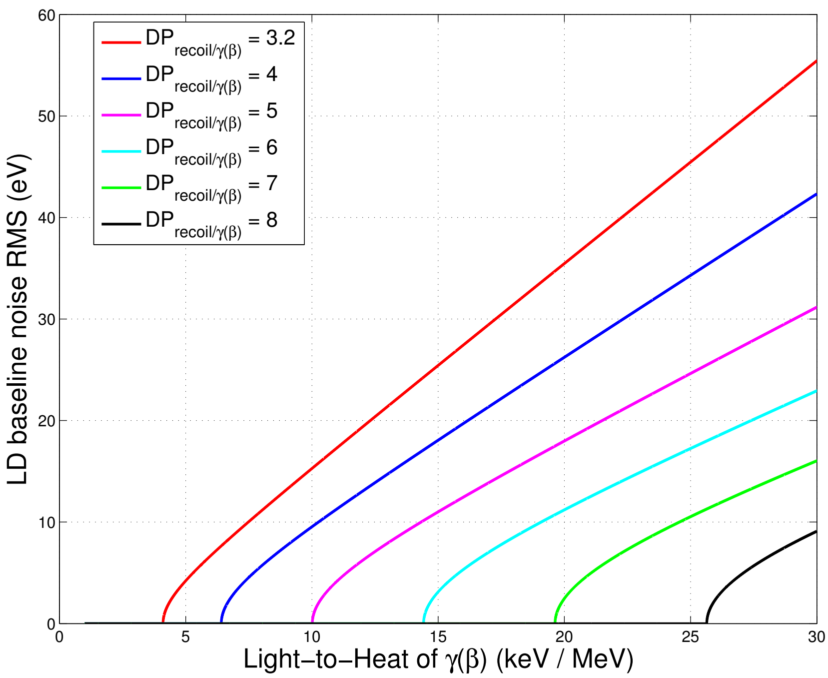

Figure 6. Discrimination power $DP_{\mathrm{recoil}/\gamma(\beta)}$ expected at 10 keV (an example of a possible dark matter search ROI). as a function of the LD noise resolution and the relative scintillation signal ($L/H_{\gamma(\beta)}$ parameter) of a scintillating bolometer. The assumed quenching factor for nuclear recoils (0.1) and an average photon energy (2.95 eV) are taken as for calcium tungstate scintillating bolometers.

3. Research and Development on Scintillating Bolometers

This section reports on development and applications of scintillating bolometers based on the following inorganic materials:

- Tungstates: $CaWO_4$, $CdWO_4$, Li_2WO_4, $Na_2W_2O_7$, $PbWO_4$, and $ZnWO_4$;
- Molybdates: $CaMoO_4$, $CdMoO_4$, Li_2MoO_4, $Li_2Mg_2(MoO_4)_3$, $Li_2Zn_2(MoO_4)_3$, $MgMoO_4$, $Na_2Mo_2O_7$, $PbMoO_4$, $SrMoO_4$, and $ZnMoO_4$;
- Borates: $Li_6Eu(BO_3)_3$ and $Li_6Gd(BO_3)_3$;
- Some other oxide scintillators: Al_2O_3, $Bi_4Ge_3O_{12}$, $LiAlO_2$, TeO_2, YVO_4, and ZrO_2;
- Selenides: $LiInSe_2$ and ZnSe;
- Alkali metal fluorides: CaF_2, LiF, and SrF_2;
- Alkali metal iodides: CsI and NaI.

The main properties of the above listed materials in terms of low-temperature scintillation detection (such as the wavelength of the maximum emission, the light-to-heat ratio for $\gamma(\beta)$'s and the quenching factor for α's) are collected in Table 3. It has to be noted that scintillator-based bolometers have typically a notable difference in the amplitude of phonon signals induced by $\gamma(\beta)$'s and α's of the same energy; this difference is exhibited as ∼(5–15)% higher than the nominal energy of α particles calibrated in the γ energy scale [74,204,347]. Such miscalibration of α's is often not corrected, resulting in a slightly lower QF_α value. More details about the data of Table 3 are given below in sections corresponding to each material. Since phonon sensors based on NTD Ge technology were and are widely used in scintillating bolometers, we consider this technology as a default option, omitting to mention in the description of detectors.

Table 3. Scintillation properties of inorganic materials used in low-temperature particle detectors with simultaneous phonon and scintillation readout. Crystal growth method(s), wavelength of the emission peak (λ_{max}) of the material at the quoted temperature, light-to-heat ratio for $\gamma(\beta)$'s, $L/H_{\gamma(\beta)}$, scintillation light quenching for α particles, QF_α, with respect to $\gamma(\beta)$s are listed. Typically used crystal growth processes are the following [348–351]: ordinary and low-temperature-gradient Czochralski (Cz and LTG Cz, respectively), Kyropoulos (Ky), Verneuil (Ve), and variations of Bridgman–Stockbarger (BS) techniques. The $L/H_{\gamma(\beta)}$ is evaluated in photons per MeV (ph/MeV) using the energy of photons corresponding to λ_{max}.

Crystal	Growth	λ_{max} (nm)	$L/H_{\gamma(\beta)}$ (keV/MeV)	$L/H_{\gamma(\beta)}$ (ph/MeV)	QF_α	Section
$CaWO_4$	Cz	420 (8 K) [261]	6.0–24	2000–8100	0.10–0.12	Section 3.1.1
			(45–52 [a])	(15,400–17,500)		ibid.
$CdWO_4$ [b]	Cz, LTG Cz	420 (8 K) [261]	14–31	5400–12,000	0.18–0.19	Section 3.1.2
Li_2WO_4(Mo)	Cz, LTG Cz	530 (8 K) [352]	0.40	170	0.26 [c]	Section 3.1.3
$Na_2W_2O_7$	LTG Cz	540 (77 K) [353]	12	5200	0.20	Section 3.1.4
$PbWO_4$	Cz	420 (4.2 K) [354]	1.8	600	0.20	Section 3.1.5
$ZnWO_4$	Cz, LTG Cz	490 (9 K) [261]	13–19	5100–9500	0.15–0.23	Section 3.1.6
$CaMoO_4$ [b]	Cz	540 (8 K) [261]	1.9–4.8	800–2100	0.13–0.22	Section 3.2.1
$CdMoO_4$	BS	550 (5 K) [355]	2.6	1200	0.16	Section 3.2.2
Li_2MoO_4 [b]	Cz, LTG Cz, BS	590 (8 K) [311]	0.55–1.0	300–500	0.17–0.23	Section 3.2.3
			(1.2–1.4 [d])	(600–700)		ibid.
$Li_2Mg_2(MoO_4)_3$	LTG Cz	585 (8 K) [356]	1.3	610	0.22	Section 3.2.4
$Li_2Zn_2(MoO_4)_3$	LTG Cz	630 (10 K) [357]	n/a	n/a	n/a	Section 3.2.5
$MgMoO_4$	Cz	520 (9 K) [358]	n/a	n/a	n/a	Section 3.2.6
$Na_2Mo_2O_7$	Cz, LTG Cz	650 (4.2 K) [359]	0.58–1.6	300–840	0.16–0.40	Section 3.2.7
$PbMoO_4$	Cz, LTG Cz	520 (10 K) [360]	5.2–12	2200–5000	0.18–0.23	Section 3.2.8
$SrMoO_4$	Cz	520 (11 K) [361]	∼1–3	400–1300	∼0.26	Section 3.2.9
$ZnMoO_4$ [b]	Cz, LTG Cz	520 (1.4 K) [362]	1.0–1.5	400–600	0.13-0.19	Section 3.2.10
			(1.8–2.1 [d])	(800–900)		ibid.
$Li_6Eu(BO_3)_3$	Cz	613 (4.2 K) [363]	6.6	3200	0.08	Section 3.3.1
$Li_6Gd(BO_3)_3$ [b]	Cz	312 (90 K) [364]	0.26	65	0.23	Section 3.3.2
Al_2O_3(Ti), pure	Ve, Ky, Cz	420 (9 K) [365]	2.5–14	850–4700	0.09–0.36	Section 3.4.1
$Bi_4Ge_3O_{12}$	Cz, LTG Cz, BS	480 (9 K) [261]	7.0–28	2700–11,000	0.17–0.18	Section 3.4.2

Table 3. *Cont.*

Crystal	Growth	λ_{max} (nm)	$L/H_{\gamma(\beta)}$ (keV/MeV)	(ph/MeV)	QF_α	Section
$LiAlO_2$	Cz	340 (300 K) [366]	1.2	300	0.52	Section 3.4.3
TeO_2 [b]	BS, Cz	500 (<15 K) [271]	∼0.04	∼20	n/a	Section 3.4.4
YVO_4	Cz	450 (80 K) [367]	59	21,000	0.20	Section 3.4.5
ZrO_2		420 (85 K) [368]	∼2	∼700	∼0.2	Section 3.4.6
$LiInSe_2$	BS	730 (173 K) [265]	14	8200	0.55	Section 3.5.1
ZnSe [b]	BS	640 (9 K) [261]	0.7–7.5	360–3900	2.6–4.6	Section 3.5.2
CaF_2(Eu)	Cz, BS	425 (15 K) [369]	14	4800	0.14–0.19	Section 3.6.1
LiF [b]	Cz, BS	365 (9 K) [370]	0.21–0.38	60–110	0.30	Section 3.6.2
SrF_2	Cz, BS	365 (4.2 K) [371]	2.9	850	0.26	Section 3.6.3
CsI	Ky, Cz, BS	340 (10 K) [264]	49–81	13,000–22,000	∼0.5	Section 3.7.1
NaI	Ky, Cz, BS	300 (10 K) [372]	37 (130 [a])	9000 (32,000)	∼0.2 [e]	Section 3.7.2

[a] An advanced light collection using a beaker-shaped light detector. [b] Including crystals produced from materials enriched in an isotope of interest. [c] Estimated for α + t events (4.8 MeV sum energy, products of neutron capture by ^{6}Li). [d] An improved light collection using two identical light detectors at the crystal top and bottom. [e] Estimated for Na nuclear recoils.

3.1. Tungstates

3.1.1. Calcium Tungstate

Calcium tungstate ($CaWO_4$)—a well-known inorganic scintillator with a 120-year history [373–375]—is among the most extensively studied absorber materials of LTDs. Scintillating bolometers based on $CaWO_4$ crystals have been widely used in the ROSEBUD ([376,377], completed) and CRESST (completed CRESST-II [226,378–382] and running CRESST-III [383]) DM search programs. Moreover, such scintillating bolometers were applied to the searches for α decays of naturally occurring tungsten isotopes [384,385] and DBD processes in ^{40}Ca and ^{180}W [386], as by-products of the aforementioned experiments. In particular, the α decay of ^{180}W has been detected in the CRESST-II experiment [385], confirming the first observation of this process done in the Solotvina DBD experiment with ^{116}Cd-enriched $CdWO_4$ scintillation detectors [387]. $CaWO_4$ represents a long-standing interest as a detector of DBD in ^{48}Ca [388–391], especially if such material can be operated as a scintillating bolometer in a EURECA-like [239] (i.e., tonne-scale) experiment.

First encouraging results for a possible DM search application of a $CaWO_4$ scintillating bolometer were reported two decades ago [392,393]. A TES-instrumented dual-readout LTD was made of a 6 g $CaWO_4$ crystal (5 × 10 × 20 mm) and a Si-on-sapphire wafer (SOS, 10 × 20 × 0.5 mm). The detector is characterized by a good scintillation signal of 8 keV/MeV for $\gamma(\beta)$'s, quenched to 29% and 13% for respectively α's and neutron-induced nuclear recoils (mainly scattering off the oxygen nuclei) [392,393]. (Later, the data have been reanalyzed with a more sophisticated pulse height determination and the quenching factors have been re-evaluated to be equal to 0.10–0.12 for nuclear recoils with energies 10–150 keV [378].) Thanks to good $CaWO_4$ scintillation properties and a good energy resolution of the LD, a particle identification down to 10 keV has been achieved [392,393].

Further prospects of $CaWO_4$ scintillating bolometers as DM detectors were then demonstrated in an underground operation of a device based on a commercial 54 g $CaWO_4$ crystal and a ⌀25 mm Ge wafer, realized in the ROSEBUD experiment at the Canfranc laboratory (LSC, Spain). The detector showed a good $L/H_{\gamma(\beta)}$ of 6 keV/MeV and a scintillation quenching of 25% and 10% for α particle and nuclear recoils, respectively, thus allowing efficient particle identification with a heat-scintillation readout [267,384,394].

An extensive R&D on $CaWO_4$ scintillating bolometers (including the Cz-based growth of radiopure crystals [395,396]), as well as their use in the DM searches at LNGS have been realized by the CRESST Collaboration. Eighteen TES-W-instrumented detector modules made of large $CaWO_4$ crystals (⌀40 × 40 mm, ∼300 g each) and either Si (30 × 30 × 0.4 mm) or SOS (⌀40 × 0.5 mm) wafers, were operated in the CRESST-II experiment. All detectors of the CRESST-II Phase 1 were made according to a conventional design. Six out of eighteen detectors of the CRESST-II Phase 2 were constructed following new designs to improve an active background suppression: (a) all supporting elements of the crystal and the LD were made of materials with scintillating properties; (b) a complete active 4π-veto system was based on a beaker-shaped LD (see below) and a carrier crystal scintillator for the main energy absorber. The CRESST-III experiment is ongoing with the help of small $CaWO_4$ crystals (20 × 20 × 10 mm, 24 g) and SOS LDs (20 × 20 × 0.4 mm), aiming at a drastic improvement of the $CaWO_4$ detector threshold and the experimental sensitivity to low-mass WIMP. A typical light signal detected by the CRESST $CaWO_4$ scintillating bolometers is ∼(1.0–2.4)% of the total energy deposited by $\gamma(\beta)$ radiation in crystals, that is ∼(10–24) keV/MeV, while the scintillation is quenched to 22% and 10% for α particles and nuclear recoils, respectively (e.g., see [397,398]). Thanks to a good scintillation efficiency of $CaWO_4$ crystals at low temperatures and high performance (i.e., low threshold) bolometric LDs, CRESST $CaWO_4$-based detector modules show a powerful particle identification down to few–ten keV region [226,281,376,378,379,381–385,396,397,399].

The study of light production and transport of CRESST-II detector modules [398] demonstrates the scintillation efficiency of $CaWO_4$ crystals is (7.4–9.2)%, while the detection efficiency is (18–28)%, or 23% on average. Additional measurements with a photomultiplier demonstrated a similar variation of the detected light, suggesting the dominant part of this variation is originated from the self absorption of the crystals (i.e., difference in the crystals quality) [398]. The detection efficiency was then improved by a factor 2 (to 34%) using two identical LDs facing a $CaWO_4$ crystal on top and bottom [398]. These results clearly show that the enhancement of the light detection with a single bolometric photodector is feasible via the detector module design optimization.

An impressive light collection optimization has been achieved with a large area, ≈60 cm^2, beaker-shaped Si absorber (with a diameter and height of 40 mm, around 6 g in weight) allowing enhancement of the scintillation signal by a factor 2.5 compared to conventional CRESTT-II detector modules [293]. In particular, the scintillation light of two identical prototypes based on $CaWO_4$ crystals (⌀35 × 38 mm, ≈220 g each) was detected by the beaker-design LDs at the level of 4.53% and 5.17% (e.g., compare with 1.95% of the average value for the conventional CRESST design [398]). It is also worth noting that the achieved baseline resolutions of such beaker-shaped devices show no degradation in performance compared to smaller CRESST-II LDs (see Table 2) [293,326].

The determination of quenching factors is essential for WIMP searches, in particular with a multi-element detector as $CaWO_4$. With this in mind, a precise measurement of quenching factors for O, Ca, and W has been realized using a $CaWO_4$ LTD irradiated by a neutron beam and the CRESST neutron-calibration data [400]. The study found that the QFs in the 10–40 keV region are typically 0.11, 0.06, and 0.02 for O, Ca, and W, respectively [400].

3.1.2. Cadmium Tungstate

Cadmium tungstate ($CdWO_4$)—a classic material for scintillation detectors [374,375]—has been actively used in rare-event search experiments with scintillating counters for about three decades (e.g., see [168,387,401–408]). $CdWO_4$-based LTDs with heat-scintillation read-out [296,409] can drastically improve the detector performance and particle identification capability compared with scintillation detectors, thus enhancing the sensitivity to rare processes. A particular interest in $CdWO_4$ scintillating bolometers is the search for DBD of ^{116}Cd, one of the most promising isotopes for 0νDBD searches from both theoretical and experimental points of view (e.g., see [168,346,406] and references therein).

The first realization of a $CdWO_4$ scintillating bolometer has been reported 15 years ago [296]; the detector was constructed from a 140 g $CdWO_4$ crystal and a SiO_2-coated Ge slab (see Table 4), and tested at LNGS. The scintillation signal ∼6 keV/MeV has been detected for γ and β particles, while the light yield for α particles, well separated from

$\gamma(\beta)$'s, is quenched to 18%. It should be emphasized that the LD calibration is done using photon statistics for the observed γ peaks and the noise resolution of this large-area device was estimated as 16 photons, that is ≈48 eV (assuming ∼3 eV/photon) [71,296], never reported later for this LD. Thus, we can speculate that such "low" $L/H_{\gamma(\beta)}$ value of the $CdWO_4$ sample is underestimated. (The results for very old 433 g $CdWO_4$ crystal, characterized by $L/H_{\gamma(\beta)} \sim 14$ keV/MeV [410], could also support this assumption.) It is interesting to note that the bolometric LD measured the scintillation peak at 2615 keV with an energy resolution of 3% FWHM, which is better than the resolutions achieved with room temperature $CdWO_4$ scintillation detectors (3.4%–5.0% [406,411,412]) developed for rare-event search experiments.

A few years later, the technical feasibility of the $CdWO_4$ scintillating bolometer approach through an array of detectors has been demonstrated using four 213 g crystals and a single 426 g sample viewed by LDs with a Ge wafer diameter of 66 and 35 mm, respectively (Table 4) [413]. In particular, a full suppression of an α-induced background has been illustrated for the 426 g $CdWO_4$ scintillating bolometer (the quenching factor for α's of ^{210}Po is around 0.18) [413]. It was also observed that some α events, ascribed to decays at the crystal surface, have a loss of the scintillation signal with respect to bulk α's.

Subsequently, an extensive investigation of a 510 g $CdWO_4$ scintillating bolometer (Table 4) has been realized [204]. Similar to previous prototypes, the detector exhibits a high $L/H_{\gamma(\beta)}$ (17.6 keV/MeV) and QF_α = 0.19. The high light yield of the $CdWO_4$ scintillator worsen the energy resolution of the heat channel because of the heat-light anti-correlation [204,414], however, it can be improved by considering the energy partition between heat and scintillation channels. It was also found that the energy resolution of 6.8% at the 2615 keV scintillation peak of the LD cannot be explained by the fluctuation of the Poisson statistics of the absorbed photons and it is probably dominated by a light yield variation due to position dependent effects.

Table 4. Results of low-temperature scintillation detection with scintillating bolometers based on natural/^{116}Cd-enriched $CdWO_4$ crystals and thin bolometric light detectors (LDs). The crystal growth method, the mass (two significant digits) and the size of the sample, the size and the material (including coating) of the coupled LD, as well as the $L/H_{\gamma(\beta)}$ and QF_α values are listed.

Cryogenic Scintillator			LD		$L/H_{\gamma(\beta)}$	QF_α	Ref.
Material	**Mass (g)**	**Size (mm)**	**Size (mm)**	**Material**	**(keV/MeV)**		
$CdWO_4$ (Cz)	140	30 × 30 × 20	⌀66 × 1	Ge+SiO_2	6 [a]	0.18	[296]
	210 (×4)	30 × 30 × 30	⌀66 × 1	Ge+SiO_2	n/a	n.a	[413]
	400	⌀40 × 40	⌀40 × 0.5	Al_2O_3+Si	15	0.18	[415,416]
	430	30 × 30 × 60	⌀35 × 0.3	Ge	n/a	0.18	[413]
	430	⌀40 × 43	⌀44 × 0.2	Ge+SiO	14	0.17	[410]
	510	⌀40 × 50	⌀36 × 1	Ge+SiO_2	18	0.19	[413]
(LTG Cz)	8	20 × 10 × 5	30 × 30 × 0.4	Si	27	n/a	[415]
$^{116}CdWO_4$ (LTG Cz)	35	28 × 27 × 6	⌀44 × 0.2	Ge+SiO	31	0.18	[346]
	580 (×2)	⌀45 × 47	⌀44 × 0.2	Ge+SiO	25–27	0.18	[417]

[a] Possibly underestimated because of the LD miscalibration, see text for details.

Recently, a 433 g $CdWO_4$-based scintillating bolometer (cylindrical sample, Table 4) has been investigated at LSC, aiming at precise investigation of the β-spectrum shape of ^{113}Cd [410]. The crystal was produced about 25 years ago [404] and for most of this period it has been stored underground, where it was also used in a low-background experiment to investigate precisely the rare β decay of ^{113}Cd [404]. The choice of this crystal for the experiment is mainly driven by the precise measurement of the Cd isotopic composition in the sample and the high crystal radiopurity [404]. The $L/H_{\gamma(\beta)}$ for 2.6 MeV γ quanta of a ^{232}Th source, measured with the help of a SiO-coated Ge LD, amounts to 14 keV/MeV. However, the light yield exhibits a strong energy dependence, dropping down to $L/H_{\gamma(\beta)}$ = 10 keV/MeV for the $\gamma(\beta)$ energy deposition in the crystal below 0.1 MeV. The LD exploits the NTL signal amplification and that allowed us to reach a low-threshold of around 60 eV (equal to 5 sigma of the noise fluctuation).

$CdWO_4$ has been also examined for potential use in DM searches exploiting the CRESST technology [415]. In particular, the low-temperature scintillation of a small and of a CRESST-size crystals (8 g and 400 g, respectively) was measured with Si and SOS LDs, respectively (Table 4). The small sample was cut from the ingot grown using the LTG Cz method [350,418]. Among two $CdWO_4$ samples, only a large crystal was equipped with a phonon sensor (TES on a small $CdWO_4$ carrier). The $L/H_{\gamma(\beta)}$ values of the small and large $CdWO_4$ samples were measured to be 27 and 14 keV/MeV respectively, which is comparable to $CaWO_4$. Thus, $CdWO_4$ is a promising alternative target to $CaWO_4$-based DM searches.

Cadmium tungstate produced from cadmium enriched in ^{116}Cd ($^{116}CdWO_4$) is preferred for both DBD and DM search experiments, because a number of ^{116}Cd nuclei per unit volume can be increased by one order of magnitude consequently reducing the amount of β-active ^{113}Cd (12% in natural Cd, 0.56 Bq/kg activity in $CdWO_4$) [350,406]. The first test of a $^{116}CdWO_4$ scintillating bolometer has been recently performed using a 35 g sample and a SiO-coated Ge LD [346]. The sample was cut from a 1.9 kg boule developed from highly purified enriched cadmium (82% enrichment in ^{116}Cd) [406]. Thanks to a high crystal quality, the measured $L/H_{\gamma(\beta)}$ of 31 keV/MeV is the highest ever achieved with $CdWO_4$ scintillating bolometers. The quenching factors for α particles and nuclear recoils were calculated as 0.18 and 0.08, respectively. The detector exhibits a small light-heat anticorrelation, with a minor impact on the detector energy resolution. Similar results have been recently obtained with two large $^{116}CdWO_4$ scintillating bolometers constructed from twin crystals of around 580 g each cut from the same ingot (the 35 g sample was produced from the same boule too) and operated one at LSC and the other at the Modane underground laboratory (LSM, France). The $L/H_{\gamma(\beta)}$ values of 27 and 25 keV/MeV were measured, thus providing an efficient separation of α-induced background [417]. The investigations of $^{116}CdWO_4$ scintillating bolometers [346,417] reinforce results of early studies with such devices based on natural crystals [204,296,413,415], confirming the good prospects of this material for a large-scale bolometric experiment to search for the ^{116}Cd 0νDBD, in particular using the advantage of multi-target approach [419].

3.1.3. Lithium Tungstate with Mo Content

Due to issues of direct crystallization of the lithium tungstate ($LiWO_4$) stoichiometric melt, such material has been produced by a solid solution crystal growth with molybdenum admixture resulting in $Li_2Mo_{1-x}W_xO_4$, where x is the molybdenum mole ratio [420]. High quality crystals have been produced from a stoichiometric mixture with x = 0.05 using Cz [420] and LTG Cz [352,421] crystal growth methods.

In 2017, this material was selected for the BASKET project [249] aiming at the development of a cryogenic detector suited to the study of CENNS in above-ground conditions. The Li (^{6}Li) content ensures the neutron detection capability, as demonstrated with other Li-containing scintillating bolometers, while the presence of a heavy target (W) increases the CENNS events detection rate [55]. Therefore, a low-threshold $LiWO_4$(Mo) scintillating bolometer is particularly interesting to be used as CENNS detector, neutron flux monitor, and/or active veto [422].

A first scintillating bolometric test of the material was done with a Cz-grown $Li_2Mo_{0.08}W_{0.92}O_4$ crystal (⌀18 × 7 mm, 8 g) coupled to a ⌀44 mm Ge LD [422]. A rather low scintillation signal ($L/H_{\gamma(\beta)}$ = 0.17 keV/MeV) was detected, but the result is affected by non-optimal light collection (the absence of a reflective film around the lateral side of the crystal and uncoated Ge wafer). However, a good α/γ separation has been achieved using the NTL amplification of the LD signals (QF_α was computed as 0.28).

A poor scintillation efficiency of the compound has been also observed in low-temperature tests of two LTG-Cz-grown samples of $Li_2Mo_{0.05}W_{0.95}O_4$ (10 × 10 × 10 mm, 4.4 g and ⌀25 × 25 mm, 52 g) [423]. In particular, the 4.4-g-based detector measured $L/H_{\gamma(\beta)}$ = 0.15 keV/MeV in conditions similar to the above mentioned test of the 8 g sample. The 52 g $Li_2Mo_{0.05}W_{0.95}O_4$ scintillating bolometer exhibited $L/H_{\gamma(\beta)}$ = 0.4 keV/MeV (quenched to 26% for α+t events) thanks to improved light collection conditions (a SiO-coated Ge LD, a reflective film at bottom and around the lateral side of the sample). An $\alpha/\gamma(\beta)$ separation has been achieved thanks to the NTL mode operation of the LD.

3.1.4. Sodium Tungstate

A Na- and/or I-containing scintillator without hygroscopic properties, in contrast to sodium iodide (and cesium iodide), can be interesting for DM searches, in particular to scrutinize the nature of the signal modulation observed in the DAMA/NaI [424] and DAMA/LIBRA [425–427] DM search experiments. Taking into account such a possible application, a sodium tungstate ($Na_2W_2O_7$) represents a great interest as a cryogenic scintillator [428]. The first bolometric operation of the material has been recently realized at LNGS using a 5.6 g $Na_2W_2O_7$ scintillation element (10 × 10 × 10 mm, LTG Cz growth) coupled to a large-area Ge LD (⌀50.8 × 0.2 mm) [429]. An efficient scintillation ($L/H_{\gamma(\beta)}$ = 12.8 keV/MeV) together with an excellent particle identification capability (QF_α = 0.20) have been observed. These results show good prospects of a $Na_2W_2O_7$-based scintillating bolometer for searches for DM particles.

3.1.5. Lead Tungstate

Thanks to the presence of the heaviest stable element (Pb) in lead tungstate ($PbWO_4$) and increased scintillation at low temperatures (e.g., [430]), this well-known scintillator is attractive for bolometric DM searches [431,432]. In addition, there are four Pb isotopes that can potentially undergo α decay, but the theoretical predictions [29] are rather pessimistic from the experimental point of view. At the same time, the $PbWO_4$ production using modern lead is a drawback of the material for rare-event searches, in particular using Pb-containing bolometers [409]. Indeed, a considerably high contamination (tens–thousands Bq/kg) of modern lead by β-active ^{210}Pb (Q_β = 63.5 keV, $T_{1/2}$ = 22.3 yr) drastically affects the background and the operation of a thermal detector. The ^{210}Pb issue can be solved by using lead produced hundreds of years ago, the so-called Roman, or ancient, or archeological lead (see [409,433,434] and references therein). The production of $PbWO_4$ crystals (Cz method) from ancient lead is reported in [407,408,435]. A first test of the material as a scintillating bolometer has been realized at LNGS with a device fabricated from a large $PbWO_4$ sample (30 × 30 × 61 mm, 454 g) and a Ge wafer (⌀36 × 1 mm) [435]. The measured $PbWO_4$ scintillation signal for $\gamma(\beta)$ interactions is reasonably good ($L/H_{\gamma(\beta)}$ = 1.78 keV/MeV), being five times lower for α particles (QF_α = 0.2) [435].

3.1.6. Zinc Tungstate

Zinc tungstate ($ZnWO_4$) has a rather long-standing interest as a detector material for the searches for DBD (^{64,70}Zn and ^{180,186}W isotopes) and DM (spin-independent and spin-dependent interactions, diurnal modulation) [96,436–440]. Such an interest is driven by a reasonable scintillation efficiency (comparable with $CaWO_4$), one of the highest radiopurity among crystal scintillators, the presence of isotopes with non-zero spin (^{67}Zn, ^{183}W), and anisotropic properties of the material.

The first test of this compound as a scintillating bolometer was done using a CRESST-like detector module with a 8 g $ZnWO_4$ crystal (20 × 10 × 5 mm, LTG Cz growth) and a SiO_2-coated silicon wafer (30 × 30 × 0.5 mm) both instrumented with W superconducting thermometers [441]. A pulse-shape difference between the $ZnWO_4$ luminescence and particles directly impinging on the LD was observed. A high scintillation signal, resulted to $L/H_{\gamma(\beta)} \sim$ 14 keV/MeV, was measured. A non-linearity of the $ZnWO_4$ light output for electron recoils was evident below ∼150 keV heat energy deposition (a curious reader can find details about a non-proportional scintillation response, for example, in [374,442,443]). The light signal for nuclear recoils is quenched to ∼10% and, thanks to that, such events can be clearly separated from $\gamma(\beta)$'s for phonon signals above 20 keV. This test shows that the light output of $ZnWO_4$ crystals is among the highest for oxide scintillators. Moreover, the $ZnWO_4$ light output can be further increased by annealing. For example, a ∼(10–30)%

improvement of a light output at room temperature has been achieved for LTG-Cz-grown $ZnWO_4$ crystals annealed at 800 °C [444].

Recently, the light collection efficiency of the CRESST conventional detector design has been investigated using a $ZnWO_4$ sample (⌀40 × 40 mm) and several $CaWO_4$ crystals [398]. The $ZnWO_4$ scintillation efficiency is estimated to be 8%, while only one fourth is detected as scintillation light (1.9%) due to ∼24% of the light collection efficiency [398]. The results obtained for the $ZnWO_4$ detector are comparable with those of the $CaWO_4$-based scintillating bolometers [398].

An anisotropy in the $ZnWO_4$ light output (at room temperature) for α particles [437,445] and nuclear recoils [445]—a key feature for the $ZnWO_4$-based detection of the diurnal asymmetry of WIMP direction [231,437]—has been also reported recently in studies of a $ZnWO_4$ scintillating bolometer (1 cm^3) with MMC readout of the phonon and scintillation channels [446].

Because of the W content, a $ZnWO_4$-based detector is also suitable for the investigation and searches for rare α decays of W isotopes [447]. Moreover, an interesting approach has been proposed in [448], where a scintillating bolometer made of a 22 g $ZnWO_4$ crystal doped with Sm isotopically enriched in ^{148}Sm to 95.54% (0.16% of $^{148}Sm_2O_3$ powder in the initial charge; Cz growth) was used for the precise measurement of the ^{148}Sm α decay half-life.

Furthermore, an internal active shield based on $ZnWO_4$ scintillators with a bolometric light readout is considered, for the first time in an array of macrobolometers, by the BINGO project [220] aiming at the development of an advanced background rejection for a possible follow-up of the CUPID tonne-scale DBD search experiment. The BINGO concept is going to be demonstrated by the MINI-BINGO small-scale experiment using lithium molybdate and tellurium dioxide crystals of natural isotopic composition with a $ZnWO_4$-based 4π active shield. As a very first step, a scintillating bolometer constructed from an optically polished small $ZnWO_4$ crystal (10 × 10 × 10 mm, 8 g, LTG Cz growth) coupled to a SiO-coated Ge LD (⌀44 × 0.2 mm) has been recently investigated at IJCLab (Orsay, France) with excellent results in terms of the detected light (∼15 keV/MeV for $\gamma(\beta)$'s) [449]. A subsequent bolometric test of low-temperature scintillation detection from a 60-mm-long $ZnWO_4$ bar (30 mm in diameter) shows a similar light yield of the material (the measured $L/H_{\gamma(\beta)}$ is ∼14 keV/MeV) [450].

3.2. Molybdates

3.2.1. Calcium Molybdate

R&D on calcium molybdate ($CaMoO_4$) scintillation detectors, in particular scintillating bolometers, for DBD search (mainly ^{100}Mo) has been going on for nearly two decades [296,451,452]. This material has also been studied for the bolometric detection of DM particles [444,453].

A good prospect for the application of $CaMoO_4$ scintillating bolometers in this field was first demonstrated 15 years ago, achieving a full $\alpha/\gamma(\beta)$ separation with a few-grams detector coupled to a Ge bolometer [296]. Later, a powerful particle identification of such detectors was shown with a massive $CaMoO_4$ crystal (158 g, ⌀40 × 35 mm) [101]. The $L/H_{\gamma(\beta)}$ was measured as 1.87 keV/MeV and the QF_α parameter was found to be ∼0.15 [101]. The investigation of the scintillation of this material, obtained with a 20 × 10 × 5 mm crystal and a 30 × 30 × 0.5 mm SiO_2-coated Si LD, instrumented by a TES W sensor, reports a $L/H_{\gamma(\beta)}$ value of 4.77 keV/MeV induced by 60 keV γ quanta of an ^{241}Am source [453].

The extensive developments of $CaMoO_4$ scintillating bolometers have been realised over the last decade for the AMoRE project [81,454]. In particular, the fabrication of high quality $CaMoO_4$ crystals from calcium depleted in ^{48}Ca and molybdenum enriched in ^{100}Mo ($^{48depl}Ca^{100}MoO_4$) has been developed [455]. The 2νDBD-activity of ^{48}Ca (in spite of 0.2% content in natural calcium [456]) can represent a major background contribution to the ^{100}Mo 0νDBD ROI [296,451,452], thus, the ^{48}Ca content in calcium used for the AMoRE crystals production is reduced below 0.001% [457]. The purification of the starting materials has been adopted to improve the crystal quality and radiopurity [81,455,458,459]. The growth of the $^{48depl}Ca^{100}MoO_4$ crystals is done using the Cz method; the double crystallization is applied to further improve the radiopurity of the ingots [81].

The main milestones achieved in the AMoRE R&D on MMC-instrumented $CaMoO_4$ scintillating bolometers can be summarized as follows:

- first single-readout $CaMoO_4$ prototypes based on small (10 × 10 × 6 mm, 2.7 g) [285] and large-volume (⌀40 × 40 mm, 216 g) [460] crystals;
- a scintillating bolometer based on a 200 g $^{48depl}Ca^{100}MoO_4$ crystal and a 2 inch Ge wafer [461,462];
- an array of five to six scintillating bolometers based on massive $^{48depl}Ca^{100}MoO_4$ crystals (∼200–400 g each; a total mass up to 1.9 kg) in the recently completed AMoRE-Pilot experiment at the Yangyang underground laboratory (Y2L, Republic of Korea) [463–465];
- a 6 kg array of thirteen $^{48depl}Ca^{100}MoO_4$ and five other ^{100}Mo-containing detectors of the AMoRE-I experiment [464–468], currently in progress at Y2L.

A highly efficient identification of α events has been demonstrated with all these dual-readout bolometers [465]. Unfortunately, the measurements lack the LD calibrations, thus, the information about the $L/H_{\gamma(\beta)}$ values is not available. The only particle identification parameter which can be extracted from the published data is QF_α, estimated as ∼0.2 [461,462]. In spite of a huge progress in the developments of $CaMoO_4$ scintillating bolometers, the AMoRE Collaboration is performing R&D on other Mo-containing crystal scintillators [468,469] for the AMoRE-II stage of the experiment (with a 200 kg scale detector array) to avoid the needs of the ^{48}Ca-depleted starting material and to mitigate the remaining issue with the purification of Ca-based compounds.

3.2.2. Cadmium Molybdate

Cadmium molybdate ($CdMoO_4$) was considered a promising scintillation material for cryogenic detectors about 15 years ago [260], in particular the luminescence of this material at 9 K was reported to be 80% of $CaWO_4$. In short, an excellent α particle identification was demonstrated with a first scintillating bolometer based on a small (10 × 10 × 5 mm) $CdMoO_4$ crystal [266,470]. In spite of the first encouraging results, the interest in this material has been reactivated only recently, in particular by proposing to use $CdMoO_4$ enriched in ^{116}Cd and ^{100}Mo for a bi-isotope search for 0νDBD [471]. As a follow-up, a first test of a large scintillating bolometer based on this compound has been recently realized with a colorless 134 g $CdMoO_4$ crystal (⌀25 × 45 mm, BS growth) and ⌀44 mm Ge LD without anti-reflective coating [472]. These measurements demonstrate good prospects for $CdMoO_4$ cryogenic scintillators; in particular, a $L/H_{\gamma(\beta)}$ value of ∼2.6 keV/MeV and a quenching to 16% for α particles ensures an excellent $\alpha/\gamma(\beta)$ separation.

3.2.3. Lithium Molybdate

Lithium molybdate (Li_2MoO_4) is the best example of recent developments of scintillation materials with a strong impact on the strategy of bolometric DBD search experiments and related activities. Li_2MoO_4 was first considered a prospective material for ^{100}Mo DBD search with LTDs about a decade ago [473]. An outstanding progress in the development of Li_2MoO_4 crystal scintillators and their application in rare-event searches with scintillating bolometers has been achieved over the last six years. Consequently, Li_2MoO_4 is now considered the most viable detector material for tonne-scale bolometric 0νDBD searches to be realized in the near future.

Going back to the first operation of a Li_2MoO_4 crystal (1.3 g; Cz growth) as a scintillating bolometer [266], it was hard to imagine such a success of the material because the results of the test were far from being appealing. In particular, the light yield was estimated to be ≈20% of the $CaMoO_4$ one [266] (i.e., $L/H_{\gamma(\beta)}$ ∼0.4 keV/MeV using $CaMoO_4$ data from [101]). Despite the poor detector performance, a hint on the $\alpha/\gamma(\beta)$ separation was demonstrated [266]. Few years later, a similar $L/H_{\gamma(\beta)}$ (0.43 keV/MeV) combined with good performance were reported for a 33 g Li_2MoO_4 scintillating bolometer [474] (from the same crystal producer of [266]). The encouraging results of this study were then reinforced by the characterization of a 151 g Li_2MoO_4 (LTG Cz growth) scintillating bolometer [311], showing excellent performance, almost doubled $L/H_{\gamma(\beta)}$ (∼0.7 keV/MeV) and a highly efficient $\alpha/\gamma(\beta)$ separation.

The results achieved with the advanced Li_2MoO_4 cryogenic scintillator [311] triggered an extensive R&D on Li_2MoO_4 scintillating bolometers recently realized within the ISOTTA and LUMINEU projects [74,345,475–477]. Currently, several R&D activities on the Li_2MoO_4 development for scintillating bolometers are ongoing world-wide: in France (CLYMENE project [478–481]), in the Republic of Korea [482–485], in China [486,487], in the United States [488,489], in Ukraine [490], in addition to the existing crystal growth technologies in Russia [74,311,473,476,491–494]. Most of these activities were and are considered part of R&D programs towards large-scale bolometric DBD search experiments CUPID [82,495,496] and AMoRE [81,483].

Moreover, ^{100}Mo-enriched crystals ($Li_2{}^{100}MoO_4$; 97% of enrichment in ^{100}Mo) have been already developed and used in the LUMINEU (4-detector array) [74,173,345] and its follow-up CUPID-Mo (20-detector array) [159,259,497–499] bolometric DBD search experiments at LSM. Despite of the modest exposure of these small-scale CUPID demonstrators, they have provided valuable physics results. Notably, the most precise measurement of the ^{100}Mo 2νDBD half-life (the second highest precision among all 2νDBD-active nuclides) [173] and the most stringent half-life limit on the 0ν-mode [159] have been achieved. Furthermore, $Li_2{}^{100}MoO_4$ bolometers will be used in the CROSS DBD search experiment (32–52 detectors) [69,118,500] and possibly in the BINGO demonstrator [220]. In addition to the enriched detectors, several crystals have been produced from molybdenum depleted in ^{100}Mo ($Li_2{}^{100depl}MoO_4$) [494] and are going to be used together with enriched ones for the investigation of the 2νDBD spectral shape. Preliminary results of the first scintillating bolometer test of the $Li_2{}^{100depl}MoO_4$ sample (Table 5) are encouraging [500]. Despite the absence of the reflective film inside the Cu holder, that caused to register a lower light [345], an excellent $\alpha/\gamma(\beta)$ separation has been achieved thanks to the good performance of the LD.

Table 5. Results of low-temperature scintillation detection with scintillating bolometers based on natural/^{100}Mo-enriched Li_2MoO_4 crystals and thin Ge LDs. The crystal growth method, the mass (two significant digits) and the size of the sample, the size and the coating of the coupled LD, as well as the $L/H_{\gamma(\beta)}$ and QF_α values are listed.

Cryogenic Scintillator			Ge LD		$L/H_{\gamma(\beta)}$	QF_α	Ref.
Material	**Mass (g)**	**Size (mm)**	**Size (mm)**	**Coating**	**(keV/MeV)**		
Li_2MoO_4 (Cz)	1.3	⌀25 × 0.9	⌀66 × 1	SiO_2	∼0.4	∼0.3	[266]
	33	⌀22 × 33	⌀36 × 1		0.43 [a]	0.22 [a]	[474]
	14	28 × 27 × 6	⌀44 × 0.2		0.91	0.24 [b]	[479]
	160	⌀40 × 40	⌀44 × 0.2		0.97	0.23 [b]	[478,479]
(LTG Cz)	150	⌀40 × 40	⌀40 × 0.05		0.68	0.23	[74,311]
	240	⌀50 × 40	⌀45 × 0.3		0.99	0.20	[74]
	240	⌀50 × 40	⌀25 × 0.03		0.12 [c]	0.17	ibid.
$Li_2{}^{100}MoO_4$ (LTG Cz)	200	⌀44 × 45	⌀45 × 0.3		0.78	0.19	[74]
	210 (×2)	⌀44 × 45	⌀44 × 0.2	SiO	0.73–0.74	0.24–0.26 [b]	[345]
	200 (×2)	⌀44 × 45	⌀44 × 0.2	SiO	0.38–0.41 [d]	0.24–0.27 [b]	ibid.
	210 (×20)	⌀44 × 45	⌀44 × 0.2	SiO	0.55–0.96 [e]	0.20	[259,498]
					(1.17–1.44 [f])		ibid.
	280	45 × 45 × 45	⌀44 × 0.2	SiO	0.64	0.20	[69]
	280 (×3)	45 × 45 × 45	⌀44 × 0.2	SiO	0.25 [g] (0.50 [g,f])	0.17	[283]
					0.55 (1.10 [f])		ibid.
$Li_2{}^{100depl}MoO_4$ (LTG Cz)	280	45 × 45 × 45	⌀44 × 0.2	SiO	0.33 [d]	0.21	[501]

[a] The $L/H_{\gamma(\beta)}$ evaluated from the data shown in Figure 7 [474] is ∼0.7 keV/MeV, in contradiction to Figures 2–4 (ibid.); this discrepancy is probably the origin of the reported QF_α = 0.43 [474]. [b] Estimated for α+t events (4.8 MeV sum energy), products of neutron capture by ^{6}Li. [c] Affected by smaller area of an LD compared to one of the faced crystal side. [d] No reflective foil, but a Cu housing. [e] Such spread is mainly due to the light collection difference imposed by the detector design (see text). [f] Combination of two identical LDs. [g] No reflective cavity, that is fully open detector structure.

Finally, $Li_2{}^{100}MoO_4$ scintillators have been selected from the list of ^{82}Se-, ^{100}Mo-, ^{116}Cd- and ^{130}Te-containing crystals for the realization of the CUPID tonne-scale bolometric experiment [82,283]. Last but not least, Li_2MoO_4 detector material is also a part of the AMoRE DBD project [81,483–485]. Several $Li_2{}^{100}MoO_4$ scintillating bolometers (few out of 18 detectors) are operating in the AMoRE-I DBD experiment [465], aiming at investigating the possibility to use Li_2MoO_4 (instead of $CaMoO_4$, see Section 3.2.1) in the large-scale AMoRE-II detector array [81]. In addition to the great interest for DBD searches, Li_2MoO_4 low-threshold scintillating bolometers are promising detectors for low-mass DM searches with a high sensitivity to spin-dependent interactions with ^{7}Li, as demonstrated for the first time in [322]. A large content of ^{7}Li can also be exploited as a target for a resonant absorption of solar axions [43,266,474,502,503]. Thanks to the 8% content of ^{6}L in natural lithium, Li_2MoO_4 scintillating bolometers can be used for neutron detection in a ROI populated only by α events [74,311,345,474,478,479,485,498]. A high radiopurity of the material [69,74,345,479,497,498] allows the suppression of the contribution of bulk/surface radioactivity down to the ROI for neutron spectroscopy.

The measurements of scintillation light with natural and ^{100}Mo-enriched Li_2MoO_4 scintillating bolometers are listed in Table 5 and can be summarized as follows:

- The Cz-grown Li_2MoO_4 crystals (developed by CLYMENE) [478,479] exhibit similar light yield to the LTG Cz produced scintillators. The amount of the detected light for a standard detector design envisaging the use of a reflective film is compatible with highly efficient particle identification in the ^{100}Mo 0νDBD ROI.
- Crystals produced by the LTG Cz growth from the purified starting materials show reproducible value of the light yield within a minor variation for the same detector structure. In particular, the largest $L/H_{\gamma(\beta)}$ (0.90 keV/MeV median value) for the 20 similar size $Li_2{}^{100}MoO_4$ detectors of CUPID-Mo has been measured for crystals viewed by a single LD (placed at bottom) [259,498]. The use of two LDs reduces the amount of the light detected by each of them to 0.64 and 0.74 keV/MeV (median values) for the bottom and top photodetectors, respectively [259,498]. A small difference in the light signals seen by the top and bottom LDs is explained by a slightly reduced entrance window for the bottom one (required to place the crystal). The combination of two LDs allows us to double the measured scintillation light signal (median $L/H_{\gamma(\beta)}$ is 1.33 keV/MeV) and, subsequently, to enhance the particle identification efficiency [159,283,498,504].
- A notably smaller photodetector area than the crystal side facing it (e.g., a factor of 3 difference [74,275]) can decrease the light collection drastically. An order of tens % difference [69,283,501] can be tolerated, because an efficient particle identification capability would be still possible without the needs of a high-performing LD.
- The absence of a reflective film around a crystal inserted inside a fully closed Cu housing, decreases the light collection by almost a factor 2 [345]. A similar reduction factor is observed for bare crystals compared to ones surrounded by the reflective film in an opened detector structure [283]. This result combined with Monte Carlo simulations of the scintillation light production, propagation, and absorption show that the surface roughness does not play an important role for Li_2MoO_4 crystals [283] (for instance, similar observations are reported for tungstates [276,277], while a stronger impact of the surface roughness on the light collection is expected, for example, for zinc molybdate [275] and tellurium dioxide [271,505]).
- Despite a large variation in the measured $L/H_{\gamma(\beta)}$, imposed by light collection efficiency, the QF_α value remains rather similar, $\sim$0.2, showing a small variation. The quenching factor for α+triton events ($QF_{\alpha+t}$), detected in neutron calibrations of Li_2MoO_4 scintillating bolometers, is about 10% larger than that of α's of similar energy. The difference in the light yield induced by α and α+t interactions in a scintillator illustrates Birck's formula (see Section 1.2): more than a half of the energy release in the ^{6}Li(n,t)α reaction is taken away by a lighter nucleus, triton, which induces a higher light output than α of the same energy loss.

In addition to Li_2MoO_4-based scintillating bolometers instrumented with NTD Ge thermistors (all listed in Table 5), other phonon sensor technologies have been recently used. Among the features of these technologies, it is important to emphasize a faster detector response and the possibility of channel multiplexing. Fast timing of heat and light signals is of special importance for ^{100}Mo-enriched bolometers to suppress the background in the ^{100}Mo 0νDBD ROI induced by random coincidences (mainly due to 2νDBD events) [205–207]. The AMoRE prototypes of Li_2MoO_4 scintillating bolometers are instrumented with MMC sensors [484,485]. Only partial scintillation-based particle separation (improved to 99.9% by the heat pulse-shape analysis) has been achieved in the measurements with a small crystal coupled to a Ge LD (15 × 15 × 0.5 mm) [484]. Conversely, an efficient particle identification around the ^{100}Mo 0νDBD ROI has been demonstrated with a much larger (⌀50 × 48 mm) crystal paired with a Ge disk (⌀50 × 0.5 mm) [485]. It was also observed that a weak hygroscopicity of the material can drastically impact the phonon signal amplitude if no precaution is taken to avoid exposition to a humid environment [485]. Another technology, employing KIDs developed within the CALDER project [286,338,506], has been used to test a Li_2MoO_4 scintillating bolometer based on a 24 g crystal (20 × 20 × 20 mm; LUMINEU sample) and a Si wafer (20 × 20 × 0.3 mm). The LD signals are characterized by a rise time of ∼0.2 ms [286], a factor 3–5 faster than ever reported for NTD-Ge-instrumented LDs. A study of the KID LD response shows that the Li_2MoO_4 scintillation decay time, measured as 85(5) µs, is constant in the 10–190 mK range [286].

3.2.4. Lithium Magnesium Molybdate

Lithium magnesium molybdate ($Li_2Mg_2(MoO_4)_3$) is another Mo-containing material recently developed and tested at low temperatures for rare-event searches [356]. The $Li_2Mg_2(MoO_4)_3$ compound contains one of the largest number of Mo atoms per crystal volume (e.g., comparable to $CaMoO_4$, and 20% more than Li_2MoO_4). The absence of hygroscopic properties of the material (in contrast to weak hygroscopicity of Li_2MoO_4) is an advantage too. An optically-clear quality $Li_2Mg_2(MoO_4)_3$ crystal growth was realized successfully using a 5N grade MoO_3 powder and the LTG Cz technique [356]. An element with a size of 19 × 14 × 10 mm and a mass of 10.2 g was produced for a bolometric test. Scintillation detection was done with the help of a SiO-coated Ge LD (⌀44 × 0.2 mm) assisted with the NTL signal amplification. The measured $L/H_{\gamma(\beta)}$ of 1.3 keV/MeV is comparable to the results of $ZnMoO_4$ (Section 3.2.10) and slightly exceeds the values reported for Li_2MoO_4 (Section 3.2.3) crystal scintillators. The scintillation induced by α particles is quenched to 22%. The detector provides an efficient particle identification satisfying the requirements of a bolometric 0νDBD search experiment and allowing the use of the material for a bolometer-based neutron detection [356]. The variety of elements with different atomic masses present in $Li_2Mg_2(MoO_4)_3$ is of particular interest for DM search applications [356].

3.2.5. Lithium Zinc Molybdate

Lithium zinc molybdate ($Li_2Zn_2(MoO_4)_3$) was developed a decade ago as a potential LTD of DBD processes in Zn and Mo isotopes (with the main interest in ^{100}Mo) [357]. A small sample (20 × 10 × 2 mm; LTG Cz growth), cut from a crystal boule grown from purified materials, was successfully operated as a single readout LTD [357]. Despite a rather low scintillation of the material detected at 223 K (∼(3–4)% of $CaMoO_4$), an increase of the $Li_2Zn_2(MoO_4)_3$ light output at low temperatures has been observed [357], opening a possibility to use $Li_2Zn_2(MoO_4)_3$ as a cryogenic scintillator.

3.2.6. Magnesium Molybdate

A possible application of magnesium molybdate ($MgMoO_4$) to rare-event searches with scintillating LTDs was investigated for the first time 15 years ago [358]. The scintillation of the material increases steeply below ∼30 K [260,507]. A bolometric test of this scintillator (89 g sample, 32 × 31 × 24 mm) has been realized with a single readout only (the assembly structure did not allow for the mounting of an LD) [101]. Moreover, the detector performances were strongly affected (possibly by a crystal crack under the glued thermistor). Despite of that issue, a clear pulse-shape difference between $\gamma(\beta)$ and α events has been demonstrated [101]. These results definitely indicate the possibility of particle identification with a $MgMoO_4$-based scintillating bolometer.

3.2.7. Sodium Molybdate

In addition to DM search applications (as for sodium tungstate, Section 3.1.4), sodium molybdate might be interesting for Mo-based DBD search experiments, in particular for the AMoRE project [508]. A good progress in the development of a large volume $Na_2Mo_2O_7$ crystals using the Cz growth has been achieved within the AMoRE R&D [508]. The light output of the $Na_2Mo_2O_7$ scintillator at 10 K was found to be 55% of the $CaMoO_4$ light yield [508], which is rather promising for scintillating bolometer applications.

A growth and low-temperature characterization of $Na_2Mo_2O_7$ and $Na_2Mo_4O_{13}$ crystals have been reported in [265]. A 1.6 g sample of $Na_2Mo_4O_{13}$ crystal grown by the vertical Bridgman method was of low quality because of the difficulties in the growing process of this compound. Despite this problem, a scintillation-assisted particle identification has been demonstrated with the $Na_2Mo_4O_{13}$ scintillating bolometer. A Cz-grown $Na_2Mo_2O_7$ sample was larger (11 g) and of better quality single crystal. An aboveground characterization of the sample at low temperatures also demonstrates a clear separation between $\gamma/\beta/\mu$-induced events and α particles [265].

A highly purified MoO_3 powder and a commercial Na_2CO_3 (4N purity grade) were used as starting materials for the LTG-Cz-based production of the $Na_2Mo_2O_7$ scintillator [429]. In a bolometric operation of a small sample (10 × 10 × 10 mm, 3.6 g), realized together with the same-size $Na_2W_2O_7$ crystal (see Section 3.1.4), the detected scintillation is characterized by $L/H_{\gamma(\beta)}$ = 1.61 keV/MeV and QF_α = 0.16 [429]. In spite of relatively modest performance of the LD (0.3 keV RMS noise), a particle identification was clearly demonstrated. Another LTG-Cz-grown $Na_2Mo_2O_7$ crystal (10 × 10 × 10 mm) together with a Ge slab (15 × 15 × 0.05 mm) were used in an MMC-instrumented scintillating bolometer [484]. Using the dual readout, the detector achieved only a partial separation of α particles from γ and β events, while the α rejection efficiency was improved to higher than 99.9% with a pulse-shape analysis of the heat channel [484].

3.2.8. Lead Molybdate

A large increase of the lead molybdate ($PbMoO_4$) fluorescence at cryogenic temperatures has been reported decades ago [430,509], emphasizing the good prospects of the material for scintillating bolometer searches for the ^{100}Mo 0νDBD [509,510]. A powerful $\alpha/\gamma(\beta)$ separation with a small, a few grams, $PbMoO_4$ scintillating bolometer was demonstrated for the first time 15 years ago [296]. As in the case of $PbWO_4$ (see Section 3.1.5), the ^{210}Pb contamination is a limiting factor of this material to be used for bolometric DBD searches [296]. However, $PbMoO_4$ remains attractive for rare-event searches [431,432], especially if ^{210}Pb-free lead can be used for the crystal production.

Recently, highly purified ancient lead samples were used for the $PbMoO_4$ growth by Cz [511] and LTG Cz [512] methods and 57 g (⌀20 × 30 mm) and 570 g (⌀44 × 55 mm) samples were cut respectively from the grown ingots for bolometric characterizations. Two scintillating bolometers based on these crystals were constructed in the same way and using similar size Ge LDs (⌀44 × 0.3 mm and ⌀44 × 0.2 mm). Low-temperature tests were realized in the same underground facility at LNGS. The material exhibits the highest scintillation yield ever reported for molybdates at low temperatures. However, the measured $L/H_{\gamma(\beta)}$ is significantly different between the modules: 5.2 and 12.0 keV/MeV for the Cz- and LTG-Cz-grown $PbMoO_4$ crystals, respectively [511,512]. This difference is probably due to higher quality (and/or purity) of the latter sample. The α particle induced scintillation is quenched to a ∼20% level for both $PbMoO_4$ samples (the QF_α parameters are 0.23 and 0.18 for the Cz- and LTG-Cz-grown crystals, respectively [511,512]).

3.2.9. Strontium Molybdate

Strontium molybdate ($SrMoO_4$) is a potential scintillation material for the searches for DBD of Sr and Mo isotopes. The feasibility of $SrMoO_4$ as a phonon-scintillation LTD, in particular a clear $\alpha/\gamma(\beta)$ separation, as well as a problem with the crystal radiopurity were demonstrated about 15 years ago [296]. In contrast to the γ and β events, the detector response to α radiation exhibits a non-linearity of the scintillation light output with the increase of particle energy. Therefore, the QF_α value can only be roughly estimated as ∼0.26.

The interest in the material has been renewed recently in view of a progress in the crystal growth (Cz method). The measurements of a $SrMoO_4$ scintillation at 11 K, carried out using the multi-photon counting technique [513], has determined its light yield to be 15(5)% of $ZnWO_4$ [361], that is $L/H_{\gamma(\beta)} \sim$ (1–3) keV/MeV taking into account the results for $ZnWO_4$ crystals (Section 3.1.6).

3.2.10. Zinc Molybdate

Zinc molybdate ($ZnMoO_4$) is another crystal scintillator extensively developed over the last decade, being considered one the most promising Mo-containing scintillation materials for bolometric experiments to search for the ^{100}Mo 0νDBD [74,344,514–517]. Early bolometric tests of the material [101,275,307,344,514,518,519] have been realized mainly within Bolux R&D Experiment, LUCIFER, and ISOTTA projects, while a technology of radiopure, natural and ^{100}Mo-enriched $ZnMoO_4$ scintillating bolometers has been developed as a part of the LUMINEU project [74,318,362,475,515–517,520–524]. The developed $ZnMoO_4$ scintillating bolometers and the results of scintillation detection with these devices are listed in Table 6.

Table 6. Results of low-temperature scintillation detection with scintillating bolometers based on natural/^{100}Mo-enriched $ZnMoO_4$ crystals and thin Ge LDs. The crystal growth method, the mass (two significant digits) and the size of the sample, the size and the coating of the coupled LD, as well as the $L/H_{\gamma(\beta)}$ and QF_α values are listed.

Cryogenic Scintillator			Ge LD		$L/H_{\gamma(\beta)}$	QF_α	Ref.
Material	Mass (g)	Size (mm)	Size (mm)	Coating	(keV/MeV)		
$ZnMoO_4$ (Cz)	20	⌀25 × 11	⌀36 × 1	SiO_2	1.1	∼0.15	[101,518]
(LTG Cz)	5.1	15 × 15 × 5	15 × 15 × 0.5		2.1 [a]	∼0.15	[275,514]
	24	⌀16 × 28	15 × 15 × 0.3		1.8 [a]	0.19	[275]
	28	⌀19 × 22	⌀36 × 1	SiO_2	1.1	0.18	[344]
	30	29 × 18 × 13	⌀36 × 1	SiO_2	0.78	0.18	ibid.
	55	⌀20 × 40	⌀50 × 0.3		0.98	0.15	[362]
	55	⌀20 × 40	⌀50 × 0.3		1.3		[523]
	55 [b]	⌀20 × 40	⌀50 × 0.3		1.1		ibid.
	150	⌀35 × 40	⌀50 × 0.3		0.96	0.16	[362]
	310	(irregular)	⌀50 × 0.3		n/a	0.15	[522]
	330	(irregular)	⌀50 × 0.3		1.5	0.17	[519]
	330	⌀50 × 40	⌀50 × 0.3			0.15–0.17	[74,522]
$Zn^{100}MoO_4$	60 (×2)	(irregular)	⌀50 × 0.3		1.0		[318]
(LTG Cz)	380 (×2)	⌀60 × 40	⌀45 × 0.2	SiO	1.2–1.3	0.13-0.17	[74]

[a] Combined value of two identical LDs. [b] Doped with tungsten to 0.5 mol%.

The low-temperature investigations of $ZnMoO_4$ found that this material is characterized by a reasonably good scintillation (see Table 6), which allows for a highly efficient particle identification in the ROI of ^{100}Mo 0νDBD. The only abnormal peculiarity, observed in scintillation-vs.-heat data of $ZnMoO_4$-based LTDs, is a tail (with a negative slope) of α lines of bulk contaminants to lower light signal values [74,101,313,518]. Since the QF_α value is lower than 1, this anomaly results in an increased separation of such α's, but worsen the α energy resolution. This feature is probably due to inclusions seen in the samples. In spite of a great progress in the development of large-mass crystal boules (about 1 kg mass) using highly purified natural/^{100}Mo-enriched molybdenum compounds [74,522], the difficulties with the $ZnMoO_4$ solidification process affect the crystal quality. It was found that doping with a small amount of W helps to mitigate the $ZnMoO_4$ growing issues and to get better quality crystals with similar low-temperature scintillation efficiency [523]. However, the growth of a large-volume crystal boule needs further R&D to improve the presently achievable crystal quality [74]. Therefore, another Mo-containing material (lithium molybdate, Section 3.2.3) has been developed as a viable alternative to zinc molybdate.

3.3. Borates

3.3.1. Lithium Europium Borate

In view of the poor scintillation of lithium fluoride, largely investigated for neutron detection (Section 3.6.2), lithium europium borate ($Li_6Eu(BO_3)_3$) was studied as a possible scintillating bolometer for neutron spectroscopy exploiting (n, α) reactions on ^{6}Li and ^{10}B [59]. In particular, a $Li_6Eu(BO_3)_3$-based LTD would have an efficiency for neutron detection similar to lithium fluoride [59]. The feasibility of this approach has been investigated with a 5 mm side cube $Li_6Eu(BO_3)_3$ scintillating bolometer irradiated by a neutron source. A good capability to distinguish three expected neutron capture reactions—^{6}Li(n, t)α, ^{10}B(n, α)^{7}Li, and ^{10}B(n, α)^{7}Li+γ—has been demonstrated [59].

$Li_6Eu(BO_3)_3$ was also considered a viable Eu-containing material to search for α decays of naturally occurring europium [525] (e.g., as an alternative to Eu-doped calcium fluoride [526], Section 3.6.1), in particular, using a $Li_6Eu(BO_3)_3$-based LTD. Such idea has been lately realized using a scintillating bolometer made of a 6.2 g $Li_6Eu(BO_3)_3$ crystal (Cz-grown) and a Ge LD ($\varnothing$44 $\times$ 0.3 mm) to detect the rare α decay of ^{151}Eu [527,528]. The material has a good scintillation at low temperatures, as exhibited by the measured $L/H_{\gamma(\beta)}$ of 6.55 keV/MeV. The α particles induced scintillation was found to be quenched to 8%, providing excellent identification capability.

3.3.2. Lithium Gadolinium Borate

Lithium gadolinium borate ($Li_6Gd(BO_3)_3$), developed two decades ago [529], is an attractive scintillation material for neutron detection thanks to the content of ^{6}Li, ^{10}B, and ^{155,157}Gd. It is worth noting that the large thermal neutron cross sections for ^{155,157}Gd(n, γ) reactions result in relatively low detection efficiency of a $Li_6Gd(BO_3)_3$-based detector to thermal neutrons as compared to, for example, $Li_6Eu(BO_3)_3$ or lithium fluoride [59]. On the contrary, such a feature of $Li_6Gd(BO_3)_3$ can be exploited to get a cleaner fast neutron spectrum near the thermal peak [59].

A small-size (5 $\times$ 5 $\times$ 5 mm) $Li_6Gd(BO_3)_3$ enriched at 95% in both isotopes ^{6}Li and ^{10}B has been investigated as a scintillating bolometer [59,371]. A poor $L/H_{\gamma(\beta)}$ (0.26 keV/MeV) has been measured. The scintillation for α particles is found to be quenched to 23% of the $\gamma(\beta)$-induced one. It is interesting to note that the scintillation yield registered for α+triton events (4.8 MeV) is 35% higher than that of ^{241}Am α's (5.5 MeV). This evidence might suggest a good scintillation of the ^{6}Li/^{10}B-enriched $Li_6Gd(BO_3)_3$ bolometer, possibly affected by non-optimal light collection conditions (e.g., caused by a low reflectivity of the cavity for the scintillation emission spectrum occurring in the ultraviolet range [530]). Indeed, such a large difference between QF_α and $QF_{\alpha+t}$ has been recently observed with an efficient Li-containing scintillator (lithium indium diselenide, Section 3.5.1).

3.4. Other Oxides

3.4.1. Aluminium Oxide

Aluminium oxide (Al_2O_3) is a very promising target for low-mass WIMP spin-independent searches allowing also investigation of the spin-dependent interactions (^{27}Al, 100% isotopic abundance) [531]. (Al_2O_3 is called sapphire for all synthetic crystals, except red-colored ones (rubies) which are with the admixture of Cr.) In particular, this material has been used in the single readout bolometric DM search detectors of the EDELWEISS/MANOLIA [532], ROSEBUD [533–535], and the CRESST (instrumented with TES W) [536,537] experiments. Scintillating bolometers based on this target (as well as bismuth germanate, Section 3.4.2, and lithium fluoride, Section 3.6.2) have been extensively developed and studied as part of the ROSEBUD DM search program [257,267,538–541]. In addition to being used as DM detector, an Al_2O_3 scintillating bolometer, operated alone or together with a ^{6}Li-containing LTD, can be exploited for the monitoring of fast neutrons (which can mimic a DM signal) [60,257,258].

A scintillating bolometer based on a Ky-grown nominally undoped sapphire (Ti content is lower than 10 ppm in weight) exhibits a good scintillation, in particular the $L/H_{\gamma(\beta)}$ values of 50 g prototypes coupled to ⌀25 mm Ge LDs were measured as 12.7–13.5 keV/MeV [267,530,538]. A very similar scintillation signal of a Ti-doped Al_2O_3 crystal (4 g, Ky growth), that is 13 keV/MeV, was detected by a Ge LD [267]. The scintillation induced by α particles and nuclear recoils is quenched to around 10% and 6%, respectively [267,538], also demonstrating the dependence of quenching factors on energy [541]. Such performance of a sapphire-based scintillating bolometer provides a powerful particle identification, down to 10 keV [539].

In the study of two scintillating bolometers made of Ve-grown undoped Al_2O_3 crystals with mass of 25 and 200 g coupled respectively to ⌀25 and ⌀40 mm Ge LDs, five times lower $L/H_{\gamma(\beta)}$ values (2.5–2.8 keV/MeV) have been measured [530]. Such a large difference in the detected scintillation of Ve- and Ky-grown Al_2O_3 crystals cannot be completely explained by the difference in the light collection efficiency (a relative factor of 1.7, originated to the difference in the reflectivity between uncoated and Ag-coated Cu cavities) [530]. The evaluated quenching factors for α's and nuclear recoils (QF_α = 0.30–0.36 and QF_{recoil} = 0.12 [530]) are 2–4 times larger than those obtained for Ky-grown crystals [267,538]. Due to a lower light output (combined with a lower scintillation quenching for nuclear recoils), a clear separation between $\gamma(\beta)$ and nuclear recoils has been achieved only down to around 60 keV [530].

Further investigations of sapphire-based scintillating bolometers have been realized with four 4–50 g crystals from several suppliers and with different concentration of Ti and Cr, as part of the SciCryo project [542]. Either Ge or Si LDs were coupled to the studied scintillators. The $L/H_{\gamma(\beta)}$ values (8–14 keV/MeV) measured for three out of four samples [542,543] are similar to previously reported results for Ky-grown crystals [267,538], while a considerably lower scintillation (2.5 keV/MeV) was detected from the fourth one [542,543]. A 50 g Al_2O_3 scintillating bolometer was also operated in the EDELWEISS set-up at LSM, demonstrating the integration of a scintillation-phonon device into the ionization-phonon detector array of the cryogenic DM search experiment [542,543]. This test, relevant for EURECA, shows the feasibility of the combination of different DM detector technologies and the use of sapphire as scintillating bolometer to act as a neutron flux monitor [542,543].

An anti-correlation between light and heat pulse amplitudes of a scintillating bolometer was reported for the first time for a sapphire-based device [538]. This observation was exploited for the analysis of the energy partition in an Al_2O_3 scintillating bolometer, fabricated from a 50 g crystal [540]. It was found that the absolute light yield is 11%, while the same amount is trapped by the crystal and the rest of the energy release goes to heat [540]. However, a significantly lower $L/H_{\gamma(\beta)}$ value is measured due to a low light collection efficiency (around 12%) [540].

3.4.2. Bismuth Germanate

Bismuth germanate ($Bi_4Ge_3O_{12}$, commonly abbreviated as BGO) is another classic scintillation material [374,375] with a long-standing interest for direct DM searches with scintillating bolometers. In particular, this material was considered a possible scintillating target for the CRESST [392] and used in the ROSEBUD [267,394,539,544–546] experiments. The content of the heaviest "stable" element, ^{209}Bi (100% abundance in natural bismuth), with non-zero spin of the ground state provides a viable target for high-mass WIMP spin-independent and spin-dependent searches.

Excellent particle identification capability of BGO scintillating bolometers was reported for the first time almost two decades ago in studies with 46 and 91 g crystals [133,267,394]. In particular, $L/H_{\gamma(\beta)}$ = 7.5 keV/MeV, QF_α = 0.17, and $QF_{recoil} \sim 0.07$ have been measured with a 46 g BGO bolometer (⌀20 × 20 mm) coupled to a Ge LD

(⌀25 × 0.1 mm), providing an efficient separation down to ∼20 keV recoil energies [133,267,539]. A detailed study of QF_α and QF_{recoil} as a function of the deposited energy in that 46 g BGO scintillating bolometer is presented in [541].

As in the case of sapphire (Section 3.4.1), the light-heat anti-correlation of the 46 g BGO scintillating bolometer [544] allowed us to determine that the absolute light yield is 5.8%, while the rest of the deposited particle energy is released in heat or trapped with a similar fraction (46% vs. 48%) [540]. At the same time, due to a low light collection efficiency (estimated as 12%), the measured $L/H_{\gamma(\beta)}$ remains much lower (7.0 keV/MeV).

The considerable contamination of BGO crystals by ^{207}Bi [96,547], which might be mitigated by a careful selection of Bi-containing starting materials, is a limiting factor for DM search applications. In any case, a BGO scintillating bolometer (especially, with a reasonably low ^{207}Bi content) represents an interest for γ and/or α spectroscopy [544,548] and related nuclear and particle physics applications. In particular, the ^{207}Bi contamination of the 46 g BGO scintillating bolometer has been exploited for the first measurement of the L/K electron capture ratio of the ^{207}Bi decay to the 1633 keV level of ^{207}Pb [549]. Moreover, excellent performance and $\alpha/\gamma(\beta)$ separation of BGO scintillating bolometers allowed us to detect, for the first time, the α decay of ^{209}Bi [133], the rarest ever observed α decay. This discovery has been made with the above-mentioned 46 and 91 g BGO scintillating bolometers. Furthermore, about twice higher $L/H_{\gamma(\beta)}$, 16.6 keV/MeV, measured with a large-volume (50 × 50 × 50 mm, 891 g) BGO scintillating bolometer working in coincidences with a SiO_2-coated Ge LD (⌀36 × 0.3 mm) was exploited to detect the ^{209}Bi α decay transition to the first excited state of ^{205}Tl [134]. It is worth noting that the LD energy resolution was measured as 3.5% FWHM at 2615 keV [134,548]. Last but not least, the operation of a 4-crystal array of 0.89-kg BGO bolometers coupled to a single Ge LD (⌀50 × 0.3 mm) at LNGS has enabled competitive searches for axioelectric absorption of solar axions [550].

Taking into account good scintillation properties of BGO and well-established growth of large-volume crystals (particularly, using the LTG Cz method [551]), this material is considered in the BINGO project as a viable alternative to $ZnWO_4$ for the development of an active shield of a bolometric DBD search experiment [449]. A first low-temperature test of the BGO-based BINGO prototype has been recently realized at IJClab using a LTG-Cz-grown sample (⌀30 × 60 mm) and two identical Ge LDs (⌀44 × 0.2 mm; only one LD, coated with SiO, was operational). The data analysis shows an efficient pulse-shape discrimination between signals induced by BGO scintillation and muons passing through the LD [449]. The $L/H_{\gamma(\beta)}$ is measured as ∼28 keV/MeV [449], which is the highest value ever reported for BGO and is twice higher than that of the same-size $ZnWO_4$ crystal investigated in the same experimental conditions (see Section 3.1.6).

3.4.3. Lithium Aluminate

A lithium aluminate ($LiAlO_2$) crystal scintillator is another Li-containing material investigated recently using a scintillating bolometer approach and applied for the searches for spin-dependent DM interactions [323,552]. One detector module based on a small $LiAlO_2$ crystal (20 × 10 × 5 mm, 2.8 g, Cz growth) with an NTD readout was tested aboveground with a CRESST-III LD instrumented with a TES sensor. (A twin sample with a TES directly deposited on the crystal was operated too, but without LD.) Another module was investigated at LNGS. It was constructed from a large sample (⌀50 × 70 mm, 373 g), cut from the same crystal boule, and equipped with both NTD and TES-on-$CaWO_4$-based-carrier sensors. A CRESST-II LD was also facing the top surface of the $LiAlO_2$ crystal. Both phonon-scintillation LTDs demonstrate good particle identification capability thanks to high-performance LDs and a reasonable light yield. In particular, the small $LiAlO_2$ scintillating bolometer is characterized with $L/H_{\gamma(\beta)}$ = 1.18 keV/MeV, $QF_{\alpha+t}$ = 0.6 and QF_{recoil} = 0.24. The quenching factor for α particles is 16% lower than that of α+t events, as found in the study of the large $LiAlO_2$ scintillating bolometer.

3.4.4. Tellurium Dioxide

Tellurium dioxide (TeO_2) is the most extensively developed and used material for DBD search experiments with pure thermal detectors. In particular, thanks to almost 30-years-long development on TeO_2 LTDs [218], 988 large-volume detectors (50 × 50 × 50 mm, 750 g) are now operating at LNGS in the first tonne-scale bolometric experiment, CUORE [77–80]. A major drawback of this material is the negligibly low scintillation of pure or doped crystals either at room or low temperatures [267–269,553]. Despite that issue, particle identification with a TeO_2 crystal operated as a scintillating bolometer, first reported in [267,554], can be realized by the detection of the Cherenkov radiation induced by $\gamma(\beta)$'s, but not α's [270] (see Section 2.1). However, as one can see in Table 7, this task is extremely challenging because of the poor amount of the emitted light ($L/H_{\gamma(\beta)} \sim$ 0.04 keV/MeV), which requires low-threshold LDs. Indeed, in order to reach about 99.9% rejection of the α background (i.e., $DP_{\alpha/\gamma(\beta)}$ = 3.2) for a TeO_2 bolometer, the baseline noise resolution of an LD is required to be ∼20 eV RMS [555], for example, comparable with the noise resolution of the best performance NTD-instrumented LDs (the same phonon sensor technology of the CUORE experiment). A feasible optimization of the light collection could relax this constraint to only ∼30 eV RMS [271]. The state-of-the-art of the Cherenkov-dominated signal detection and particle identification with TeO_2 crystals, operated using a scintillating bolometer approach, is reported in Table 7.

Table 7. Results of low-temperature scintillation and Cherenkov radiation detection with scintillating bolometers based on natural/^{130}Te-enriched TeO_2 crystals and thin LDs. The mass (two significant digits) and the size of the sample, the size, the material (including coating), the sensor technology, and the baseline noise RMS of the coupled LD, as well as the $L/H_{\gamma(\beta)}$ value and the achieved $DP_{\alpha/\gamma(\beta)}$ at the ^{130}Te 0νDBD ROI are listed.

TeO_2		LD				$L/H_{\gamma(\beta)}$	$DP_{\alpha/\gamma(\beta)}$	Refs.
Mass (g)	Size (mm)	Size (mm)	Material	Sensor	Noise (eV)	(eV/MeV)		
6.0	10 × 10 × 10	20 × 20 × 0.6	Si	NTD Ge [a]	∼28	∼5	4.7	[321]
23	20 × 20 × 10	20 × 20 × 0.5	Si	TES IrAu [a]	8	30	3.6	[334]
26	13 × 15 × 21	⌀25 × 0.05	Ge	NTD Ge	16	50	2.4	[267,315]
120 [b]	30 × 24 × 28	⌀66 × 1	Ge+SiO_2	NTD Ge	97	75	1.4	[319]
290	⌀40 × 40	⌀40 × 0.5	Al_2O_3+Si	TES W	23	48	3.7	[325]
440 [c]	36 × 38 × 52	⌀44 × 0.2	Ge	NTD Ge [a]	35	58	2.7	[299]
440 [c]	36 × 38 × 52	⌀44 × 0.2	Ge+SiO	NTD Ge [a]	25	61	3.5	[299]
750	50 × 50 × 50	⌀50 × 0.3	Ge	NTD Ge	72	45	n/a	[555]
750	50 × 50 × 50	⌀44 × 0.2	Ge	NTD Ge [a]	19	35	2.6	[556]
780	51 × 51 × 51	⌀44 × 0.2	Ge+SiO	NTD Ge [a]	10	26	3.2	[269]
780	51 × 51 × 51	⌀44 × 0.2	Ge+SiO	NTD Ge	20	58	3.6	[301]

[a] A signal amplification based on the NTL effect [305,306] was exploited. [b] A Sm-doped crystal. [c] A crystal produced from tellurium enriched in ^{130}Te.

3.4.5. Yttrium Orthovanadate

Yttrium orthovanadate (YVO_4), given its large mass fraction of vanadium (about 18%), is an attractive compound for the investigation of the 4-fold-forbidden β decay of ^{50}V, in particular using a bolometric technology [557]. The first characterization of the YVO_4 material using a scintillating bolometer technique has been realized with a Cz-grown undoped crystal (⌀18 × 20 mm, 22 g) viewed by a Ge LD [557]. The YVO_4 scintillating bolometer shows an efficient scintillation at low temperatures: the measured $L/H_{\gamma(\beta)}$ is 59.4 keV/MeV. (An order of magnitude lower light signal is seen in Figure 5 [557] compared to Figure 4 and results presented ibid., seems to be due to the LD miscalibration. Indeed, YVO_4 has a rather high light output at room temperature (6300–11,000 photons/MeV [558,559] and a significantly increased scintillation efficiency with the temperature decrease (a factor 5 gained light yield at ∼140 K compared to one at room temperature [559]).) The scintillation light for α particles is quenched to 20% [557], thus providing an excellent particle identification capability. Thanks to the encouraging results of this bolometric test, an innovative approach based on triple coincidence between YVO_4, TeO_2 and Ge LTDs has been proposed [557] to detect the rare β transition of ^{50}V to the first excited state of ^{50}Cr, improving the present knowledge on the ^{50}V decay scheme [560].

3.4.6. Zirconium Dioxide

Zirconium dioxide (ZrO_2) is potentially interesting to search for DBD of Zr isotopes [34,296,561,562], especially ^{96}Zr, an isotope with one of the largest $Q_{\beta\beta}$-value. An operation of a small ZrO_2 sample (0.14 g) as a scintillating bolometer has been realized about a decade ago [208,470]. The ZrO_2 scintillation has been detected with the help of a Ge LD (⌀35 × 0.3 mm), allowing for a separation between $\gamma(\beta)$ and α events. No ZrO_2 $L/H_{\gamma(\beta)}$ is reported, but a poor scintillation light output of the material together with Li_2MoO_4 is concluded from the low-temperature tests [208,470]. Using a rough comparison of a light signal amplitude induced by similar energy deposition in the ZrO_2 detector and a neighbour scintillating bolometer (cesium iodide) operated in the same assembly [470], the ZrO_2 light yield is estimated as ∼2% of cesium iodide (or $L/H_{\gamma(\beta)} \sim 2$ keV/MeV, using results presented in Section 3.7.1) and the QF_α parameter is evaluated as ∼0.2.

3.5. Selenides

3.5.1. Lithium Indium Diselenide

Lithium indium diselenide ($LiInSe_2$) has been under development as a neutron detector material for several years [265] and it can potentially be interesting for the searches for 0νDBD of Se isotopes and/or solar neutrino detection. However, the presence of the β-active ^{115}In ($T_{1/2}$ = 4.4 × 10^{14} yr) with almost 96% abundance in natural indium limits a suitable crystal mass of a bolometric detector to ∼10 g, in which the ^{115}In activity of around 1 Bq is the maximum acceptable in order to avoid serious pile-up issues. On the contrary, such cryogenic detector can be used to investigate the 4-fold-forbidden β decay of ^{115}In, particularly its spectral shape would help to disentangle a possible quenching of the axial-vector coupling constant and this information is important for theoretical predictions on 0νDBD rate [30]. With this aim, a small $LiInSe_2$ crystal (19 × 15 × 8 mm, 10.2 g, BS growth) was operated as a scintillating bolometer [265,563,564]. A Ge LD (⌀44 × 0.2 mm) with the NTL signal amplification was used to detect the $LiInSe_2$ scintillation. The measured notable $L/H_{\gamma(\beta)}$ (14 keV/MeV [265]) does not require a high-performance LD, but it is important for the control of pile-ups and for the reconstruction of the spectrum at near threshold energy. The quenching of scintillation light was found to be 55% and 79%, respectively, for α particles of ^{210}Po and α+t events from thermal neutron captures by ^{6}Li [265]. Thus, $LiInSe_2$ is extremely promising as a scintillating bolometer for neutron spectroscopy because the products of the neutron capture can be detected in the region free of $\alpha/\beta/\gamma/\mu$-induced radiation.

3.5.2. Zinc Selenide

Zinc selenide (ZnSe) as a potential scintillation detector for DBD searches was first studied about 30 years ago [436], while it has been actively used in scintillating bolometers only over the last decade. The main developments of ZnSe scintillating bolometers were realized within the Bolux R&D Experiment [347] and LUCIFER [312,565–567] projects. Furthermore, 24 ^{82}Se-enriched (Zn^{82}Se; 96% enrichment) and two natural crystals developed by the LUCIFER Collaboration have been used in the CUPID-0 DBD search experiment, realized over the last four years [75,157,169,193,568–572].

The first investigation of ZnSe scintillating bolometers [347] reports comprehensively the features of the material at low temperatures, which were then confirmed and extended by further studies of natural and ^{82}Se-enriched ZnSe crystals. The findings related to the ZnSe scintillation detection can be summarized as follows:

- A good $L/H_{\gamma(\beta)}$ of several keV/MeV and a large spread (up to a factor 10) among samples are observed (see Table 8). A large variation in the light yield was also reported in studies of ZnSe scintillation at low temperatures with a bolometric photodetector [262].

- Light and heat signals exhibit correlation [347,565,570,573] (in contrast to other efficient scintillation materials showing anti-correlation). Taking into account that this feature (and anti-correlation as well) deteriorates the energy resolution of a bolometer, a simultaneous detection of heat and scintillation signals is thus needed to improve the energy resolution of ZnSe-based scintillating bolometers [347,565,570,573].
- A scintillation signal induced by an α particle is few times higher than the one of $\gamma(\beta)$'s of the same energy. Therefore, the QF_α parameter is larger than 1, and amounts to $\sim$3–5 (see Table 8), in contrast to other scintillation materials tested with a scintillating bolometer approach.
- The QF_α dependence on an α source position (e.g., about 20% difference for a source irradiating different crystal sides) is reported [347]. A small difference (around 12%) in the QF_α is found between surface and bulk α events [565,573].
- The reduction of scintillation light is observed for some α events (similar to surface α events in a $CdWO_4$ scintillating bolometer, see Section 3.1.2), which are then leaking into the band of $\gamma(\beta)$ events spoiling particle identification [347,565,569,573]. Moreover, the number of events in the tail of the α population depends on the crystal surface quality (optical or rough) facing the α source [347].
- Scintillation light signals induced by α's are faster than those of $\gamma(\beta)$'s, thus a highly efficient particle identification can be done using a pulse-shape analysis of signals acquired by a bolometric LD [312,347,565,568,569,571,573,574]. The particle-dependent difference in the pulse-shape also affects the QF_α estimate. Indeed, if one uses the pulse area (instead of the signal maximum amplitude obtained with the optimal filtering technique) as an energy estimate, the QF_α value is reduced by a factor 1.5, but still higher than 1 [347].
- A thermal treatment of ZnSe crystals (under an argon atmosphere) improves their homogeneity and reduces microcracks [575,576]. However, the pulse-shape, the signal amplitude, and the light yield of scintillating bolometers based on the annealed ZnSe crystals are found to be deteriorated [575]. It is interesting to note that the QF_α parameter is found to be less than 1 [575]. These observations suggest changes of the annealed crystal defect structure (affecting the bolometric performance of the material) and reductions of the luminescence centers or changes their nature (affecting the light yield and the kinetics of luminescence) [575]. A subsequent characterization shows that the donor-acceptor pairs consisting of Zn vacancies and Al donors, present in as-grown material with concentrations of the order of ppm and responsible for the good scintillation properties, are lost during the ZnSe thermal treatment [576]. Therefore, more studies are needed (and some are proposed in [576]) to understand the influence of the defects present in ZnSe aiming at the optimization of ZnSe-based scintillating bolometers.

Despite the complexity of the ZnSe growth process (which affects the crystal quality and radiopurity) and the features of ZnSe scintillating bolometers (which affect the detector performance), the results of the LUCIFER project and the CUPID-0 experiment proof good prospects of this material for high-sensitivity searches for the ^{82}Se 0νDBD. In particular, thanks to the scintillation-based rejection of α events, CUPID-0 has achieved the lowest background in the 0νDBD ROI ever reported for a bolometric experiment [571] and has set the most stringent limit on the ^{82}Se 0νDBD half-life [157,568]. It is worth noting that the ^{82}Se 2νDBD has been measured with the best precision ever reported for such process [169]. Therefore, ZnSe scintillators remain promising for a large-scale bolometric DBD search experiment, particularly exploiting a multi-target array of scintillating bolometers [419].

Table 8. Results of low-temperature scintillation detection with scintillating bolometers based on natural/^{82}Se-enriched ZnSe crystals and thin Ge LDs. The crystal growth method, the mass (two significant digits) and the size of the sample, the size and the coating of the coupled LD, as well as the $L/H_{\gamma(\beta)}$ and QF_{α} values are listed.

Material	Cryogenic Scintillator Mass (g)	Cryogenic Scintillator Size (mm)	Ge LD Size (mm)	Ge LD Coating	$L/H_{\gamma(\beta)}$ (keV/MeV)	QF_{α}	Ref.
ZnSe (BS)	38	⌀20 × 21	⌀66 × 1	SiO_2	1.3	4.4	[347]
	120	⌀41 × 17	⌀36 × 1	SiO_2	7.5	4.2	ibid.
	340	⌀40 × 50	⌀66 × 1	SiO_2	4.6	3.0	ibid.
	430	⌀44 × 49	⌀50 × 0.3	SiO_2	6.4	4.6	[565,573]
	430 [a]	⌀44 × 49	⌀50 × 0.3	SiO_2	3.2	0.69	[575]
	460	⌀45 × 55	⌀50 × 0.3	SiO_2	∼2.6	3.4	[566]
	460	⌀45 × 55	⌀50 × 0.3	SiO_2	∼2.6	2.6	ibid.
	460	⌀45 × 55	⌀50 × 0.3	SiO_2	6.1	3.0	ibid.
	490 [b] (×12)	⌀48 × 52	⌀50 × 0.3	SiO_2	4.4 [a]	n/a	[567]
	(110–560)				(0.7–6.3)	n/a	ibid.
$Zn^{82}Se$ (BS)	440 (×3)	⌀44 × 55	⌀44 × 0.2	SiO	3.3–5.2	2.7	[312]
	430 (×24)	⌀44 × 54	⌀44 × 0.2	SiO	n/a	n/a	[75]
	(0.17–0.48)				n/a	n/a	ibid.

[a] The same sample used in [565,573], but after the thermal treatment. [b] A median value of 12 ZnSe scintillating bolometers including four crystals studied in [565,566].

3.6. *Alkali Metal Fluorides*

3.6.1. Calcium Fluoride

Calcium fluoride (CaF_2), particularly Eu-doped, is a well-known scintillation material [374,375] with a long history of applications to the searches for DBD of calcium isotopes (see, e.g., [577–583] and references therein). This material is especially interesting for the search for 0νDBD of ^{48}Ca (the nuclide with the largest transition energy $Q_{\beta\beta}$), particularly with CaF_2 scintillating bolometers [287]. There is also remarkable interest in CaF_2 as a target for DM searches (in particular spin-dependent interactions with ^{19}F) [291,579,584,585]. A Eu-doped CaF_2 can also be used for the investigation of α decay of natural europium [526] (the first observation of the α decay of ^{151}Eu was done using a CaF_2 room-temperature scintillation detector [526]).

As mentioned in Section 2.4, CaF_2(Eu) crystal scintillators were used in first composite bolometers, developed in the 1990's, with a simultaneous detection of phonons (by a thermistor) and photons (with either a photodiode [287–289] or a bolometric LD [290,291]). These studies show that the Eu (paramagnetic element) doping at the level of 0.01% to 0.07% does not affect the bolometric performance of a CaF_2(Eu) thermal detector [287] and that a 0.03% doping concentration maximizes the scintillation yield [289]. The operation of gram-scale CaF_2(Eu) scintillating bolometers (based on 2 g [287–289] and 0.3 g [290,291]) crystals) demonstrates the discrimination of α particles thanks to the heat-scintillation dual readout. The QF_{α} of 0.14(1) for ∼5–6-MeV α's was reported in [291]. A similar value of the quenching (0.18) was obtained in bolometric measurements of the scintillation emitted by a 20 g CaF_2(Eu) crystal under α and γ irradiation [267]; the $L/H_{\gamma(\beta)}$ value was measured to be ∼14 keV/MeV. In spite of such good scintillation properties at low temperatures, no R&D on CaF_2 scintillating bolometers have been realized until recently. It can be explained by the fact that more appealing materials (e.g., $CaWO_4$) were investigated and used for DM search applications. The very low isotopic abundance of ^{48}Ca (0.2% [456]) combined with the not-yet-possible industrial enrichment in this isotope [35] is a limiting factor for CaF_2-based DBD search experiments.

The interest in developments of pure / Eu-doped CaF_2 scintillating bolometers has been renewed recently [586–588], in particular within the CANDLES project [217]. Two scintillating bolometers based on CaF_2 and CaF_2(0.17% Eu) crystals (312 g, ⌀50 × 50 mm each) and 2 in. Ge wafers, both with MMC phonon readout as in the AMoRE experiment, have demonstrated an efficient particle identification [586,587]. A significantly higher $\alpha/\gamma(\beta)$ separation has been achieved for the Eu-doped detector [587], thanks to the enhanced light output of the doped sample. A QF_{α} = 0.17 is found for ∼5-MeV α events, in agreement with early investigations. The R&D is ongoing to improve both the energy resolution of CaF_2(Eu)-based LTDs (possibly affected by the spin-lattice interaction of paramagnetic Eu ions) and to understand the large distribution of the α-induced scintillation measured with the undoped CaF_2 scintillating bolometer [587,588].

3.6.2. Lithium Fluoride

Lithium fluoride (LiF) is among the pioneering materials investigated extensively as thermal detectors for DM searches (e.g., see [589–591]) and remains attractive for such applications [531]. Indeed, the content of only light nuclei in LiF provides sensitivity to low-mass WIMP. ^{7}Li and ^{19}F are viable targets for the investigation of spin-dependent interactions. Moreover, a large content in ^{7}Li makes LiF suitable for the searches for resonant absorption of solar axions [502,503]. Furthermore, the presence of ^{6}Li in a Li-containing bolometer can be exploited for neutron spectroscopy, as demonstrated for the first time with LiF LTDs [589,591].

A first operation of a LiF-based scintillating bolometer (16 g crystal coupled to ⌀25-mm Ge LD) was realized about 15 year ago [267,554] and this study reports a low scintillation of the material ($L/H_{\gamma(\beta)}$ = 0.38 keV/MeV). The scintillation light for α particles and nuclear recoils was found to be quenched to 29% and 15%, respectively. Events induced by the thermal and fast neutron captures by ^{6}Li were clearly separated form $\gamma/\beta/\mu$ events, but not from α's (despite of ∼20% more light detected for α+t events of the same energy release as α's). Similar results were achieved with a twice massive LiF scintillating bolometer operated aboveground [592] and underground [545]. Since such low light yield did not provide particle discrimination at low thresholds, this material was considered only for neutron detection in further studies with natural and ^{6}Li-enriched LiF scintillating bolometers [59,60,254,255,257,258,371]. In particular, a scintillating bolometer prototype based on a 32 g ^{6}LiF crystal (⌀25 × 25 mm, 95% enrichment in ^{6}Li) has been operated successfully [59,371]. The measured $L/H_{\gamma(\beta)}$ is twice lower (0.21 keV/MeV [371]) than that of the 16 g LiF detector reported in [267], but α particle identification above 2 MeV was clearly demonstrated with the ^{6}LiF scintillating bolometer.

3.6.3. Strontium Fluoride

Strontium fluoride (SrF_2) can potentially be used in searches for DBD of Sr isotopes and DM particles [371]. A 54 g SrF_2 scintillation crystal (⌀25 × 25 mm) and a Ge wafer with the same diameter were coupled together in a scintillating bolometer module tested aboveground [371,593]. An excellent $\alpha/\gamma(\beta)$ separation has been achieved, in particular thanks to a good scintillation ($L/H_{\gamma(\beta)}$ = 2.9 keV/MeV) and quenching to 26% and 10% for α particles and nuclear recoils, respectively [371]. The crystal was found to be contaminated by ^{226}Ra (0.5 Bq/kg), ^{210}Po (0.07 Bq/kg) and ^{228}Th (0.02 Bq/kg) [371]; it was used to study the light output in fast subsequent α decays. In particular, a positive correlation between the light yield of ^{224}Ra and ^{220}Rn α emitters indicates a light output position dependence in SrF_2 [371,593]. It is also worth noting the particle identification capability of SrF_2 by using either heat or scintillation signals [593].

3.7. Alkali Metal Iodides

3.7.1. Cesium Iodide

Cesium iodide (CsI) is among the oldest discovered and widely used inorganic scintillators [374,375]. This material, doped with Tl to enhance light output, is actively used in scintillation detectors for DM searches [594–603]. Undoped CsI is very attractive for bolometric searches for DM signals [415,604,605], particularly for the detection of the annual modulation of the DM rate [606]. Indeed, a low light yield of CsI at room temperature (a factor ∼20 lower than the light yield of Tl-doped cesium and sodium iodides [607]) can be about an order of magnitude higher at 3.4–10 K [264,608]. At the same time, a weak hygroscopicity and a low hardness of CsI has to be taken into account for bolometric operation. Moreover, a low Debye temperature of the material and thus a high specific heat expected at low temperatures is the main issue which would affect the bolometric performance (in particular, it would result in a low signal amplitude affecting the detector energy resolution and threshold).

A large scintillation signal together with an efficient particle identification of a CsI scintillating bolometer, made of a small cubic crystal (10 × 10 × 10 mm) and a Ge LD (⌀35 × 0.3 mm), has been reported about a decade ago [470]. More detailed study of the material as scintillating LTD has been then realized using the CRESST detection technology [415]. The $L/H_{\gamma(\beta)}$ of a small (20 × 10 × 5 mm) and a CRESST-size (⌀40 × 40 mm) CsI crystals measured with SOS LDs (⌀40 × 0.4 mm each) was found to be enormous: 71 and 49 keV/MeV, respectively. On the contrary, a small phonon signal, measured by a TES on a small sapphire carrier glued onto the large CsI, was the reason of an order of magnitude worse energy resolution than that of the same-size $CaWO_4$ bolometer. The large difference in the light yield might be explained by the difference in the samples' shape and size (i.e., difference in the internal trapping of scintillation light).

These observations were also confirmed by further low-temperature tests of two CsI crystals of the same size (30 × 30 × 30 mm, 122 g), but from different producers [604]. The phonon readout was done using a small $CdWO_4$-based carrier with a W TES evaporated on it. The scintillation was detected with the help of a SOS LD (⌀40 × 0.46 mm) with the same TES-based readout. The $L/H_{\gamma(\beta)}$ of the detector modules was measured as 81 and 65 keV/MeV. It was also observed that the light yield of both CsI crystals at 10 keV is around 10% higher than at 120 keV. The results of the detection of nuclear recoils (from an α source) in the DM search ROI were found to be unclear, requiring a dedicated study with a neutron source, while no α region is shown in [604]. Concerning particle identification, we can quote $QF_\alpha \sim 0.5$, which was measured at 3.4–10 K with an undoped CsI crystal viewed by two photomultipliers and using an optical cryostat with an experimental space encapsulated in a glove box [608].

3.7.2. Sodium Iodide

Sodium iodide, doped with Tl to improve light output, is a "standard" in the world of inorganic scintillators and the most extensively used material in scintillation detectors [374,375]. Both pure and Tl-doped NaI exhibit a huge light yield at low temperatures (at ∼2 K), which amounts to about 65% of the light output of NaI(Tl) at room temperature [263]. Therefore, a NaI-based LTD with particle identification is of a great interest for DM search experiments [585,605,606,609], in particular aiming at the investigation of the nature of the galactic DM signature detected in the DAMA/LIBRA and DAMA/NaI experiments with room-temperature NaI(Tl) scintillation detectors (e.g., see [424–427] and references therein). However, in addition to a low Debye temperature (as in the case of CsI, Section 3.7.1), a high hygroscopicity of NaI is a challenge for bolometric applications of this material.

In order to mitigate the hygroscopicity issue and therefore to simplify the mounting and operation of a NaI-based LTD, a vapor-deposited parylene (poly-p-xylylene) coating of NaI(Tl) and NaI crystals has been demonstrated to be a viable solution [610].

The development of another technology of NaI scintillating bolometers is now ongoing withing the COSINUS project [241,611]. The first prototype [612] was fabricated using a 66 g undoped NaI (30 × 30 × 20 mm) attached to a $CdWO_4$-based carrier (⌀39 × 1.6 mm), equipped with a TES W sensor. The LD was made of a SOS wafer (⌀40 × 0.5 mm) with a W TES deposited on it. A reflective film without scintillating properties (LuMirror™) was placed around the NaI crystal. The detector module was housed in an air-tight copper container, which was then evacuated using a dedicated cryogenic valve opening during the cool-down. The $L/H_{\gamma(\beta)}$ of this prototype was measured to be 37 keV/MeV [612], close to the final COSINUS design goal of 40 keV/MeV [611].

The second prototype [294] was made of the same-size undoped NaI, while a Si beaker (⌀40 × 38 mm, the wall thickness is about 0.6 mm), foreseen for the final detector design, was used as LD and active shield. Thanks to significantly improved light collection provided by such a photodetector (see also Section 3.1.1), a huge $L/H_{\gamma(\beta)}$ of 131 keV/MeV, never reported for scintillating bolometers, has been measured [294,295].

4. Conclusions

Active developments of scintillating bolometers have been ongoing over the past three decades aiming at the implementation of low-temperature particle detectors for rare-event searches (as rare alpha and beta decays, double-beta decay, dark matter, neutrino detection) and/or for a background control in these experiments (e.g., neutron detection). An important feature of such devices is the detection of the scintillation light emitted by a cryogenic scintillator that allows an event-by-event particle identification, a crucial tool for background rejection. In most cases, the scintillation of low-temperature devices is detected using an auxiliary (thin) bolometer.

This review reports on scintillation of low-temperature detectors based on different scintillation materials (used as particle energy absorbers). Among them we find tungstates ($CaWO_4$, $CdWO_4$, Li_2WO_4, $Na_2W_2O_7$, $PbWO_4$, $ZnWO_4$), molybdates ($CaMoO_4$, $CdMoO_4$, Li_2MoO_4, $Li_2Mg_2(MoO_4)_3$, $Li_2Zn_2(MoO_4)_3$, $MgMoO_4$, $Na_2Mo_2O_7$, $PbMoO_4$, $SrMoO_4$, $ZnMoO_4$), borates ($Li_6Eu(BO_3)_3$, $Li_6Gd(BO_3)_3$), and some other oxide scintillators (Al_2O_3, $Bi_4Ge_3O_{12}$, $LiAlO_2$, TeO_2, YVO_4, ZrO_2) together with selenides ($LiInSe_2$, ZnSe) and alkali halides (CaF_2, LiF, SrF_2, CsI, NaI). Some of the considered scintillators have been also produced from starting materials enriched or depleted in isotopes of interest for rare-event searches.

A particular interest of this review is devoted to the measurements of particle-dependent scintillation of materials, represented by the fraction of the energy detected by a photodetector to the energy measured as a heat of a cryogenic scintillator (light-to-heat ratio). The amount of scintillation light measured by a photodetector plays an important role for particle identification capability of a scintillating bolometer and defines the performance requirements of the light detector. Taking into account that most of the scintillating bolometer tests follow "universal" detector design (i.e., a scintillator inside a reflective cavity is viewed by a bolometric photodetector), the scintillation efficiency of the material largely contributes to the observed difference in the light-to-heat values, $\sim$0.1–100 keV/MeV, of the investigated compounds. At the same time, an optimization of the light output and light collection efficiency can also be a viable way to enhance the scintillation signal measured by the light detector.

Thanks to the extensive R&D on scintillating bolometers realized over the last 30 years, some of the reported materials have already been used in frontier searches for rare-event processes. Moreover, new experiments, in particular with a tonne-scale array of scintillating bolometers, are under development. Furthermore, known scintillation materials of advanced quality and new ones are still appealing for a wide field of applications of cryogenic scintillators, as well as for a possible improvement and/or extension of the physics goals achievable with the presently developed scintillating bolometers. Therefore, investigations of low-temperature detectors based on new or advanced scintillation materials are greatly encouraged.

Funding: This research received no external funding.

Institutional Review Board Statement: Not applicable.

Informed Consent Statement: Not applicable.

Data Availability Statement: No new data were created or analyzed in this study. Data sharing is not applicable to this article.

Acknowledgments: The author is grateful to Andrea Giuliani, Pierre de Marcillac and anonymous Reviewers for their careful reading of this manuscript and their many insightful comments and suggestions.

Conflicts of Interest: The author declares no conflict of interest.

Abbreviations

The following abbreviations are used in this manuscript:

0νDBD	neutrinoless double-beta decay
2νDBD	two-neutrino double-beta decay
BGO	$Bi_4Ge_3O_{12}$
BS	Bridgman–Stockbarger
CENNS	coherent elastic neutrino-nucleus scattering
Cz	Czochralski
DBD	double-beta decay
DM	dark matter
DP	discrimination power
KID	kinetic inductance detector
Ky	Kyropoulos
LD	light detector
L/H	light-to-heat
LNGS	Laboratori Nazionali del Gran Sasso
LSC	Laboratorio Subterráneo de Canfranc
LSM	Laboratoire Souterrain de Modane
LTD	low-temperature detector
LTG Cz	low-temperature-gradient Czochralski
MMC	metallic magnetic calorimeter
n/a	not available
NTD	neutron-transmutation-doped
NTL	Neganov-Trofimov-Luke
QET	quasiparticle-trap-assisted electrothermal feedback transition-edge sensor
QF	quenching factor
R&D	research and development
RMS	root mean square
ROI	region-of-interest
SM	Standard Model
SOS	silicon-on-sapphire
TES	transition-edge sensor
Ve	Verneuil
Y2L	Yangyang laboratory
WIMP	weakly interactive massive particles

References

1. Fiorini, E.; Niinikoski, T. Low-temperature calorimeters for rare decays. *Nucl. Instrum. Methods Phys. Res. A* **1984**, *224*, 83. [CrossRef]
2. Moseley, S.H.; Mather, J.C.; McCammon, D. Thermal detectors as x-ray spectrometers. *J. Appl. Phys.* **1984**, *56*, 1257. [CrossRef]
3. Gonzalez-Mestres, L.; Perret-Gallix, D. Detection of low energy solar neutrinos and galactic dark matter with crystal scintillators. *Nucl. Instrum. Methods Phys. Res. A* **1989**, *279*, 382–387. [CrossRef]
4. Alessandrello, A.; Camin, D.V.; Fiorini, E.; Giuliani, A.; Buraschi, M.; Pignatel, G. Bolometric detection of particles. *Nucl. Instrum. Methods Phys. Res. A* **1989**, *279*, 142–147. [CrossRef]
5. Stodolsky, L. Neutrino and dark-matter detection at low temperature. *Phys. Today* **1991**, *44*, 24–32. [CrossRef]
6. Giuliani, A.; Sanguinetti, S. Phonon-mediated particle detectors: Physics and materials. *Mat. Sci. Eng. R* **1993**, *11*, 1–52. [CrossRef]
7. Young, B.A. Phonon-mediated particle detection: An overview. *Nucl. Phys. B (Proc. Suppl.)* **1993**, *32*, 127–137. [CrossRef]
8. Richards, P.L. Bolometers for infrared and millimeter waves. *J. Appl. Phys.* **1994**, *76*, 1. [CrossRef]
9. Twerenbold, D. Cryogenic particle detectors. *Rep. Prog. Phys.* **1996**, *59*, 349–426. [CrossRef]
10. Booth, B.; Cabrera, N.; Fiorini, E. Low-temperature particle detectors. *Annu. Rev. Nucl. Part. Sci.* **1996**, *46*, 471–532. [CrossRef]
11. Booth, N.E.; Goldie, D.J. Superconducting particle detectors. *Supercond. Sci. Technol.* **1996**, *9*, 493–516. [CrossRef]
12. Kraus, H. Superconductive bolometers and calorimeters. *Supercond. Sci. Technol.* **1996**, *9*, 827–842. [CrossRef]
13. Alessandrello, A.; Brofferio, C.; Camin, D.V.; Cremonesi, O.; Fiorini, E.; Giuliani, A.; Nucciotti, A.; Pavan, M.; Pessina, G.; Previtali, E.; et al. Low temperature thermal detectors in searches for rare events. *Czech. J. Phys.* **1998**, *48*, 133. [CrossRef]
14. Giuliani, A. Particle and radiation detection with low-temperature devices. *Physica B* **2000**, *280*, 501–508. [CrossRef]
15. Pretzl, K. Cryogenic calorimeters in astro and particle physics. *Nucl. Instrum. Methods Phys. Res. A* **2000**, *454*, 114–127. [CrossRef]
16. McCammon, D. Physics of low-temperature microcalorimeters. *Nucl. Instrum. Methods Phys. Res. A* **2004**, *520*, 11–15. [CrossRef]

17. Enss, C. (Ed.) *Cryogenic Particle Detection*; Springer: Berlin/Heidelberg, Germany, 2005.
18. Eitel, K. Direct Dark Matter search with heat-and-ionization detectors. *Prog. Part. Nucl. Phys.* **2006**, *57*, 366–374. [CrossRef]
19. Enss, C.; McCammon, D. Physical principles of low temperature detectors: Ultimate performance limits and current detector capabilities. *J. Low Temp. Phys.* **2008**, *151*, 5–24. [CrossRef]
20. Giuliani, A. Neutrino Physics with Low-Temperature Detectors. *J. Low Temp. Phys.* **2012**, *167*, 991–1003. [CrossRef]
21. Ullom, J.N.; Bennett, D.A. Review of superconducting transition-edge sensors for x-ray and gamma-ray spectroscopy. *Supercond. Sci. Technol.* **2015**, *28*, 084003. [CrossRef]
22. Nucciotti, A. The use of low temperature detectors for direct measurements of the mass of the electron neutrino. *Adv. High Energy Phys.* **2016**, *2016*, 9153024. [CrossRef]
23. Pirro, S.; Mauskopf, P. Advances in bolometer technology for fundamental physics. *Annu. Rev. Nucl. Part. Sci.* **2017**, *67*, 161. [CrossRef]
24. Poda, D.; Giuliani, A. Low background techniques in bolometers for double-beta decay search. *Int. J. Mod. Phys. A* **2017**, *32*, 1743012. [CrossRef]
25. Bellini, F. Potentialities of the future technical improvements in the search of rare nuclear decays by bolometers. *Int. J. Mod. Phys. A* **2018**, *33*, 1843003. [CrossRef]
26. Biassoni, M.; Cremonesi, O. Search for neutrino-less double beta decay with thermal detectors. *Progr. Part. Nucl. Phys.* **2020**, *114*, 103803. [CrossRef]
27. Beretta, M.; Pagnanini, L. Development of cryogenic detectors for neutrinoless double beta decay searches with CUORE and CUPID. *Appl. Sci.* **2021**, *11*, 1606. [CrossRef]
28. Kittel, C. (Ed.) *Introduction to Solid State Physics [Global Edition]*; John Wiley & Sons: Hoboken, NJ, USA, 2018.
29. Belli, P.; Bernabei, R.; Danevich, F.A.; Incicchitti, A.; Tretyak, V.I. Experimental searches for rare alpha and beta decays. *Eur. Phys. J. A* **2019**, *55*, 140. [CrossRef]
30. Haaranen, M.; Srivastava, P.C.; Suhonen, J. Forbidden nonunique β decays and effective values of weak coupling constants. *Phys. Rev. C* **2016**, *93*, 034308. [CrossRef]
31. Suhonen, J.T. Value of the axial-vector coupling strength in β and $\beta\beta$ decays: A review. *Front. Phys.* **2017**, *5*, 55. [CrossRef]
32. Kostensalo, J.; Suhonen, J. Beta-spectrum shapes of forbidden β decays. *Int. J. Mod. Phys. A* **2018**, *33*, 1843008. [CrossRef]
33. Tretyak, V.I.; Zdesenko, Y.G. Tables of double beta decay data. *At. Data Nucl. Data Tables* **1995**, *61*, 43–90. [CrossRef]
34. Tretyak, V.I.; Zdesenko, Y.G. Tables of double beta decay data—An update. *At. Data Nucl. Data Tables* **2002**, *80*, 83–116. [CrossRef]
35. Giuliani, A.; Poves, A. Neutrinoless double-beta decay. *Adv. High Energy Phys.* **2012**, *2012*, 857016. [CrossRef]
36. Dolinski, M.J.; Poon, A.W.P.; Rodejohann, W. Neutrinoless double-beta decay: Status and prospects. *Annu. Rev. Nucl. Part. Sci.* **2019**, *69*, 219–251. [CrossRef]
37. Barabash, A.S. Precise half-life values for two-neutrino double-β decay: 2020 Review. *Universe* **2020**, *6*, 159. [CrossRef]
38. Ellis, J.; Flores, R.A. Elastic supersymmetric relic-nucleus scattering revisited. *Phys. Lett. B* **1991**, *263*, 259–266. [CrossRef]
39. Bednyakov, V.A.; Šimkovic, F. Nuclear spin structure in dark matter search: The finite momentum transfer Limit. *Phys. Part. Nuclei* **2005**, *37*, S106–S128. [CrossRef]
40. Matarrese, S.; Colpi, M.; Gorini, V.; Moschella, U. (Eds.) *Dark Matter and Dark Energy: A Challenge for Modern Cosmology*; Springer: Cham, Switzerland, 2011.
41. Roszkowski, L.; Sessolo, E.M.; Trojanowski, S. WIMP dark matter candidates and searches—Current status and future prospects. *Rep. Prog. Phys.* **2018**, *81*, 066201. [CrossRef]
42. Moriyama, S. Proposal to search for a monochromatic component of solar axions using ^{57}Fe. *Phys. Rev. Lett.* **1995**, *75*, 3222. [CrossRef]
43. Krčmar, M.; Krečak, Z.; Ljubičič, A.; Stipčević, M.; Bradley, D.A. Search for solar axions using ^{7}Li. *Phys. Rev. D* **2001**, *64*, 115016. [CrossRef]
44. Jakovčić, K.; Krečak, Z.; Krčmar, M.; Ljubičič, A. Search for solar hadronic axions using ^{83}Kr. *Radiat. Phys. Chem.* **2004**, *71*, 793–794. [CrossRef]
45. Derbin, A.V.; Bakhlanov, S.B.; Egorov, A.I.; Mitropolsky, I.A.; Muratova, V.N.; Semenov, D.A.; Unzhakov, E.V. Search for solar axions generated by the Primakoff effect with resonance absorption by ^{169}Tm. *Bull. Russ. Acad. Sci. Phys.* **2010**, *74*, 481–486. [CrossRef]
46. Abdelhameed, A.H.; Bakhlanov, S.V.; Bauer, P.; Bento, A.; Bertoldo, E.; Canonica, L.; Derbin, A.V.; Drachnev, I.S.; Iachellini, N.F.; Fuchs, D.; et al. New limits on the resonant absorption of solar axions obtained with a ^{169}Tm-containing cryogenic detector. *Eur. Phys. J. C* **2020**, *80*, 376. [CrossRef]
47. Ejiri, H.; Engel, J.; Hazama, R.; Krastev, P.; Kudomi, N.; Robertson, R.G.H. Spectroscopy of double-beta and inverse-beta decays from ^{100}Mo for neutrinos. *Phys. Rev. Lett.* **2000**, *85*, 2917. [CrossRef]
48. Ejiri, H.; Engel, J.; Kudomi, N. Supernova-neutrino studies with ^{100}Mo. *Phys. Lett. B* **2002**, *530*, 27–32. [CrossRef]
49. Zuber, K. Spectroscopy of low energy solar neutrinos using CdTe detectors. *Phys. Lett. B* **2003**, *571*, 148–154. [CrossRef]
50. Ejiri, H.; Elliott, S.R. Solar neutrino interactions with the double-β decay nuclei ^{82}Se, ^{100}Mo, and ^{150}Nd. *Phys. Rev. C* **2017**, *95*, 055501. [CrossRef]
51. Billard, J.; Figueroa-Feliciano, E.; Strigari, L. Implication of neutrino backgrounds on the reach of next generation dark matter direct detection experiments. *Phys. Rev. D* **2014**, *89*, 023524. [CrossRef]

52. Gütlein, A.; Angloher, G.; Bento, A.; Bucci, C.; Canonica, L.; Erb, A.; Feilitzsch, F.V.; Iachellini, N.F.; Gorla, P.; Hauff, D.; et al. Impact of coherent neutrino nucleus scattering on direct dark matter searches based on $CaWO_4$ crystals. *Astropart. Phys.* **2015**, *69*, 44–49. [CrossRef]
53. Billard, J.; Johnston, J.; Kavanagh, B.J. Prospects for exploring new physics in coherent elastic neutrino-nucleus scattering. *J. Cosmol. Astropart. Phys.* **2018**, *11*, 016. [CrossRef]
54. Akimov, D.Y.; Belov, V.A.; Bolozdynya, A.I.; Efremenko, Y.V.; Konovalov, A.M.; Kumpan, A.V.; Rudik, D.G.E.; Sosnovtsev, V.V.E.; Khromov, A.V.; Shakirov, A.V.; et al. Coherent elastic neutrino scattering on atomic nucleus: Recently discovered type of low-energy neutrino interaction. *Phys. Usp.* **2019**, *62*, 166–178. [CrossRef]
55. Angloher, G.; Ardellier-Desages, F.; Bento, A.; Canonica, L.; Erhart, A.; Ferreiro, N.; Friedl, M.; Ghete, V.M.; Hauff, D.; Kluck, H.; et al. Exploring CEνNS with NUCLEUS at the Chooz Nuclear Power Plant. *Eur. Phys. J. C* **2019**, *79*, 1018. [CrossRef]
56. Galindo-Uribarri, A.; Miranda, O.G.; Sanchez Garcia, G. A novel approach for the study of CEvNS. *arXiv* **2020**, arXiv:hep-ph/2011.10230.
57. Eijk, C.W.E. Inorganic scintillators for thermal neutron detection. *Radiat. Meas.* **2004**, *38*, 337–342. [CrossRef]
58. Bell, Z.W.; Carpenter, D.A.; Cristy, S.S.; Lamberti, V.E.; Burger, A.; Woodfield, B.F.; Niedermayr, T.; Dragos Hau, I.; Labov, S.E.; Friedrich, S.; et al. Neutron detection with cryogenics and semiconductors. *Phys. Status Solidi C* **2005**, *2*, 1592–1605. [CrossRef]
59. Martínez, M.; Coron, N.; Ginestra, C.; Gironnet, J.; Gressier, V.; Leblanc, J.; de Marcillac, P.; Redon, T.; Di Stefano, P.; Torres, L.; et al. Scintillating bolometers for fast neutron spectroscopy in rare events searches. *J. Phys. Conf. Ser.* **2012**, *375*, 012025. [CrossRef]
60. Coron, N.; Cuesta, C.; García, E.; Ginestra, C.; Gironnet, J.; de Marcillac, P.; Martínez, M.; Ortigoza, Y.; de Solórzano, A.O.; Puimedón, J.; et al. Neutron spectrometry with scintillating bolometers of LiF and sapphire. *IEEE Trans. Nucl. Sci.* **2016**, *63*, 1967–1975. [CrossRef]
61. Pietropaolo, A.; Angelone, M.; Bedogni, R.; Colonna, N.; Hurd, A.J.; Khaplanov, A.; Murtas, F.; Pillon, M.; Piscitelli, F.; Schooneveld, E.M.; et al. Neutron detection techniques from μeV to GeV. *Phys. Rep.* **2020**, *875*, 1–65. [CrossRef]
62. White, G.K.; Meeson, J. *Experimental Techniques in Low-Temperature Physics*; Oxford University Press: Oxford, UK, 2002.
63. Enss, C.; Hunklinger, S. *Low-Temperature Physics*; Springer: Berlin/Heidelberg, Germany, 2005.
64. Ekin, J.W. *Experimental Techniques for Low-Temperature Measurements: Cryostat Design, Material Properties and Superconductor Critical-Current Testing*; Oxford University Press: Oxford, UK, 2006.
65. Pobell, F. *Matter and Methods at Low Temperatures*; Springer: Berlin/Heidelberg, Germany, 2007.
66. Ventura, G.; Risegari, L. *The Art of Cryogenics*; Elsevier: Amsterdam, The Netherlands, 2010.
67. Zhao, Z.; Wang, C. (Eds.) *Cryogenic Engineering and Technologies: Principles and Applications of Cryogen-Free Systems*; CRC Press: Boca Raton, FL, USA, 2019.
68. Armengaud, E.; Arnaud, Q.; Augier, C.; Benoît, A.; Bergé, L.; Bergmann, T.; Billard, J.; De Boissière, T.; Bres, G.; Broniatowski, A. Performance of the EDELWEISS-III experiment for direct dark matter searches. *J. Instrum.* **2017**, *12*, P08010. [CrossRef]
69. Armatol, A.; Armengaud, E.; Armstrong, W.; Augier, C.; Avignone, F.T., III; Azzolini, O.; Bandac, I.C.; Barabash, A.S.; Bari, G.; et al. A CUPID $Li_2{}^{100}MoO_4$ scintillating bolometer tested in the CROSS underground facility. *J. Instrum.* **2021**, *16*, P02037. [CrossRef]
70. Gorla, P.; Bucci, C.; Pirro, S. Complete elimination of 1K Pot vibrations in dilution refrigerators. *Nucl. Instrum. Methods Phys. Res. A* **2004**, *520*, 641–643. [CrossRef]
71. Pirro, S. Further developments in mechanical decoupling of large thermal detectors. *Nucl. Instrum. Methods Phys. Res. A* **2006**, *559*, 672. [CrossRef]
72. Olivieri, E.; Billard, J.; De Jesus, M.; Juillard, A.; Leder, A. Vibrations on pulse tube based dry dilution refrigerators for low noise measurements. *Nucl. Instrum. Methods Phys. Res. A* **2017**, *858*, 73. [CrossRef]
73. Lee, C.; Jo, H.S.; Kang, C.S.; Kim, G.B.; Kim, I.; Kim, S.R.; Kim, Y.H.; Lee, H.J.; So, J.H.; Yoon, Y.S. Vibration isolation system for cryogenic phonon-scintillation calorimeters. *J. Instrum.* **2017**, *12*, C02057. [CrossRef]
74. Armengaud, E.; Augier, C.; Barabash, A.S.; Beeman, J.W.; Bekker, T.B.; Bellini, F.; Benoît, A.; Bergé, L.; Bergmann, T.; Billard, J.; et al. Development of ^{100}Mo-containing scintillating bolometers for a high-sensitivity neutrinoless double-beta decay search. *Eur. Phys. J. C* **2017**, *77*, 785. [CrossRef]
75. Azzolini, O.; Barrera, M.T.; Beeman, J.W.; Bellini, F.; Beretta, M.; Biassoni, M.; Brofferio, C.; Bucci, C.; Canonica, L.; Capelli, S.; et al. CUPID-0: The first array of enriched scintillating bolometers for $0\nu\beta\beta$ decay investigations. *Eur. Phys. J. C* **2018**, *78*, 428. [CrossRef]
76. D'Addabbo, A.; Bucci, C.; Canonica, L.; Di Domizio, S.; Gorla, P.; Marini, L.; Nucciotti, A.; Nutini, I.; Rusconi, C.; Welliver, B. An active noise cancellation technique for the CUORE pulse tube cryocoolers. *Cryogenics* **2018**, *93*, 56–65. [CrossRef]
77. Alduino, C.; Alessandria, F.; Balata, M.; Biare, D.; Biassoni, M.; Bucci, C.; Caminata, A.; Canonica, L.; Cappelli, L.; Ceruti, G.; et al. The CUORE cryostat: An infrastructure for rare event searches at millikelvin temperatures. *Cryogenics* **2019**, *102*, 9–21. [CrossRef]
78. Alduino, C.; Alessandria, F.; Alfonso, K.; Andreotti, E.; Arnaboldi, C.; Avignone, F.T., III; Azzolini, O.; Balata, M.; Bandac, I.; Banks, T.I.; et al. First results from CUORE: A search for lepton number violation via $0\nu\beta\beta$ decay of ^{130}Te. *Phys. Rev. Lett.* **2018**, *120*, 132501. [CrossRef] [PubMed]
79. Adams, D.Q.; Alduino, C.; Alfonso, K.; Avignone, F.T., III; Azzolini, O.; Bari, G.; Bellini, F.; Benato, G.; Biassoni, M.; Branca, A.; et al. Improved limit on neutrinoless double-beta decay in ^{130}Te with CUORE. *Phys. Rev. Lett.* **2020**, *124*, 122501. [CrossRef] [PubMed]

80. Adams, D.Q.; Alduino, C.; Alfonso, K.; Avignone, F.T., III; Azzolini, O.; Bari, G.; Bellini, F.; Benato, G.; Beretta, M.; Biassoni, M.; et al. High sensitivity neutrinoless double-beta decay search with one tonne-year of CUORE data. *arXiv* **2021**, arXiv:nucl-ex/2104.06906.
81. Alenkov, V.; Aryal, P.; Beyer, J.; Boiko, R.S.; Boonin, K.; Buzanov, O.; Chanthima, N.; Chernyak, M.K.; Choi, J.; Choi, S.; et al. Technical design report for the AMoRE $0\nu\beta\beta$ decay search experiment. *arXiv* **2015**, arXiv:physics.ins-det/1512.05957.
82. Armstrong, W.R.; Chang, C.; Hafidi, K.; Lisovenko, M.; Novosad, V.; Pearson, J.; Polakovic, T.; Wang, G.; Yefremenko, V.; Zhang, J.; et al. CUPID pre-CDR. *arXiv* **2019**, arXiv:physics.ins-det/1907.09376.
83. Heusser, G. Low-radioactivity background techniques. *Annu. Rev. Nucl. Part. Sci.* **1995**, *45*, 543–590. [CrossRef]
84. Bucci, C.; Capelli, S.; Carrettoni, M.; Clemenza, M.; Cremonesi, O.; Gironi, L.; Gorla, P.; Maiano, C.; Nucciotti, A.; Pattavina, L.; et al. Background study and Monte Carlo simulations for large-mass bolometers. *Eur. Phys. J. A* **2009**, *41*, 155–168. [CrossRef]
85. Pattavina, L. Radon-Induced Surface Contaminations in Neutrinoless Double Beta Decay and Dark Matter Experiments. Ph.D. Thesis, Institut de Physique Nucléaire de Lyon, Lyon, France, 2011.
86. Pattavina, L. Radon induced surface contaminations in low background experiments. *AIP Conf. Proc.* **2013**, *1549*, 82–85.
87. Artusa, D.R.; Avignone, F.T.; Azzolini, O.; Balata, M.; Banks, T.I.; Bari, G.; Beeman, J.; Bellini, F.; Bersani, A.; Biassoni, M.; et al. Exploring the neutrinoless double beta decay in the inverted neutrino hierarchy with bolometric detectors. *Eur. Phys. J. C* **2014**, *74*, 3096. [CrossRef]
88. Ejiri, H.; Elliott, S.R. Charged current neutrino cross section for solar neutrinos, and background to $\beta\beta(0\nu)$ experiments. *Phys. Rev. C* **2014**, *89*, 055501. [CrossRef]
89. Bernabei, R.; Belli, P.; Dai, C.J. Adopted low background techniques and analysis of radioactive trace impurities. *Int. J. Mod. Phys. A* **2016**, *31*, 1642003. [CrossRef]
90. Abgrall, N.; Arnquist, I.J.; Avignone, F.T., III; Back, H.O.; Barabash, A.S.; Bertrand, F.E.; Boswell, M.; Bradley, A.W.; Brudanin, V.; Busch, M.; et al. The MAJORANA DEMONSTRATOR radioassay program. *Nucl. Instrum. Methods Phys. Res. A* **2016**, *828*, 22–36. [CrossRef]
91. Best, A.; Görres, J.; Junker, M.; Kratz, K.L.; Laubenstein, M.; Long, A.; Nisi, S.; Smith, K.; Wiescher, M. Low energy neutron background in deep underground laboratories. *Nucl. Instrum. Methods Phys. Res. A* **2016**, *812*, 1–6. [CrossRef]
92. Zhang, C.; Mei, D.; Kudryavtsev, V.A.; Fiorucci, S. Cosmogenic activation of materials used in rare event search experiments. *Astropart. Phys.* **2016**, *84*, 62–69. [CrossRef]
93. Cebrián, S. Cosmogenic activation of materials. *Int. J. Mod. Phys. A* **2017**, *32*, 1743006. [CrossRef]
94. Westerdale, S.; Meyers, P.D. Radiogenic neutron yield calculations for low-background experiments. *Nucl. Instrum. Methods Phys. Res. A* **2017**, *875*, 57–64. [CrossRef]
95. Danevich, F.A. Radiopure tungstate and molybdate crystal scintillators for double beta decay experiments. *Int. J. Mod. Phys. A* **2017**, *32*, 1743008. [CrossRef]
96. Danevich, F.A.; Tretyak, V.I. Radioactive contamination of scintillators. *Int. J. Mod. Phys. A* **2018**, *33*, 1843007. [CrossRef]
97. Amare, J.; Castel, J.; Cebrián, S.; Coarasa, I.; Cuesta, C.; Dafni, T.; Galán, J.; García, E.; Garza, J.G.; Iguaz, F.J.; et al. Cosmogenic production of tritium in dark matter detectors. *Astropart. Phys.* **2018**, *97*, 96–105. [CrossRef]
98. Cebrián, S. Cosmogenic activation in double beta decay experiments. *Universe* **2020**, *6*, 162. [CrossRef]
99. Laubenstein, M.; Lawson, I. Low background radiation detection techniques and mitigation of radioactive backgrounds. *Front. Phys.* **2020**, *8*, 577734. [CrossRef]
100. Gironi, L. Scintillating bolometers for double beta decay search. *Nucl. Instrum. Methods Phys. Res. A* **2010**, *617*, 478–481. [CrossRef]
101. Arnaboldi, C.; Brofferio, C.; Cremonesi, O.; Gironi, L.; Pavan, M.; Pessina, G.; Pirro, S.; Previtali, E. A novel technique of particle identification with bolometric detectors. *Astropart. Phys.* **2011**, *34*, 797–804. [CrossRef]
102. Gironi, L. Development of Cryogenic Detectors for Rare Event Searches. Ph.D. Thesis, Università degli Studi di Milano, Milan, Italy, 2011.
103. Spooner, N.J.C.; Bewick, A.; Homer, G.J.; Smith, P.F.; Lewin, J.D. Demonstration of nuclear recoil discrimination for low temperature dark matter detectors, by measurement of simultaneous ionization and thermal pulses in silicon. *Phys. Lett. B* **1991**, *273*, 333–337. [CrossRef]
104. Shutt, T.; Ellman, B.; Barnes, P.D., Jr; Cummings, A.; Da Silva, A.; Emes, J.; Giraud-Héraud, Y.; Haller, E.E.; Lange, A.E.; Ross, R.R.; et al. Measurement of ionization and phonon production by nuclear recoils in a 60 g crystal of germanium at 25 mK. *Phys. Rev. Lett.* **1992**, *69*, 3425. [CrossRef]
105. Brink, P.L.; Cabrera, B.; Castle, J.P.; Cooley, J.; Novak, L.; Ogburn, R.W.; Pyle, M.; Ruderman, J.; Tomada, A.; Young, B.A.; et al. First test runs of a dark-matter detector with interleaved ionization electrodes and phonon sensors for surface-event rejection. *Nucl. Instrum. Methods Phys. Res. A* **2006**, *559*, 414–416. [CrossRef]
106. Broniatowski, A.; Defay, X.; Armengaud, E.; Bergé, L.; Benoit, A.; Besida, O.; Blümer, J.; Chantelauze, A.; Chapellier, M.; Chardin, G.; et al. A new high-background-rejection dark matter Ge cryogenic detector. *Phys. Lett. B* **2009**, *681*, 305–309. [CrossRef]
107. Agnese, R.; Anderson, A.J.; Balakishiyeva, D.; Basu Thakur, R.; Bauer, D.A.; Borgland, A.; Brandt, D.; Brink, P.L.; Bunker, R.; Cabrera, B.; et al. Demonstration of surface electron rejection with interleaved germanium detectors for dark matter searches. *Appl. Phys. Lett.* **2013**, *103*, 164105. [CrossRef]
108. Agnese, R.; Anderson, A.J.; Aramaki, T.; Arnquist, I.; Baker, W.; Barker, D.; Thakur, R.B.; Bauer, D.A.; Borgland, A.; Bowles, M.A.; et al. Projected sensitivity of the SuperCDMS SNOLAB experiment. *Phys. Rev. D* **2017**, *95*, 082002. [CrossRef]

109. Arnaud, Q.; Armengaud, E.; Augier, C.; Benoît, A.; Bergé, L.; Billard, J.; Broniatowski, A.; Camus, P.; Cazes, A.; Chapellier, M.; et al. Optimizing EDELWEISS detectors for low-mass WIMP searches. *Phys. Rev. D* **2018**, *97*, 022003. [CrossRef]
110. Hellmig, J.; Gaitskell, R.J.; Abusaidi, R.; Cabrera, B.; Clarke, R.M.; Emes, J.; Nam, S.W.; Saab, T.; Sadoulet, B.; Seitz, D.; et al. The CDMS II Z-sensitive ionization and phonon germanium detector. *Nucl. Instrum. Methods Phys. Res. A* **2000**, *444*, 308–311. [CrossRef]
111. Juillard, A.; Marnieros, S.; Dolgorouky, Y.; Bergé, L.; Collin, S.; Fiorucci, S.; Lalu, F.; Dumoulin, L. Development of Ge/NbSi detectors for EDELWEISS-II with identification of near-surface events. *Nucl. Instrum. Methods Phys. Res. A* **2006**, *559*, 393–395. [CrossRef]
112. Nones, C.; Bergé, L.; Collin, S.; Dumoulin, L.; Juillard, A.; Marnieros, S.; Olivieri, E. New TeO_2/NbSi detectors for rare event search. *J. Low Temp. Phys.* **2008**, *151*, 871–876. [CrossRef]
113. Olivieri, E.; Bergé, L.; Chapellier, M.; Collin, S.; Dolgorouky, Y.; Dumoulin, L.; Juillard, A.; Marnieros, S.; Nones, C. Modelling of the surface-event identification mechanism in Ge detectors equipped with NbSi thin films. *J. Low Temp. Phys.* **2008**, *151*, 884–890. [CrossRef]
114. Marnieros, S.; Bergé, L.; Broniatowski, A.; Chapellier, M.; Collin, S.; Crauste, O.; Defay, X.; Dolgorouky, Y.; Dumoulin, L.; Juillard, A.; et al. Surface event rejection of the EDELWEISS cryogenic Germanium detectors based on NbSi thin film sensors. *J. Low Temp. Phys.* **2008**, *151*, 835–840. [CrossRef]
115. Nones, C. Identification of surface events in massive bolometers for the search of rare events. *Nuovo Cimento B* **2010**, *125*, 417–437.
116. Schnagl, J.; Angloher, G.; Feilitzsch, F.V.; Huber, M.; Jochum, J.; Lanfranchi, J.; Sarsa, M.L.; Wänninger, S. First tests on phonon threshold spectroscopy. *Nucl. Instrum. Methods Phys. Res. A* **2000**, *444*, 245–248. [CrossRef]
117. Nones, C.; Bergé, L.; Dumoulin, L.; Marnieros, S.; Olivieri, E. Superconducting aluminum layers as pulse shape modifiers: An innovative solution to fight against surface background in neutrinoless double beta decay experiments. *J. Low Temp. Phys.* **2012**, *167*, 1029–1034. [CrossRef]
118. Bandac, I.C.; Barabash, A.S.; Bergé, L.; Brière, M.; Bourgeois, C.; Carniti, P.; Chapellier, M.; de Combarieu, M.; Dafinei, I.; Danevich, F.A.; et al. The $0\nu2\beta$-decay CROSS experiment: Preliminary results and prospects. *J. High Energy Phys.* **2020**, *1*, 018. [CrossRef]
119. Khalife, H.; Bergé, L.; Chapellier, M.; Dumoulin, L.; Giuliani, A.; Loaiza, P.; de Marcillac, P.; Marnieros, S.; Marrache-Kikuchi, C.A.; Nones, C.; et al. The CROSS experiment: Rejecting surface events by PSD induced by superconducting films. *J. Low Temp. Phys.* **2020**, *199*, 19. [CrossRef]
120. Bandac, I.C.; Barabash, A.S.; Bergé, L.; Bourgeois, C.; Calvo-Mozota, J.M.; Carniti, P.; Chapellier, M.; de Combarieu, M.; Dafinei, I.; Danevich, F.A.; et al. Phonon-mediated crystal detectors with metallic film coating capable of rejecting α and β events induced by surface radioactivity. *Appl. Phys. Lett.* **2021**, *118*, 184105. [CrossRef]
121. Sangiorgio, S.; Barucci, M.; Foggetta, L.; Giuliani, A.; Jug, G.; Nones, C.; Pasca, E.; Pedretti, M.; Pessina, G.; Risegari, L.; et al. Innovations in low-temperature calorimeters: Surface sensitive bolometers for background rejection and capacitive bolometers for higher energy resolution. *Proc. SPIE* **2004**, *5540*, 165–176.
122. Foggetta, L.; Giuliani, A.; Nones, C.; Pedretti, M.; Sangiorgio, S. Surface-sensitive macrobolometers for the identification of external charged particles. *Appl. Phys. Lett.* **2005**, *86*, 134106. [CrossRef]
123. Nones, C.; Foggetta, L.; Giuliani, A.; Pedretti, M.; Salvioni, C.; Sangiorgio, S. A new method for background rejection with surface sensitive bolometers. *Nucl. Instrum. Methods Phys. Res. A* **2006**, *559*, 355–357. [CrossRef]
124. Pedretti, M.; Cremonesi, O.; Foggetta, L.; Giachero, A.; Giuliani, A.; Gorla, P.; Nones, C.; Pavan, M.; Salvioni, C.; Sangiorgio, S. A new technique for the identification of surface background: The surface sensitive bolometers. *J. Low Temp. Phys.* **2008**, *151*, 841–847. [CrossRef]
125. Foggetta, L.; Giuliani, A.; Nones, C.; Pedretti, M.; Sangiorgio, S. Surface-sensitive macrobolometers for the identification of external charged particles. *Astropart. Phys.* **2011**, *34*, 809–821. [CrossRef]
126. Birks, J.B. Scintillations from organic Ccrystals: Specific fluorescence and relative response to different radiations. *Proc. Phys. Soc. A* **1951**, *64*, 874–877. [CrossRef]
127. Birks, J.B. *The Theory and Practice of Scintillation Counting*; Pergamon Press: Oxford, UK, 1964.
128. Tretyak, V.I. Semi-empirical calculation of quenching factors for ions in scintillators. *Astropart. Phys.* **2010**, *33*, 40. [CrossRef]
129. Geiger, H.; Nuttall, J.M. LVII. The ranges of the α particles from various radioactive substances and a relation between range and period of transformation. *Ph. Mag.* **1911**, *22*, 613–621. [CrossRef]
130. Qi, C.; Liotta, R.J.; Wyss, R. Generalization of the Geiger-Nuttall law and alpha clustering in heavy nuclei. *J. Phys. Conf. Ser.* **2012**, *381*, 012131. [CrossRef]
131. Qi, C.; Andreyev, A.N.; Huyse, M.; Liotta, R.J.; Van Duppen, P.; Wyss, R. On the Validity of the Geiger-Nuttall alpha-decay law and its microscopic basis. *Phys. Lett. B* **2014**, *734*, 203–206. [CrossRef]
132. Wang, M.; Audi, G.; Kondev, F.G.; Huang, W.J.; Naimi, S.; Xu, X. The AME2016 atomic mass evaluation * (II). Tables, graphs and references. *Chin. Phys. C* **2017**, *41*, 030003. [CrossRef]
133. de Marcillac, P.; Coron, N.; Dambier, G.; Leblanc, J.; Moalic, J.P. Experimental detection of α-particles from the radioactive decay of natural bismuth. *Nature* **2003**, *422*, 876–878. [CrossRef] [PubMed]
134. Beeman, J.W.; Biassoni, M.; Brofferio, C.; Bucci, C.; Capelli, S.; Cardani, L.; Carrettoni, M.; Clemenza, M.; Cremonesi, O.; Ferri, E.; et al. First measurement of the partial widths of ^{209}Bi decay to the ground and to the first excited states. *Phys. Rev. Lett.* **2012**, *108*, 062501.

135. Gove, N.B.; Martin, M.J. Log-f tables for beta decay. *At. Data Nucl. Data Tables* **1971**, *10*, 205–219. [CrossRef]
136. Singh, B.; Rodriguez, J.L.; Wong, S.S.M.; Tuli, J.K. Review of logft values in β decay. *Nucl. Data Sheets* **1998**, *84*, 487–563. [CrossRef]
137. Haaranen, M.; Kotila, J.; Suhonen, J. Spectrum-shape method and the next-to-leading-order terms of the β-decay shape factor. *Phys. Rev. C* **2017**, *95*, 024327. [CrossRef]
138. Suhonen, J.; Kostensalo, J. Double β decay and the axial strength. *Front. Phys.* **2019**, *7*, 29. [CrossRef]
139. Gysbers, P.; Hagen, G.; Holt, J.D.; Jansen, G.R.; Morris, T.D.; Navrátil, P.; Papenbrock, T.; Quaglioni, S.; Schwenk, A.; Stroberg, S.R.; et al. Discrepancy between experimental and theoretical β-decay rates resolved from first principles. *Nat. Phys.* **2019**, *15*, 428–431. [CrossRef]
140. Märkisch, B.; Mest, H.; Saul, H.; Wang, X.; Abele, H.; Dubbers, D.; Klopf, M.; Petoukhov, A.; Roick, C.; Soldner, T.; et al. Measurement of the weak axial-vector coupling constant in the decay of free neutrons using a pulsed cold neutron beam. *Phys. Rev. Lett.* **2019**, *122*, 242501. [CrossRef]
141. Hirsch, M.; Muto, K.; Oda, T.; Klapdor-Kleingrothaus, H.V. Nuclear structure calculation of $\beta^+\beta^+$, β^+/EC and EC/EC decay matrix elements. *Z. Phys. A* **1994**, *347*, 151–160. [CrossRef]
142. Suhonen, J.; Civitarese, O. Weak-interaction and nuclear-structure aspects of nuclear double beta decay. *Phys. Rep.* **1998**, *300*, 123–214. [CrossRef]
143. Vergados, J.D. The neutrinoless double beta decay from a modern perspective. *Rep. Prog. Phys.* **2002**, *361*, 1–56. [CrossRef]
144. Kotila, J.; Iachello, F. Phase space factors for $\beta^+\beta^+$ decay and competing modes of double-β decay. *Phys. Rev. C* **2013**, *87*, 024313. [CrossRef]
145. Saakyan, R. Two-neutrino double-beta decay. *Annu. Rev. Nucl. Part. Sci.* **2013**, *63*, 503–529. [CrossRef]
146. Maalampi, J.; Suhonen, J. Neutrinoless double β^+/EC decays. *Adv. High Energy Phys.* **2013**, *2013*, 505874. [CrossRef]
147. Kotila, J.; Barea, J.; Iachello, F. Neutrinoless double-electron capture. *Rev. Mod. Phys.* **2020**, *92*, 045007. [CrossRef]
148. Belli, P.; Bernabei, R.; Boiko, R.S.; Cappella, F.; Caracciolo, V.; Cerulli, R.; Danevich, F.A.; di Vacri, M.L.; Incicchitti, A.; Kropivyansky, B.N.; et al. First search for 2ε and $\varepsilon\beta^+$ processes in ^{168}Yb. *Nucl. Phys. A* **2019**, *990*, 64–78. [CrossRef]
149. Vergados, J.D.; Ejiri, H.; Šimkovic, F. Theory of neutrinoless double-beta decay. *Rep. Prog. Phys.* **2012**, *75*, 106301. [CrossRef]
150. Päs, H.; Rodejohann, W. Neutrinoless double-beta decay. *New J. Phys.* **2015**, *17*, 115010. [CrossRef]
151. Vergados, J.D.; Ejiri, H.; Šimkovic, F. Neutrinoless double beta decay and neutrino mass. *Int. J. Mod. Phys. E* **2016**, *25*, 1630007. [CrossRef]
152. Vissani, F. Signal of neutrinoless double beta decay, neutrino spectrum and oscillation scenarios. *J. High Energy Phys.* **1999**, *6*, 022. [CrossRef]
153. Arnold, R.; Augier, C.; Baker, J.D.; Barabash, A.S.; Basharina-Freshville, A.; Blondel, S.; Blot, S.; Bongrand, M.; Brudanin, V.; Busto, J.; et al. Results of the search for neutrinoless double-β decay in ^{100}Mo with the NEMO-3 experiment. *Phys. Rev. D* **2015**, *92*, 072011. [CrossRef]
154. Gando, A.; Gando, Y.; Hachiya, T.; Hayashi, A.; Hayashida, S.; Ikeda, H.; Inoue, K.; Ishidoshiro, K.; Karino, Y.; Koga, M.; et al. Search for majorana neutrinos near the inverted mass hierarchy region with KamLAND-Zen. *Phys. Rev. Lett.* **2016**, *117*, 082503. [CrossRef]
155. Anton, G.; Badhrees, I.; Barbeau, P.S.; Beck, D.; Belov, V.; Bhatta, T.; Breidenbach, M.; Brunner, T.; Cao, G.F.; Cen, W.R.; et al. Search for neutrinoless double-β decay with the complete EXO-200 dataset. *Phys. Rev. Lett.* **2019**, *123*, 161802. [CrossRef]
156. Alvis, S.I.; Arnquist, I.J.; Avignone, F.T., III; Barabash, A.S.; Barton, C.J.; Basu, V.; Bertrand, F.E.; Bos, B.; Busch, M.; Buuck, M.; et al. Search for neutrinoless double-β decay in ^{76}Ge with 26 kg yr of exposure from the Majorana Demonstrator. *Phys. Rev. C* **2019**, *100*, 025501. [CrossRef]
157. Azzolini, O.; Beeman, J.W.; Bellini, F.; Beretta, M.; Biassoni, M.; Brofferio, C.; Bucci, C.; Capelli, S.; Cardani, L.; Carniti, P.; et al. Final result of CUPID-0 phase-I in the search for the ^{82}Se neutrinoless double-β decay. *Phys. Rev. Lett.* **2019**, *123*, 032501. [CrossRef]
158. Agostini, M.; Araujo, G.R.; Bakalyarov, A.M.; Balata, M.; Barabanov, I.; Baudis, L.; Bauer, C.; Bellotti, E.; Belogurov, S.; Bettini, A.; et al. Final results of GERDA on the search for neutrinoless double-β decay. *Phys. Rev. Lett.* **2020**, *125*, 252502. [CrossRef]
159. Armengaud, E.; Augier, C.; Barabash, A.S.; Bellini, F.; Benato, G.; Benoît, A.; Beretta, M.; Bergé, L.; Billard, J.; Borovlev, Y.A.; et al. New limit for neutrinoless double-beta decay of ^{100}Mo from the CUPID-Mo experiment. *Phys. Rev. Lett.* **2021**, *126*, 181802. [CrossRef]
160. Belli, P.; Bernabei, R.; Cappella, F.; Caracciolo, V.; Cerulli, R.; Incicchitti, A.; Merlo, V. Double beta decay to excited states of daughter nuclei. *Universe* **2020**, *6*, 239. [CrossRef]
161. Barabash, A.S. Double beta decay to the excited states: Review. *AIP Conf. Proc.* **2017**, *1894*, 020002.
162. Albert, J.B.; Auger, M.; Auty, D.J.; Barbeau, P.S.; Beauchamp, E.; Beck, D.; Belov, V.; Benitez-Medina, C.; Bonatt, J.; Breidenbach, M.; et al. Improved measurement of the $2\nu\beta\beta$ half-life of ^{136}Xe with the EXO-200 detector. *Phys. Rev. C* **2014**, *89*, 015502. [CrossRef]
163. Arnold, R.; Augier, C.; Barabash, A.S.; Basharina-Freshville, A.; Blondel, S.; Blot, S.; Bongrand, M.; Brudanin, V.; Busto, J.; Caffrey, A.J.; et al. Investigation of double beta decay of ^{100}Mo to excited states of ^{100}Ru. *Nucl. Phys. A* **2014**, *925*, 25–36. [CrossRef]
164. Balata, M.; D'Andrea, V.; di Vacri, A.; Junker, M.; Laubenstein, M.; Macolino, C.; Zavarise, P.; Pandola, L.; Borowicz, D.; Frodyma, N.; et al. Results on $\beta\beta$ decay with emission of two neutrinos or Majorons in ^{76}Ge from GERDA Phase I. *Eur. Phys. J. C* **2015**, *75*, 416.

165. Arnold, R.; Augier, C.; Baker, J.D.; Barabash, A.S.; Basharina-Freshville, A.; Blondel, S.; Blot, S.; Bongrand, M.; Brudanin, V.; Busto, J.; et al. Measurement of the $2\nu\beta\beta$ decay half-life of ^{150}Nd and a search for $2\nu\beta\beta$ decay processes with the full exposure from the NEMO-3 detector. *Phys. Rev. D* **2016**, *94*, 072003. [CrossRef]
166. Arnold, R.; Augier, C.; Baker, J.D.; Barabash, A.S.; Basharina-Freshville, A.; Blondel, S.; Blot, S.; Bongrand, M.; Boursette, D.; Brudanin, V.; et al. Measurement of the $2\nu\beta\beta$ decay half-life and search for the $0\nu\beta\beta$ decay of ^{116}Cd with the NEMO-3 detector. *Phys. Rev. D* **2017**, *95*, 012007. [CrossRef]
167. Arnold, R.; Augier, C.; Barabash, A.S.; Basharina-Freshville, A.; Blondel, S.; Blot, S.; Bongrand, M.; Boursette, D.; Brudanin, V.; Busto, J.; et al. Final results on ^{82}Se double beta decay to the ground state of ^{82}Kr from the NEMO-3 experiment. *Eur. Phys. J. C* **2018**, *78*, 821. [CrossRef]
168. Barabash, A.S.; Belli, P.; Bernabei, R.; Cappella, F.; Caracciolo, V.; Cerulli, R.; Chernyak, D.M.; Danevich, F.A.; d'Angelo, S.; Incicchitti, A.; et al. Final results of the Aurora experiment to study 2β decay of ^{116}Cd with enriched $^{116}CdWO_4$ crystal scintillators. *Phys. Rev. D* **2018**, *98*, 092007. [CrossRef]
169. Azzolini, O.; Beeman, J.W.; Bellini, F.; Beretta, M.; Biassoni, M.; Brofferio, C.; Bucci, C.; Capelli, S.; Cardani, L.; Carniti, P.; et al. Evidence of single state sominance in the two-neutrino double-β decay of ^{82}Se with CUPID-0. *Phys. Rev. Lett.* **2019**, *123*, 262501. [CrossRef]
170. Kasperovych, D.V.; Barabash, A.S.; Belli, P.; Bernabei, R.; Boiko, R.S.; Cappella, F.; Caracciolo, V.; Cerulli, R.; Danevich, F.A.; Di Marco, A.; et al. Study of double-β decay of ^{150}Nd to the first 0^+ excited level of ^{150}Sm. *AIP Conf. Proc.* **2019**, *2165*, 020014.
171. Gando, A.; Gando, Y.; Hachiya, T.; Ha Minh, M.; Hayashida, S.; Honda, Y.; Hosokawa, K.; Ikeda, H.; Inoue, K.; Ishidoshiro, K.; et al. Precision analysis of the ^{136}Xe two-neutrino $\beta\beta$ spectrum in KamLAND-Zen and its impact on the quenching of nuclear matrix elements. *Phys. Rev. Lett.* **2019**, *122*, 192501. [CrossRef]
172. Arnold, R.; Augier, C.; Barabash, A.S.; Basharina-Freshville, A.; Blondel, S.; Blot, S.; Bongr, M.; Boursette, D.; Brudanin, V.; Busto, J.; et al. Detailed studies of ^{100}Mo two-neutrino double beta decay in NEMO-3. *Eur. Phys. J. C* **2019**, *79*, 440. [CrossRef]
173. Armengaud, E.; Augier, C.; Barabash, A.S.; Bellini, F.; Benato, G.; Benoît, A.; Beretta, M.; Bergé, L.; Billard, J.; Borovlev, Y.A.; et al. Precise measurement of $2\nu\beta\beta$ decay of ^{100}Mo with the CUPID-Mo detection technology. *Eur. Phys. J. C* **2020**, *80*, 674. [CrossRef]
174. Polischuk, O.G.; Barabash, A.S.; Belli, P.; Bernabei, R.; Boiko, R.S.; Cappella, F.; Caracciolo, V.; Cerulli, R.; Danevich, F.A.; Di Marco, A.; et al. Double beta decay of ^{150}Nd to the first 0^+ excited level of ^{150}Sm. *Phys. Scr.* **2021**, *96*, 085302. [CrossRef]
175. Adams, D.Q.; Alduino, C.; Alfonso, K.; Avignone, F.T., III; Azzolini, O.; Bari, G.; Bellini, F.; Benato, G.; Biassoni, M.; Branca, A.; et al. Measurement of the $2\nu\beta\beta$ decay half-life of ^{130}Te with CUORE. *Phys. Rev. Lett.* **2021**, *126*, 171801. [CrossRef]
176. Engel, J.; Menéndez, J. Status and future of nuclear matrix elements for neutrinoless double-beta decay: A review. *Rep. Prog. Phys.* **2017**, *80*, 046301. [CrossRef]
177. Suhonen, J.T. Impact of the quenching of g_A on the sensitivity of $0\nu\beta\beta$ experiments. *Phys. Rev. C* **2017**, *96*, 055501. [CrossRef]
178. Rodin, V.A.; Faessler, A.; Šimkovic, F.; Vogel, P. Assessment of uncertainties in QRPA $0\nu\beta\beta$-decay nuclear matrix elements. *Nucl. Phys. A* **2006**, *766*, 107–131; Erratum in **2007**, *793*, 213–215. [CrossRef]
179. Kortelainen, M.; Suhonen, J. Nuclear matrix elements of $0\nu\beta\beta$ decay with improved short-range correlations. *Phys. Rev. C* **2007**, *76*, 024315. [CrossRef]
180. Šimkovic, F.; Faessler, A.; Rodin, V.; Engel, J. Anatomy of the $0\nu\beta\beta$ nuclear matrix elements. *Phys. Rev. C* **2008**, *77*, 045503. [CrossRef]
181. Šimkovic, F.; Dvornický, R.; Štefánik, D.; Faessler, A. Improved description of the $2\nu\beta\beta$-decay and a possibility to determinethe effective axial-vector coupling constant. *Phys. Rev. C* **2018**, *97*, 034315. [CrossRef]
182. Abad, J.; Morales, A.; Núñez-Lagos, R.; Pacheco, A.F. An estimation of the rates of (two-neutrino) double beta decay and related processes. *J. Phys. Colloques* **1984**, *45*, C3-147–C3-150. [CrossRef]
183. Civitarese, O.; Suhonen, J. Is the single-state dominance realized in double-β-decay transitions? *Phys. Rev. C* **1998**, *58*, 1535. [CrossRef]
184. Šimkovic, F.; Domin, P.; Semenov, S.V. The single state dominance hypothesis and the two-neutrino double beta decay of ^{100}Mo. *J. Phys. G* **2001**, *27*, 2233–2240. [CrossRef]
185. Kotila, J.; Iachello, F. Phase-space factors for double-β decay. *Phys. Rev. C* **2012**, *85*, 034316. [CrossRef]
186. Domin, P.; Kovalenko, S.; Šimkovic, F.; Semenov, S.V. Neutrino accompanied $\beta^{\pm}\beta^{\pm}$, β^{+}/EC and EC/EC processes within single state dominance hypothesis. *Nucl. Phys. A* **2005**, *753*, 337–363. [CrossRef]
187. Moreno, O.; Álvarez-Rodríguez, R.; Sarriguren, P.; Moya de Guerra, E.; Šimkovic, F.; Faessler, A. Single- and low-lying-states dominance in two-neutrino double-beta decay. *J. Phys. G* **2008**, *36*, 015106. [CrossRef]
188. Suhonen, J.; Civitarese, O. Single and double beta decays in the A = 100, A = 116 and A = 128 triplets of isobars. *Nucl. Phys. A* **2014**, *924*, 1–23. [CrossRef]
189. Arnold, R.; Augier, C.; Baker, J.; Barabash, A.; Brudanin, V.; Caffrey, A.J.; Egorov, V.; Guyonnet, J.L.; Hubert, F.; Hubert, P.; et al. Study of 2β-decay of ^{100}Mo and ^{82}Se using the NEMO3 detector. *JETP Lett.* **2004**, *80*, 377–381. [CrossRef]
190. Díaz, J.S. Limits on Lorentz and CPT violation from double beta decay. *Phys. Rev. D* **2014**, *89*, 036002. [CrossRef]
191. Díaz, J.S. Neutrinos as Probes of Lorentz Invariance. *Adv. High Energy Phys.* **2014**, *2014*, 962410. [CrossRef]
192. Albert, J.B.; Barbeau, P.S.; Beck, D.; Belov, V.; Breidenbach, M.; Brunner, T.; Burenkov, A.; Cao, G.F.; Chambers, C.; Cleveland, B.; et al. First search for Lorentz and CPT violation in double beta decay with EXO-200. *Phys. Rev. D* **2016**, *93*, 072001. [CrossRef]

193. Azzolini, O.; Beeman, J.W.; Bellini, F.; Beretta, M.; Biassoni, M.; Brofferio, C.; Bucci, C.; Capelli, S.; Cardani, L.; Carniti, P.; et al. First search for Lorentz violation in double beta decay with scintillating calorimeters. *Phys. Rev. D* **2019**, *100*, 092002. [CrossRef]
194. Niţescu, O.; Ghinescu, S.; Stoica, S. Lorentz violation effects in $2\nu\beta\beta$ decay. *J. Phys. G* **2020**, *47*, 055112. [CrossRef]
195. Niţescu, O.; Ghinescu, S.; Mirea, M.; Stoica, S. Probing Lorentz violation in $2\nu\beta\beta$ using single electron spectra and angular correlations. *Phys. Rev. D* **2021**, *103*, 031701. [CrossRef]
196. Blum, K.; Nira, Y.; Shavit, M. Neutrinoless double-beta decay with massive scalar emission. *Phys. Lett. B* **2018**, *785*, 354–361. [CrossRef]
197. Cepedello, R.; Deppisch, F.F.; González, L.; Hati, C.; Hirsch, M. Neutrinoless Double-β Decay with Nonstandard Majoron Emission. *Phys. Rev. Lett* **2019**, *122*, 181801. [CrossRef]
198. Deppisch, F.F.; Graf, L.; Šimkovic, F. Searching for new physics in two-neutrino double beta decay. *Phys. Rev. Lett.* **2020**, *125*, 171801. [CrossRef]
199. Barabash, A.S.; Dolgov, A.D.; Dvornický, R.; Šimkovic, F.; Smirnov, A.Y. Statistics of neutrinos and the double beta decay. *Nucl. Phys. B* **2007**, *783*, 90–111. [CrossRef]
200. Bolton, P.D.; Deppisch, F.F.; Gráf, L.; Šimkovic, F. Two-neutrino double beta decay with sterile neutrinos. *Phys. Rev. D* **2021**, *103*, 055019. [CrossRef]
201. Agostini, M.; Bossio, E.; Ibarra, A.; Marcano, X. Search for light exotic fermions in double-beta decays. *Phys. Lett. B* **2021**, *815*, 136127. [CrossRef]
202. Deppisch, F.F.; Graf, L.; Rodejohann, W.; Xu, X.J. Neutrino self-interactions and double beta decay. *Phys. Rev. D* **2020**, *102*, 051701. [CrossRef]
203. Alduino, C.; Alfonso, K.; Artusa, D.R.; Avignone, F.T., III; Azzolini, O.; Banks, T.I.; Bari, G.; Beeman, J.W.; Bellini, F.; Bersani, A.; et al. Measurement of the two-neutrino double-beta decay half-life of ^{130}Te with the CUORE-0 experiment. *Eur. Phys. J. C* **2017**, *77*, 13. [CrossRef]
204. Arnaboldi, C.; Beeman, J.W.; Cremonesi, O.; Gironi, L.; Pavan, M.; Pessina, G.; Pirro, S.; Previtali, E. $CdWO_4$ scintillating bolometer for Double Beta Decay: Light and heat anticorrelation, light yield and quenching factors. *Astropart. Phys.* **2010**, *34*, 143–150. [CrossRef]
205. Chernyak, D.M.; Danevich, F.A.; Giuliani, A.; Olivieri, E.; Tenconi, M.; Tretyak, V.I. Random coincidence of $2\nu2\beta$ decay events as a background source in bolometric $0\nu2\beta$ decay experiments. *Eur. Phys. J. C* **2012**, *72*, 1989. [CrossRef]
206. Chernyak, D.M.; Danevich, F.A.; Giuliani, A.; Mancuso, M.; Nones, C.; Olivieri, E.; Tenconi, M.; Tretyak, V.I. Rejection of randomly coinciding events in $ZnMoO_4$ scintillating bolometers. *Eur. Phys. J. C* **2014**, *74*, 2913. [CrossRef]
207. Chernyak, D.M.; Danevich, F.A.; Dumoulin, L.; Giuliani, A.; Mancuso, M.; De Marcillac, P.; Marnieros, S.; Nones, C.; Olivieri, E.; Poda, D.V.; et al. Rejection of randomly coinciding events in $Li_2{}^{100}MoO_4$ scintillating bolometers using light detectors based on the Neganov-Luke effect. *Eur. Phys. J. C* **2017**, *77*, 3. [CrossRef]
208. Pirro, S. Scintillating bolometers for next generation double beta decay. In Proceedings of the International Workshop on Double Beta Decay and Neutrinos, Hawaii, HA, USA, 11–13 October 2009.
209. AMoRE-Advanced Mo-Based Rare Process Experiment. Available online: https://amore.ibs.re.kr/ (accessed on 30 June 2021).
210. ISOTope Trace Analysis. Available online: http://isotta.in2p3.fr/ (accessed on 30 June 2021).
211. LUCIFER-Low Background Underground Cryogenic Installation for Elusive Rates. Available online: https://web.infn.it/lucifer/ (accessed on 30 June 2021).
212. CUPID-0. Available online: https://www.lngs.infn.it/en/cupid-eng (accessed on 30 June 2021).
213. Luminescent Underground Molybdenum Investigation for NEUtrino Mass and Nature. Available online: http://lumineu.in2p3.fr/ (accessed on 30 June 2021).
214. CUPID-Mo. Available online: https://cupid-mo.mit.edu/ (accessed on 30 June 2021).
215. Czochralski Growth of Li_2MoO_4 crYstals for the Scintillating boloMeters Used in the Rare EveNts sEarches. Available online: http://clymene.in2p3.fr/ (accessed on 30 June 2021).
216. Cryogenic Rare-Event Observatory with Surface Sensitivity. Available online: https://cordis.europa.eu/project/id/742345 (accessed on 30 June 2021).
217. CANDLES- CAlcium Fluoride for the Study of Neutrinos and Dark Matters by Low Energy Spectrometer. Available online: http://www.rcnp.osaka-u.ac.jp/candles/index.html (accessed on 30 June 2021).
218. Brofferio, C.; Dell'Oro, S. The saga of neutrinoless double beta decay search with TeO_2 thermal detectors. *Rev. Sci. Instrum.* **2018**, *89*, 121502. [CrossRef]
219. CUORE Upgrade with Particle Identification. Available online: https://cupid-i.lngs.infn.it (accessed on 30 June 2021).
220. Bi-Isotope $0\nu2\beta$ Next Generation Observatory. Available online: https://cordis.europa.eu/project/id/865844 (accessed on 30 June 2021).
221. Luković, V.; Cabella, P.; Vittorio, N. Dark matter in cosmology. *Int. J. Mod. Phys. A* **2014**, *29*, 1443001. [CrossRef]
222. Arun, K.; Gudennavar, S.B.; Sivaram, C. Dark matter, dark energy, and alternate models: A review. *Adv. Space Res.* **2017**, *60*, 166–186. [CrossRef]
223. Bertone, G.; Tait, T.M.P. A new era in the search for dark matter. *Nature* **2018**, *562*, 51–56. [CrossRef]
224. Schumann, M. Direct detection of WIMP dark matter: Concepts and status. *J. Phys. G* **2019**, *46*, 103003. [CrossRef]

225. Stark, M.; Boslau, O.; Feilitzsch, F.; Goldstra, P.; Jochum, J.; Kemmer, J.; Potzel, W.; Rau, W. Application of the Neganov-Luke effect to low-threshold light detectors. *Nucl. Instrum. Methods Phys. Res. A* **2005**, *545*, 738–743. [CrossRef]
226. Angloher, G.; Bauer, M.; Bavykina, I.; Bento, A.; Bucci, C.; Ciemniak, C.; Deuter, G.; von Feilitzsch, F.; Hauff, D.; Huff, P.; et al. Results from 730 kg days of the CRESST-II Dark Matter search. *Eur. Phys. J. C* **2012**, *72*, 1971. [CrossRef]
227. Spergel, D.N. Motion of the Earth and the detection of weakly interacting massive particles. *Phys. Rev. D* **1988**, *37*, 1353. [CrossRef]
228. Belli, P.; Bernabei, R.; Bacci, C.; Incicchitti, A.; Prosperi, D. Identifying a "dark matter" signal by nonisotropic scintillation detector. *Il Nuovo Cim. C* **1992**, *15*, 473–479. [CrossRef]
229. Bernabei, R.; Belli, P.; Nozzoli, F.; Incicchitti, A. Anisotropic scintillators for WIMP direct detection: Revisited. *Eur. Phys. J. C* **2003**, *28*, 203–209. [CrossRef]
230. Shimizu, Y.; Minowa, M.; Sekiya, H.; Inoue, Y. Directional scintillation detector for the detection of the wind of WIMP. *Nucl. Instrum. Methods Phys. Res. A* **2003**, *496*, 347–352. [CrossRef]
231. Cappella, F.; Bernabei, R.; Belli, P.; Caracciolo, V.; Cerulli, R.; Danevich, F.A.; d'Angelo, A.; Di Marco, A.; Incicchitti, A.; Poda, D.V.; et al. On the potentiality of the $ZnWO_4$ anisotropic detectors to measure the directionality of Dark Matter. *Eur. Phys. J. C* **2013**, *73*, 2276. [CrossRef]
232. Rare Objects SEarch with Bolometers UndergrounD. Available online: http://www.unizar.es/lfnae/rosebud/ (accessed on 31 December 2020).
233. CREST-Cryogenic Rare Event Search with Superconducting Thermometers. Available online: http://www.cresst.de/ (accessed on 30 June 2021).
234. Cryogenic Dark Matter Search. Available online: http://cdms.berkeley.edu/ (accessed on 31 December 2020).
235. EDELWEISS-Expérience pour DEtecter Les WIMP En Site Souterrain. Available online: http://edelweiss.in2p3.fr/ (accessed on 30 June 2021).
236. EURECA-European Underground Rare Event Calorimeter Array. Available online: https://www.eureca.kit.edu/ (accessed on 30 June 2021).
237. Kraus, H.; Armengaud, E.; Bauer, M.; Bavykina, I.; Benoit, A.; Bento, A.; Blümer, J.; Bornschein, L.; Broniatowski, A.; Burghart, G.; et al. EURECA—The Future of cryogenicDark Matter Ddtection in Europe. *PoS* **2008**, *idm2008*, 013.
238. Kraus, H.; Armengaud, E.; Bauer, M.; Bavykina, I.; Benoit, A.; Bento, A.; Blümer, J.; Bornschein, L.; Broniatowski, A.; Burghart, G.; et al. EURECA—Setting the scene for scintillators. In Proceedings of the 1st International Workshop on Radiopure Scintillators for EURECA (RPScint 2008), Kyiv, Ukraine, 9–10 September 2008.
239. Angloher, G.; Armengaud, E.; Augier, C.; Benoit, A.; Bergmann, T.; Blümer, J.; Broniatowski, A.; Brudanin, V.; Camus, P.; Cazes, A.; et al. EURECA Conceptual Design Report. *Phys. Dark Universe* **2014**, *3*, 41–74. [CrossRef]
240. Angloher, G.; Bento, A.; Bucci, C.; Canonica, L.; Erb, A.; Feilitzsch, F.V.; Iachellini, N.F.; Gorla, P.; Gütlein, A.; Hauff, D.; et al. Probing low WIMP masses with the next generation of CRESST detector. *arXiv* **2015**, arXiv:astro-ph.IM/1503.08065.
241. COSINUS-Cryogenic Observatory for SIgnals Seen in Next-Generation Underground Searches. Available online: https://www.lngs.infn.it/en/cosinus-eng (accessed on 30 June 2021).
242. Peccei, R.D.; Quinn, H.R. CP conservation in the presence of pseudoparticles. *Phys. Rev. Lett.* **1977**, *38*, 1440. [CrossRef]
243. Peccei, R.D.; Quinn, H.R. Constraints imposed by CP conservation in the presence of pseudoparticles. *Phys. Rev. D* **1977**, *16*, 1791. [CrossRef]
244. Irastorza, I.G.; Redondo, J. New experimental approaches in the search for axion-like particles. *Prog. Part. Nucl. Phys.* **2018**, *102*, 89–159. [CrossRef]
245. Freedman, D.Z. Coherent effects of a weak neutral current. *Phys. Lett. B* **1974**, *9*, 1389. [CrossRef]
246. Drukier, A.; Stodolsky, L. Principles and applications of a neutral current detector for neutrino physics and astronomy. *Phys. Rev. D* **1984**, *30*, 2295. [CrossRef]
247. Akimov, D.; Albert, J.B.; An, P.; Awe, C.; Barbeau, P.S.; Becker, B.; Belov, V.; Brown, A.; Bolozdynya, A.; Cabrera-Palmer, B.; et al. Observation of coherent elastic neutrino-nucleus scattering. *Science* **2017**, *357*, 1123. [CrossRef]
248. Monroe, J.; Fisher, P. Neutrino backgrounds to dark matter searches. *Phys. Rev. D* **2007**, *76*, 033007. [CrossRef]
249. BASKET-Bolometers At Sub-KeV Energy Thresholds. Available online: http://irfu.cea.fr/Phocea/Page/index.php?id=861 (accessed on 30 June 2021).
250. Thulliez, L.; Lhuillier, D.; Cappella, F.; Casali, N.; Cerulli, R.; Chalil, A.; Chebboubi, A.; Dumonteil, E.; Erhart, A.; Giuliani, A.; et al. Calibration of nuclear recoils at the 100 eV scale using neutron capture. *arXiv* **2021**, arXiv:physics.ins-det/2011.13803.
251. Brooks, F.D.; Klein, H. Neutron spectrometry: Historical review and present status. *Nucl. Instrum. Methods Phys. Res. A* **2002**, *476*, 1–11. [CrossRef]
252. Klein, H.; Brooks, F.D. Scintillation detectors for fast neutrons. *PoS* **2006**, *FNDA2006*, 097.
253. Cieślak, M.J.; Gamage, K.A.A.; Glover, R. Critical review of scintillating crystals for neutron detection. *Crystals* **2019**, *9*, 480. [CrossRef]
254. Gironnet, J.; van den Brandt, B.; Coron, N.; Hautle, P.; Filges, U.; Konter, J.A.; de Marcillac, P.; Ortigoza, Y.; Puimedon, J.; Rolon, T.; et al. Neutron spectroscopy with ^{6}LiF bolometers. *AIP Conf. Proc.* **2009**, *1185*, 751–754.
255. Ginestra, C. Fast Neutron Spectrometry by Bolometers Lithium Target for the Reduction of Background Experiences of Direct Detection of Dark Matter. Ph.D. Thesis, Université Paris Sud XI, Orsay, France, 2010. (In French)

256. Dumazert, J.; Coulon, R.; Lecomte, Q.; Bertrand, G.H.V.; Hamel, M. Gadolinium for neutron detection in current nuclear instrumentation research: A review. *Nucl. Instrum. Methods Phys. Res. A* **2018**, *882*, 53–68. [CrossRef]
257. Coron, N.; Cuesta, C.; Domange, J.; García, E.; Gironnet, J.; Leblanc, J.; de Marcillac, P.; Martínez, M.; Ortigoza, Y.; de Solórzano, A.O.; et al. Detection of fast neutrons with LiF and Al_2O_3 scintillating bolometers. *J. Phys. Conf. Ser.* **2010**, *203*, 012139. [CrossRef]
258. Coron, N.; Cuesta, C.; García, E.; Ginestra, C.; Gironnet, J.; de Marcillac, P.; Martínez, M.; Ortigoza, Y.; Pobes, C.; Puimedón, J.; et al. Measurement of the differential neutron flux inside a lead shielding in a cryogenic experiment. *J. Phys. Conf. Ser.* **2012**, *375*, 012018. [CrossRef]
259. Armengaud, E.; Augier, C.; Barabash, A.S.; Bellini, F.; Benato, G.; Benoît, A.; Beretta, M.; Bergé, L.; Billard, J.; Borovlev, Y.A.; et al. The CUPID-Mo experiment for neutrinoless double-beta decay: Performance and prospects. *Eur. Phys. J. C* **2020**, *80*, 44. [CrossRef]
260. Mikhailik, V.B.; Kraus, H. Cryogenic scintillators in searches for extremely rare events. *J. Phys. D* **2006**, *39*, 1181–1191. [CrossRef]
261. Mikhailik, V.B.; Kraus, H. Performance of scintillation materials at cryogenic temperatures. *Phys. Status Solidi B* **2010**, *247*, 1583. [CrossRef]
262. Dafinei, I.; Fasoli, M.; Ferroni, F.; Mihokova, E.; Orio, F.; Pirro, S.; Vedda, A. Low temperature scintillation in ZnSe crystals. *IEEE Trans. Nucl. Sci.* **2010**, *57*, 1470–1474. [CrossRef]
263. Sailer, C.; Lubsandorzhiev, B.; Strandhagen, C.; Jochum, J. Low temperature light yield measurements in NaI and NaI(Tl). *Eur. Phys. J. C* **2012**, *72*, 2061. [CrossRef]
264. Mikhailik, V.B.; Kapustyanyk, V.; Tsybulskyi, V.; Rudyk, V.; Kraus, H. Luminescence and scintillation properties of CsI: A potential cryogenic scintillator. *Phys. Status Solidi B* **2015**, *252*, 804–810. [CrossRef]
265. Tower, J.; Winslow, L.; Churilov, A.; Ogorodnik, Y.; Hong, H.; Glodo, J.; van Loef, E.; Giuliani, A.; Poda, D.; Leder, A.; et al. New scintillating bolometer crystals for rare particle detection. *Nucl. Instrum. Methods Phys. Res. A* **2020**, *954*, 162300. [CrossRef]
266. Barinova, O.P.; Danevich, F.A.; Degoda, V.Y.; Kirsanova, S.V.; Kudovbenko, V.M.; Pirro, S.; Tretyak, V.I. First test of Li_2MoO_4 crystal as a cryogenic scintillating bolometer. *Nucl. Instrum. Methods Phys. Res. A* **2010**, *613*, 54–57. [CrossRef]
267. Coron, N.; Dambier, G.; Leblanc, E.; Leblanc, J.; de Marcillac, P.; Moalic, J.P. Scintillating and particle discrimination properties of selected crystals for low-temperature bolometers: From LiF to BGO. *Nucl. Instrum. Methods Phys. Res. A* **2004**, *520*, 159–162. [CrossRef]
268. Dafinei, I.; Dujardin, C.; Longo, E.; Vignati, M. Low temperature photoluminescence of pure and doped paratellurite (TeO_2) crystals. *Phys. Status Solidi A* **2007**, *204*, 1567–1570. [CrossRef]
269. Bergé, L.; Chapellier, M.; De Combarieu, M.; Dumoulin, L.; Giuliani, A.; Gros, M.; de Marcillac, P.; Marnieros, S.; Nones, C.; Novati, V.; et al. Complete event-by-event $\alpha/\gamma(\beta)$ separation in a full-size TeO_2 CUORE bolometer by Neganov-Luke-magnified light detection. *Phys. Rev. C* **2018**, *97*, 032501. [CrossRef]
270. Tabarelli de Fatis, T. Cerenkov emission as a positive tag of double beta decays in bolometric experiments. *Eur. Phys. J. C* **2010**, *65*, 359–361. [CrossRef]
271. Casali, N. Model for the Cherenkov light emission of TeO_2 cryogenic calorimeters. *Astropart. Phys.* **2017**, *91*, 44–50. [CrossRef]
272. Frank, T. Development of Scintillating Calorimeters for Discrimination of Nuclear Recoils and Fully Ionizing Events. Ph.D. Thesis, Technische Universität München, Munich, Germany, 2002.
273. Ninković, J. Investigation of $CaWO_4$ Crystals for Simultaneous Phonon-Light Detection in the CRESST Dark Matter Search. Ph.D. Thesis, Technische Universität München, Munich, Germany, 2005.
274. Wahl, D. Optimisation of Light Collection in Inorganic Scintillators for Rare Event Searches. Ph.D. Thesis, University of Oxford, Oxford, UK, 2005.
275. Chernyak, D.M.; Danevich, F.A.; Degoda, V.Y.; Dmitruk, I.M.; Ferri, F.; Galashov, E.N.; Giuliani, A.; Ivanov, I.M.; Kobychev, V.V.; Mancuso, M.; et al. Optical, luminescence and thermal properties of radiopure $ZnMoO_4$ crystals used in scintillating bolometers for double beta decay search. *Nucl. Instrum. Methods Phys. Res. A* **2013**, *729*, 856. [CrossRef]
276. Danevich, F.A.; Kobychev, R.V.; Kobychev, V.V.; Kraus, H.; Mikhailik, V.B.; Mokina, V.M. Optimization of light collection from crystal scintillators for cryogenic experiments. *Nucl. Instrum. Methods Phys. Res. A* **2014**, *744*, 41–47. [CrossRef]
277. Danevich, F.A.; Kobychev, V.V.; Kobychev, R.V.; Kraus, H.; Mikhailik, V.B.; Mokina, V.M.; Solsky, I.M. Impact of geometry on light collection efficiency of scintillation detectors for cryogenic rare event searches. *Nucl. Instrum. Meth. B* **2014**, *336*, 26–30. [CrossRef]
278. Janecek, M.; Moses, W.W. Optical reflectance measurements for commonly used reflectors. *IEEE Trans. Nucl. Sci.* **2008**, *55*, 2432–2437. [CrossRef]
279. Janecek, M. Reflectivity Spectra for Commonly Used Reflectors. *IEEE Trans. Nucl. Sci.* **2012**, *59*, 490–497. [CrossRef]
280. Langenkämper, A.; Ulrich, A.; Defay, X.; Feilitzsch, F.; Lanfranchi, J.C.; Mondragón, E.; Münster, A.; Oppenheimer, C.; Potzel, W.; Roth, S.; et al. Low-temperature relative reflectivity measurements of reflective and scintillating foils used in rare event searches. *Nucl. Instrum. Methods Phys. Res. A* **2018**, *884*, 40–44. [CrossRef]
281. Lang, R.F.; Angloher, G.; Bauer, M.; Bavykina, I.; Bento, A.; Brown, A.; Bucci, C.; Ciemniak, C.; Coppi, C.; Deuter, G.; et al. Discrimination of recoil backgrounds in scintillating calorimeters. *Astropart. Phys.* **2010**, *33*, 60–64. [CrossRef]
282. Biassoni, M.; Brofferio, C.; Bucci, C.; Canonica, L.; di Vacri, M.L.; Gorla, P.; Pavan, M.; Yeh, M. Rejection of alpha surface background in non-scintillating bolometric detectors: The ABSuRD project. *J. Low Temp. Phys.* **2016**, *184*, 879–884. [CrossRef]
283. Armatol, A.; Armengaud, E.; Armstrong, W.; Augier, C.; Avignone, F.T.; Azzolini, O.; Barabash, A.; Bari, G.; Barresi, A.; Baudin, D.; et al. Characterization of cubic $Li_2{}^{100}MoO_4$ crystals for the CUPID experiment. *Eur. Phys. J. C* **2021**, *81*, 104. [CrossRef]

284. Baselmans, J. Kinetic inductance detectors. *J. Low Temp. Phys.* **2012**, *167*, 292–304. [CrossRef]
285. Lee, S.J.; Choi, J.H.; Danevich, F.A.; Jang, Y.S.; Kang, W.G.; Khanbekov, N.; Kim, H.J.; Kim, I.H.; Kim, S.C.; Kim, S.K.; et al. The development of a cryogenic detector with $CaMoO_4$ crystals for neutrinoless double beta decay search. *Astropart. Phys.* **2011**, *34*, 732–737. [CrossRef]
286. Casali, N.; Cardani, L.; Colantoni, I.; Cruciani, A.; Di Domizio, S.; Martinez, M.; Pettinari, G.; Vignati, M. Phonon and light read out of a Li_2MoO_4 crystal with multiplexed kinetic inductance detectors. *Eur. Phys. J. C* **2019**, *79*, 724. [CrossRef]
287. Alessandrello, A.; Bashkirov, V.; Brofferio, C.; Camin, D.V.; Cremonesi, O.; Fiorini, E.; Gervasio, G.; Giuliani, A.; Pavan, M.; Pessina, G.; et al. Development of a thermal scintillating detector for double beta decay of ^{48}Ca. *Nucl. Phys. B (Proc. Suppl.)* **1992**, *28*, 233–235. [CrossRef]
288. Alessandrello, A.; Bashkirov, V.; Brofferio, C.; Camin, D.V.; Cremonesi, O.; Fiorini, E.; Gervasio, G.; Giuliani, A.; Pavan, M.; Pessina, G.; et al. Search for double beta decay of ^{130}Te with a cryogenic thermal detector and simultaneous detection of light and thermal signals in a cryogenic CaF_2 detector. In Proceedings of the 12th Moriond Workshop on Progress in Atomic Physics, Neutrinos and Gravitation, Les Arcs, Savoie, France, 25 January–1 February 1992.
289. Alessandrello, A.; Bashkirov, V.; Brofferio, C.; Bucci, C.; Camin, D.V.; Cremonesi, O.; Fiorini, E.; Gervasio, G.; Giuliani, A.; Nucciotti, A.; et al. A scintillating bolometer for experiments on double beta decay. *Phys. Lett. B* **1998**, *420*, 109–113. [CrossRef]
290. Bobin, C. Bolomètres Massifs et Détection de la Matière Noire non Baryonique. Ph.D. Thesis, Université Claude Bernard Lyon-1, Lyon, France, 1995.
291. Bobin, C.; Berkes, I.; Hadjout, J.P.; Coron, N.; Leblanc, J.; De Marcillac, P. Alpha/gamma discrimination with a CaF_2(Eu) target bolometer optically coupled to a composite infrared bolometer. *Nucl. Instrum. Methods Phys. Res. A* **1997**, *386*, 453–457. [CrossRef]
292. Zhang, X.; Lin, J.; Mikhailik, V.B.; Kraus, H. Cryogenic phonon–scintillation detectors with PMT readout for rare event search experiments. *Astropart. Phys.* **2016**, *79*, 31–40. [CrossRef]
293. Angloher, G.; Bauer, P.; Bento, A.; Bucci, C.; Canonica, L.; Defay, X.; Erb, A.; Feilitzsch, F.V.; Iachellini, N.F.; Gorla, P.; et al. Performance of a CRESST-II detector module with true 4π-veto. *arXiv* **2017**, arXiv:astro-ph.IM/1708.01581.
294. Schäffner, K.; Angloher, G.; Carniti, P.; Cassina, L.; Gironi, L.; Gotti, C.; Gütlein, A.; Mancuso, M.; Di Marco, N.; Pagnanini, L.; et al. A NaI-based cryogenic scintillating calorimeter: Results from a COSINUS prototype detector. *J. Low Temp. Phys.* **2018**, *193*, 1174–1181. [CrossRef]
295. Reindl, F.; Angloher, G.; Carniti, P.; Cassina, L.; Gironi, L.; Gotti, C.; Gütlein, A.; Maino, M.; Mancuso, M.; Di Marco, N.; et al. Results of the first NaI scintillating calorimeter prototypes by COSINUS. *J. Phys. Conf. Ser.* **2020**, *1342*, 012099. [CrossRef]
296. Pirro, S.; Beeman, J.W.; Capelli, S.; Pavan, M.; Previtali, E.; Gorla, P. Scintillating double-beta-decay bolometers. *Phys. At. Nucl.* **2006**, *69*, 2109. [CrossRef]
297. Beeman, J.W.; Gentils, A.; Giuliani, A.; Mancuso, M.; Pessina, G.; Plantevin, O.; Rusconi, C. Effect of SiO_2 coating in bolometric Ge light detectors for rare event searches. *Nucl. Instrum. Methods Phys. Res. A* **2013**, *709*, 22–28. [CrossRef]
298. Mancuso, M.; Beeman, J.W.; Giuliani, A.; Dumoulin, L.; Olivieri, E.; Pessina, G.; Plantevin, O.; Rusconi, C.; Tenconi, M. An experimental study of antireflective coatings in Ge light detectors for scintillating bolometers. *EPJ Web Conf.* **2014**, *65*, 04003. [CrossRef]
299. Artusa, D.R.; Avignone, F.T., III; Beeman, J.W.; Dafinei, I.; Dumoulin, L.; Ge, Z.; Giuliani, A.; Gotti, C.; de Marcillac, P.; Marnieros, S.; et al. Enriched TeO_2 bolometers with active particle discrimination: Towards the CUPID experiment. *Phys. Lett. B* **2017**, *767*, 321. [CrossRef]
300. Hansen, E.V.; DePorzio, N.; Winslow, L. Characterization of single layer anti-reflective coatings for bolometer-based rare event searches. *J. Instrum.* **2017**, *12*, P09018. [CrossRef]
301. Barucci, M.; Beeman, J.W.; Caracciolo, V.; Pagnanini, L.; Pattavina, L.; Pessina, G.; Pirro, S.; Rusconi, C.; Schäffner, K. Cryogenic light detectors with enhanced performance for rare event physics. *Nucl. Instrum. Methods Phys. Res. A* **2019**, *935*, 150. [CrossRef]
302. Isaila, C.; Ciemniak, C.; Feilitzsch, F.; Gütlein, A.; Kemmer, J.; Lachenmaier, T.; Lanfranchi, J.C.; Pfister, S.; Potzel, W.; Roth, S.; et al. Low-temperature light detectors: Neganov-Luke amplification and calibration. *Phys. Lett. B* **2012**, *716*, 160. [CrossRef]
303. Novati, V.; Bergé, L.; Dumoulin, L.; Giuliani, A.; Mancuso, M.; de Marcillac, P.; Marnieros, S.; Olivieri, E.; Poda, D.V.; Tenconi, M.; et al. Charge-to-heat transducers exploiting the Neganov-Trofimov-Luke effect for light detection in rare-event searches. *Nucl. Instrum. Methods Phys. Res. A* **2019**, *940*, 320–327. [CrossRef]
304. Piperno, G.; Pirro, S.; Vignati, M. Optimizing the energy threshold of light detectors coupled to luminescent bolometers. *J. Instrum.* **2011**, *6*, P10005. [CrossRef]
305. Neganov, B.; Trofimov, V. USSR patent No 1037771. *Otkrytiya Izobret.* **1985**, *146*, 215.
306. Luke, P.N. Voltage-assisted calorimetric ionization detector. *J. Appl. Phys.* **1988**, *64*, 6858. [CrossRef]
307. Beeman, J.W.; Danevich, F.A.; Degoda, V.Y.; Galashov, E.N.; Giuliani, A.; Ivanov, I.M.; Mancuso, M.; Marnieros, S.; Nones, C.; Pessina, G.; et al. An Improved $ZnMoO_4$ scintillating bolometer for the search for neutrinoless double beta decay of ^{100}Mo. *J. Low Temp. Phys.* **2012**, *167*, 1021. [CrossRef]
308. Tenconi, M. Development of Luminescent Bolometers and Light Detectors for Neutrinoless Double Beta Decay Search. Ph.D. Thesis, Université Paris-Sud, Orsay, France, 2015.
309. Coron, N.J.; de Marcillac, P.; Leblanc, J.; Dambier, G.; Moalic, J.P. Highly sensitive large-area bolometers for scintillation studies below 100 mK. *Opt. Eng.* **2004**, *43*, 1568. [CrossRef]

310. Pirro, S.; Arnaboldi, C.; Beeman, J.W.; Pessina, G. Development of bolometric light detectors for double beta decay searches. *Nucl. Instrum. Methods Phys. Res. A* **2006**, *559*, 361–363. [CrossRef]
311. Bekker, T.B.; Coron, N.; Danevich, F.A.; Degoda, V.Y.; Giuliani, A.; Grigorieva, V.D.; Ivannikova, N.V.; Mancuso, M.; de Marcillac, P.; Moroz, I.M.; et al. Aboveground test of an advanced Li_2MoO_4 scintillating bolometer to search for neutrinoless double beta decay of ^{100}Mo. *Astropart. Phys.* **2016**, *72*, 38. [CrossRef]
312. Artusa, D.R.; Balzoni, A.; Beeman, J.W.; Bellini, F.; Biassoni, M.; Brofferio, C.; Camacho, A.; Capelli, S.; Cardani, L.; Carniti, P.; et al. First array of enriched Zn^{82}Se bolometers to search for double beta decay. *Eur. Phys. J. C* **2016**, *76*, 364. [CrossRef]
313. Mancuso, M. Development and Optimization of Scintillating Bolometers and Innovative Light Detectors for the Search for Neutrinoless Double Beta Decay. Ph.D. Thesis, Université Paris-Sud, Orsay, France, 2016.
314. Zolotarova, A. Study and Selection of Scintillating Crystals for the Bolometric Search for Neutrinoless Double Beta Decay. Ph.D. Thesis, Université Paris-Saclay, Saint-Aubin, France, 2018.
315. Novati, V. Sensitivity Enhancement of the CUORE Experiment Via the Development of Cherenkov Hybrid TeO_2 Bolometers. Ph.D. Thesis, Université Paris-Saclay, Orsay, France, 2018.
316. Tenconi, M.; Chernyak, D.; Danevich, F.; Giuliani, A.; Mancuso, M.; Marnieros, S.; Olivieri, E.; Rusconi, C. Bolometric light detectors for Neutrinoless Double Beta Decay search. *PoS* **2012**, *PhotoDet 2012*, 072.
317. Beeman, J.W.; Bellini, F.; Casali, N.; Cardani, L.; Dafinei, I.; Di Domizio, S.; Ferroni, F.; Gironi, L.; Nagorny, S.; Orio, F.; et al. Characterization of bolometric Light Detectors for rare event searches. *J. Instrum.* **2013**, *8*, P07021. [CrossRef]
318. Barabash, A.S.; Chernyak, D.M.; Danevich, F.A.; Giuliani, A.; Ivanov, I.M.; Makarov, E.P.; Mancuso, M.; Marnieros, S.; Nasonov, S.G.; Nones, C.; et al. Enriched Zn^{100}MoO$_4$ scintillating bolometers to search for $0\nu2\beta$ decay of ^{100}Mo with the LUMINEU experiment. *Eur. Phys. J. C* **2014**, *74*, 3133. [CrossRef]
319. Beeman, J.W.; Bellini, F.; Cardani, L.; Casali, N.; Dafinei, I.; Di Domizio, S.; Ferroni, F.; Orio, F.; Pessina, G.; Pirro, S.; et al. Discrimination of α and β/γ interactions in a TeO_2 bolometer. *Astropart. Phys.* **2012**, *35*, 558–562. [CrossRef]
320. Biassoni, M.; Brofferio, C.; Capelli, S.; Cassina, L.; Clemenza, M.; Cremonesi, O.; Faverzani, M.; Ferri, E.; Giachero, A.; Gironi, L.; et al. Large area Si low-temperature light detectors with Neganov-Luke effect. *Eur. Phys. J. C* **2015**, *75*, 480. [CrossRef]
321. Gironi, L.; Biassoni, M.; Brofferio, C.; Capelli, S.; Carniti, P.; Cassina, L.; Clemenza, M.; Cremonesi, O.; Faverzani, M.; Ferri, E.; et al. Cerenkov light identification with Si low-temperature detectors with Neganov-Luke effect-enhanced sensitivity. *J. Instrum.* **2016**, *94*, 054608. [CrossRef]
322. Abdelhameed, A.H.; Angloher, G.; Bauer, P.; Bento, A.; Bertoldo, E.; Bucci, C.; Canonica, L.; D'Addabbo, A.; Defay, X.; Di Lorenzo, S.; et al. First results on sub-GeV spin-dependent dark matter interactions with ^{7}Li. *Eur. Phys. J. C* **2019**, *79*, 630. [CrossRef]
323. Bertoldo, E.; Abdelhameed, A.H.; Angloher, G.; Bauer, P.; Bento, A.; Breier, R.; Bucci, C.; Canonica, L.; D'Addabbo, A.; Di Lorenzo, S.; et al. Lithium-containing crystals for light dark matter search experiments. *J. Low Temp. Phys.* **2020**, *199*, 510–518. [CrossRef]
324. Pantić, E. Performance of Cryogenic Light Detectors in the CRESST-II Dark Matter Search. Ph.D. Thesis, Technische Universität München, Munich, Germany, 2008.
325. Schäffner, K.; Angloher, G.; Bellini, F.; Casali, N.; Ferroni, F.; Hauff, D.; Nagorny, S.S.; Pattavina, L.; Petricca, F.; Pirro, S.; et al. Particle discrimination in TeO_2 bolometers using light detectors read out by transition edge sensors. *Astropart. Phys.* **2015**, *69*, 30–36. [CrossRef]
326. Rothe, J.; Angloher, G.; Bauer, P.; Bento, A.; Bucci, C.; Canonica, L.; D'Addabbo, A.; Defay, X.; Erb, A.; Feilitzsch, F.V.; et al. TES-Based Light Detectors for the CRESST Direct Dark Matter Search. *J. Low Temp. Phys.* **2018**, *193*, 1160–1166. [CrossRef]
327. Di Stefano, P.C.F.; Frank, T.; Angloher, G.; Bruckmayer, M.; Cozzini, C.; Hauff, D.; Pröbst, F.; Rutzinger, S.; Seidel, W.; Stodolsky, L.; et al. Textured silicon calorimetric light detector. *J. Appl. Phys.* **2003**, *94*, 6887–6891. [CrossRef]
328. Petricca, F. Dark Matter Search with Cryogenic Phonon-Light Detectors. Ph.D. Thesis, Ludwig-Maximilians-Universität, Munich, Germany, 2005.
329. Ren, R.; Bathurst, C.; Chang, Y.Y.; Chen, R.; Fink, C.W.; Hong, Z.; Kurinsky, N.A.; Mast, N.; Mishra, N.; Novati, V.; et al. Design and characterization of a phonon-mediated cryogenic particle detector with an eV-scale threshold and 100 keV-scale dynamic range. *arXiv* **2020**, arXiv:physics.ins-det/2012.12430.
330. Fink, C.W.; Watkins, S.L.; Aramaki, T.; Brink, P.L.; Camilleri, J.; Defay, X.; Ganjam, S.; Kolomensky, Y.G.; Mahapatra, R.; Mirabolfathi, N.; et al. Performance of a large area photon detector for rare event search applications. *Appl. Phys. Lett.* **2021**, *118*, 022601. [CrossRef]
331. Isaila, C.; Boslau, O.; Coppi, C.; Feilitzsch, F.; Goldstraß, P.; Jagemann, T.; Jochum, J.; Kemmer, J.; Lachenmaier, T.; Lanfranchi, J.C.; et al. Scintillation light detectors with Neganov–Luke amplification. *Nucl. Instrum. Methods Phys. Res. A* **2006**, *559*, 399. [CrossRef]
332. Isaila, C. Development of Cryogenic Light Detectors with Neganov-Luke Amplification for the Dark Matter Experiments CRESST and EURECA. Ph.D. Thesis, Technische Universität München, Munich, Germany, 2010.
333. Willers, M. Background Suppression in TeO_2 Bolometers with Neganov-Luke Amplified Cryogenic Light Detectors. Ph.D. Thesis, Technische Universität München, Munich, Germany, 2015.
334. Willers, M.; Feilitzsch, F.V.; Gütlein, A.; Münster, A.; Lanfranchi, J.C.; Oberauer, L.; Potzel, W.; Roth, S.; Schönert, S.; Sivers, M.V.; et al. Neganov-Luke amplified cryogenic light detectors for the background discrimination in neutrinoless double beta decay search with TeO_2 bolometers. *J. Instrum.* **2015**, *10*, P03003. [CrossRef]

335. Singh, V.; Armstrong, W.; Benato, G.; Beretta, M.; Chang, C.L.; Fujikawa, B.K.; Hafidi, K.; Hansen, E.; Huang, R.; Karapetrov, G.; et al. Development of transition-edge sensor based large area photon detectors for CUPID. In Proceedings of the XXIX International (online) Conference on Neutrino Physics and Astrophysics (Neutrino 2020), Minneapolis, MI, USA, 22 June–2 July 2020.
336. Cardani, L.; Casali, N.; Colantoni, I.; Cruciani, A.; Bellini, F.; Castellano, M.G.; Cosmelli, C.; D'Addabbo, A.; Di Domizio, S.; Martinez, M.; et al. High sensitivity phonon-mediated kinetic inductance detector with combined amplitude and phase read-out. *Appl. Phys. Lett.* **2017**, *110*, 033504. [CrossRef]
337. Cardani, L.; Casali, N.; Cruciani, A.; Le Sueur, H.; Martinez, M.; Bellini, F.; Calvo, M.; Castellano, M.G.; Colantoni, I.; Cosmelli, C.; et al. Al/Ti/Al phonon-mediated KIDs for UV–vis light detection over large areas. *Supercond. Sci. Technol.* **2018**, *31*, 075002. [CrossRef]
338. Cardani, L.; Casali, N.; Colantoni, I.; Cruciani, A.; Di Domizio, S.; Martinez, M.; Pettinacci, V.; Pettinari, G.; Vignati, M. Final results of CALDER: Kinetic inductance light detectors to search for rare events. *arXiv* **2021**, arXiv:physics.ins-det/2104.06850.
339. Lee, H.J.; So, J.H.; Kang, C.S.; Kim, G.B.; Kim, S.R.; Lee, J.H.; Lee, M.K.; Yoon, W.S.; Kim, Y.H. Development of a scintillation light detector for a cryogenic rare-event-search experiment. *Nucl. Instrum. Methods Phys. Res. A* **2015**, *784*, 508–512. [CrossRef]
340. Jeon, J.A.; Kim, H.L.; Kim, I.; Kim, S.G.; Kim, S.R.; Kim, T.S.; Kim, Y.H.; Kwon, D.H.; Lee, H.; Song, J.H.; et al. Study on phonon amplification of Neganov-Luke light detectors. *J. Low Temp. Phys.* **2020**, *199*, 883–890. [CrossRef]
341. Gray, D.; Enss, C.; Fleischmann, A.; Gastaldo, L.; Hassel, C.; Hengstler, D.; Kempf, S.; Loidl, M.; Navick, X.F.; Rodrigues, M. The first tests of a large-area light detector equipped with metallic magnetic calorimeters for scintillating bolometers for the LUMINEU neutrinoless double beta decay search. *J. Low Temp. Phys.* **2016**, *184*, 904–909. [CrossRef]
342. Gatti, E.; Manfredi, P. Processing the signals from solid-state detectors in elementary-particle physics. *Riv. Nuovo Cim.* **1986**, *9*, 1. [CrossRef]
343. Radeka, V.; Karlovac, N. Least-square-error amplitude measurement of pulse signals in presence of noise. *Nucl. Instrum. Meth.* **1967**, *52*, 86–92. [CrossRef]
344. Beeman, J.W.; Bellini, F.; Capelli, S.; Cardani, L.; Casali, N.; Dafinei, I.; Di Domizio, S.; Ferroni, F.; Galashov, E.N.; Gironi, L.; et al. $ZnMoO_4$: A promising bolometer for neutrinoless double beta decay searches. *Astropart. Phys.* **2012**, *35*, 813. [CrossRef]
345. Poda, D.V. ^{100}Mo-enriched Li_2MoO_4 scintillating bolometers for $0\nu2\beta$ decay search: From LUMINEU to CUPID-0/Mo projects. *AIP Conf. Proc.* **2017**, *1894*, 020017.
346. Barabash, A.S.; Danevich, F.A.; Gimbal-Zofka, Y.; Giuliani, A.; Mancuso, M.; Konovalov, S.I.; de Marcillac, P.; Marnieros, S.; Nones, C.; Novati, V.; et al. First test of an enriched $^{116}CdWO_4$ scintillating bolometer for neutrinoless double-beta-decay searches. *Eur. Phys. J. C* **2016**, *76*, 487. [CrossRef]
347. Arnaboldi, C.; Capelli, S.; Cremonesi, O.; Gironi, L.; Pavan, M.; Pessina, G.; Pirro, S. Characterization of ZnSe scintillating bolometers for Double Beta Decay. *Astropart. Phys.* **2011**, *34*, 344–353. [CrossRef]
348. Scheel, H.J. Historical aspects of crystal growth technology. *J. Cryst. Growth* **2000**, *211*, 1–12. [CrossRef]
349. Dhanaraj, G.; Byrappa, K.; Prasad, V.; Dudley, M. (Eds.) *Springer Handbook of Crystal Growth*; Springer: Berlin/Heidelberg, Germany, 2010.
350. Shlegel, V.N.; Borovlev, Y.A.; Grigoriev, D.N.; Grigorieva, V.D.; Danevich, F.A.; Ivannikova, N.V.; Postupaeva, A.G.; Vasiliev, Y.V. Recent progress in oxide scintillation crystals development by low-thermal gradient Czochralski technique for particle physics experiments. *J. Instrum.* **2017**, *12*, C08011. [CrossRef]
351. Barabash, A.S.; Belli, P.; Bernabei, R.; Cappella, F.; Caracciolo, V.; Cerulli, R.; Danevich, F.A.; Di Marco, A.; Incicchitti, A.; Kasperovych, D.V.; et al. Low background scintillators to investigate rare processes. *J. Instrum.* **2020**, *15*, C07037. [CrossRef]
352. Degoda, V.Y.; Danevich, F.A.; Grigorieva, V.D.; Podust, G.P.; Shlegel, V.N.; Stanovyy, O. Luminescence of $Li_2Mo_{1-0.05}W_{0.05}O_4$ crystal under X-ray excitation. *Optik* **2020**, *206*, 164273. [CrossRef]
353. Ryadun, A.A.; Rakhmanova, M.I.; Grigorieva, V.D. Photoluminescence properties of perspective bolometric crystals $Na_2Mo_2O_7$ and $Na_2W_2O_7$ grown by low-thermal-gradient Czochralski technique. *Opt. Mat.* **2020**, *99*, 109537. [CrossRef]
354. Kolobanov, V.N.; Kamenskikh, I.A.; Mikhailin, V.V.; Shpinkov, I.N.; Spassky, D.A.; Zadneprovsky, B.I.; Potkin, L.I.; Zimmerer, G. Optical and luminescent properties of anisotropic tungstate crystals. *Nucl. Instrum. Methods Phys. Res. A* **2002**, *486*, 496–503. [CrossRef]
355. Itoh, M. Luminescence study of self-trapped excitons in $CdMoO_4$. *J. Lumin.* **2012**, *132*, 645–651. [CrossRef]
356. Danevich, F.A.; Degoda, V.Y.; Dulger, L.L.; Dumoulin, L.; Giuliani, A.; de Marcillac, P.; Marnieros, S.; Nones, C.; Novati, V.; Olivieri, E.; et al. Growth and characterization of a $Li_2Mg_2(MoO_4)_3$ scintillating bolometer. *Nucl. Instrum. Methods Phys. Res. A* **2018**, *889*, 89–96. [CrossRef]
357. Bashmakova, N.V.; Danevich, F.A.; Degoda, V.Y.; Dmitruk, I.M.; Kudovbenko, V.M.; Kutovyi, S.Y.; Mikhailin, V.V.; Nagorny, S.S.; Nikolaiko, A.S.; Nisi, S. $Li_2Zn_2(MoO_4)_3$ crystal as a potential detector for ^{100}Mo 2β-decay search. *Funct. Mater.* **2009**, *16*, 266–274.
358. Mikhailik, V.B.; Kraus, H.; Itoh, M.; Iri, D.; Uchida, M. Radiative decay of self-trapped excitons in $CaMoO_4$ and $MgMoO_4$ crystals. *J. Phys. Condens. Matter* **2005**, *17*, 7209. [CrossRef]
359. Spassky, D.A.; Kozlova, N.S.; Brik, M.G.; Nagirnyi, V.; Omelkov, S.; Buzanov, O.A.; Buryi, M.; Laguta, V.; Shlegel, V.N.; Ivannikova, N.V. Luminescent, optical and electronic properties of $Na_2Mo_2O_7$ single crystals. *J. Lumin.* **2017**, *192*, 1264–1272. [CrossRef]
360. Spassky, D.A.; Ivanov, S.N.; Kolobanov, V.N.; Mikhailin, V.V.; Zemskov, V.N.; Zadneprovski, B.I.; Potkin, L.I. Optical and luminescent properties of the lead and barium molybdates. *Radiat. Meas.* **2004**, *38*, 607–610. [CrossRef]

361. Mikhailik, V.B.; Elyashevskyi, Y.; Kraus, H.; Kim, H.J.; Kapustianyk, V.; Panasyuk, M. Temperature dependence of scintillation properties of $SrMoO_4$. *Nucl. Instrum. Methods Phys. Res. A* **2015**, *792*, 1–5. [CrossRef]
362. Bergé, L.; Boiko, R.S.; Chapellier, M.; Chernyak, D.M.; Coron, N.; Danevich, F.A.; Decourt, R.; Degoda, V.Y.; Devoyon, L.; Drillien, A.; et al. Purification of molybdenum, growth and characterization of medium volume $ZnMoO_4$ crystals for the LUMINEU program. *J. Instrum.* **2014**, *9*, P06004. [CrossRef]
363. Belhoucif, R.; Velázquez, M.; Petit, Y.; Pérez, O.; Glorieux, B.; Viraphong, O.; de Marcillac, P.; Coron, N.; Torres, L.; Véron, E.; et al. Growth and spectroscopic properties of ^{6}Li- and ^{10}B-enriched crystals for heat-scintillation cryogenic bolometers used in the rare events searches. *CrystEngComm* **2013**, *15*, 3785–3792. [CrossRef]
364. Ogorodnikov, I.N.; Poryvay, N.E.; Sedunova, I.N.; Tolmachev, A.V.; Yavetskiy, R.P. Thermally stimulated recombination processes and luminescence in $Li_6(Y,Gd,Eu)(BO_3)_3$ crystals. *Phys. Solid State* **2011**, *53*, 263–270. [CrossRef]
365. Mikhailik, V.B.; Kraus, H.; Balcerzyk, M.; Czarnacki, W.; Moszyński, M.; Mykhaylyk, M.S.; Wahl, D. Low-temperature spectroscopic and scintillation characterisation of Ti-doped Al_2O_3. *Nucl. Instrum. Methods Phys. Res. A* **2005**, *546*, 523–534. [CrossRef]
366. Yanagida, T.; Fujimoto, Y.; Koshimizu, M.; Kawano, N.; Okada, G.; Kawaguchi, N. Comparative Studies of Optical and Scintillation Properties between $LiGaO_2$ and $LiAlO_2$ Crystals. *J. Phys. Soc. Jpn.* **2017**, *86*, 094201. [CrossRef]
367. Pankratov, V.; Grigorjeva, L.; Millers, D.; Yochum, H.M. Intrinsic luminescence and energy transfer processes in pure and doped YVO_4 crystals. *Phys. Status Solidi C* **2007**, *4*, 801–804. [CrossRef]
368. Smits, K.; Millers, D.; Grigorjeva, L.; Fidelus, J.D.; Lojkowski, W. Comparison of ZrO_2:Y nanocrystals and macroscopic single crystal luminescence. *J. Phys. Conf. Ser.* **2007**, *93*, 012035. [CrossRef]
369. Tsuboi, T.; Silfsten, P. The lifetime of Eu^{2+} fluorescence in CaF_2:Eu^{2+} crystals. *J. Phys. Condens. Matter* **1991**, *3*, 9163. [CrossRef]
370. Nakonechnyi, S.; Kärner, T.; Lushchik, A.; Lushchik, C.; Babin, V.; Feldbach, E.; Kudryavtseva, I.; Liblik, P.; Pung, L.; Vasil'chenko, E. Low-temperature excitonic, electron–hole and interstitial-vacancy processes in LiF single crystals. *J. Phys. Condens. Matter* **2005**, *18*, 379. [CrossRef]
371. Ginestra, C. Characterization of Scintillating Bolometers for Particle Detection and Installation of a Bolometric Test Facility in the University of Zaragoza. Ph.D. Thesis, Universidad de Zaragoza, Zaragoza, Spain, 2013.
372. Shiran, N.; Boiaryntseva, I.; Gektin, A.; Gridin, S.; Shlyakhturov, V.; Vasuykov, S. Luminescence and radiation resistance of undoped NaI crystals. *Mater. Res. Bull.* **2014**, *59*, 13–17. [CrossRef]
373. Edison, T.A. Communication to Lord Kelvin. *Nature* **1896**, *53*, 470–474.
374. McGregor, D.S. Materials for gamma-ray spectrometers: Inorganic scintillators. *Annu. Rev. Mater. Res.* **2018**, *48*, 245–277. [CrossRef]
375. Dorenbos, P. The quest for high resolution γ-ray scintillators. *Opt. Mat. X* **2019**, *1*, 100021. [CrossRef]
376. Cebrián, S.; Coron, N.; Dambier, G.; de Marcillac, P.; García, E.; Irastorza, I.G.; Leblanc, J.; Morales, A.; Morales, J.; de Solórzano, A.O.; et al. First underground light versus heat discrimination for dark matter search. *Phys. Lett. B* **2003**, *563*, 48–52. [CrossRef]
377. Cebrián, S.; Coron, N.; Dambier, G.; García, E.; Irastorza, I.G.; Leblanc, J.; de Marcillac, P.; Morales, A.; Morales, J.; de Solórzano, A.O.; et al. Bolometric WIMP search at Canfranc with different absorbers. *Astropart. Phys.* **2004**, *21*, 23–34. [CrossRef]
378. Angloher, G.; Bucci, C.; Christ, P.; Cozzini, C.; Von Feilitzsch, F.; Hauff, D.; Henry, S.; Jagemann, T.; Jochum, J.; Kraus, H.; et al. Limits on WIMP dark matter using scintillating $CaWO_4$ cryogenic detectors with active background suppression. *Astropart. Phys.* **2005**, *23*, 325–339. [CrossRef]
379. Angloher, G.; Bauer, M.; Bavykina, I.; Bento, A.; Brown, A.; Bucci, C.; Ciemniak, C.; Coppi, C.; Deuter, G.; Von Feilitzsch, F.; et al. Commissioning run of the CRESST-II dark matter search. *Astropart. Phys.* **2009**, *31*, 270–276. [CrossRef]
380. Brown, A.; Henry, S.; Kraus, H.; McCabe, C. Extending the CRESST-II commissioning run limits to lower masses. *Phys. Rev. D* **2012**, *85*, 021301. [CrossRef]
381. Angloher, G.; Bento, A.; Bucci, C.; Canonica, L.; Erb, A.; von Feilitzsch, F.; Iachellini, N.F.; Gorla, P.; Gütlein, A.; Hauff, D.; et al. Results on low mass WIMP using an upgraded CRESST-II detector. *Eur. Phys. J. C* **2014**, *74*, 3184. [CrossRef]
382. Angloher, G.; Bento, A.; Bucci, C.; Canonica, L.; Defay, X.; Erb, A.; von Feilitzsch, F.; Iachellini, N.F.; Gorla, P.; Gütlein, A.; et al. Results on light dark matter particles with a low-threshold CRESST-II detector. *Eur. Phys. J. C* **2016**, *76*, 25. [CrossRef]
383. Abdelhameed, A.H.; Angloher, G.; Bauer, P.; Bento, A.; Bertoldo, E.; Bucci, C.; Canonica, L.; D'Addabbo, A.; Defay, X.; Di Lorenzo, S.; et al. First results from the CRESST-III low-mass dark matter program. *Phys. Rev. D* **2019**, *100*, 102002. [CrossRef]
384. Cebrián, S.; Coron, N.; Dambier, G.; De Marcillac, P.; Garcia, E.; Irastorza, I.G.; Leblanc, J.; Morales, A.; Morales, J.; de Solorzano, A.O.; et al. Improved limits for natural α radioactivity of tungsten with a $CaWO_4$ scintillating bolometer. *Phys. Lett. B* **2003**, *556*, 14–20. [CrossRef]
385. Cozzini, C.; Angloher, G.; Bucci, C.; von Feilitzsch, F.; Hauff, D.; Henry, S.; Jagemann, T.; Jochum, J.; Kraus, H.; Majorovits, B.; et al. Detection of the natural α decay of tungsten. *Phys. Rev. C* **2004**, *70*, 064606. [CrossRef]
386. Angloher, G.; Bauer, M.; Bauer, P.; Bavykina, I.; Bento, A.C.; Bucci, C.; Canonica, L.; Ciemniak, C.; Defay, X.; Deuter, G.; et al. New limits on double electron capture of ^{40}Ca and ^{180}W. *J. Phys. G* **2016**, *43*, 095202. [CrossRef]
387. Danevich, F.A.; Georgadze, A.S.; Kobychev, V.V.; Nagorny, S.S.; Nikolaiko, A.S.; Ponkratenko, O.A.; Tretyak, V.I.; Zdesenko, S.Y.; Zdesenko, Y.G.; Bizzeti, P.G.; et al. α activity of natural tungsten isotopes. *Phys. Rev. C* **2003**, *67*, 014310. [CrossRef]
388. Zdesenko, Y.G.; Avignone, F.T., III; Brudanin, V.B.; Danevich, F.A.; Nagorny, S.S.; Solsky, I.M.; Tretyak, V.I. Scintillation properties and radioactive contamination of $CaWO_4$ crystal scintillators. *Nucl. Instrum. Methods Phys. Res. A* **2005**, *538*, 657–667. [CrossRef]

389. Zdesenko, Y.G.; Avignone, F.T., III; Brudanin, V.B.; Danevich, F.A.; Kobychev, V.V.; Kropivyansky, B.N.; Nagorny, S.S.; Tretyak, V.I.; Vylov, T. CARVEL experiment with $^{48}CaWO_4$ crystal scintillators for the double β decay study of ^{48}Ca. *Astropart. Phys.* **2005**, *23*, 249–263. [CrossRef]
390. Danevich, F.A.; Georgadze, A.S.; Kobychev, V.V.; Kropivyansky, B.N.; Nagorny, S.S.; Nikolaiko, A.S.; Poda, D.V.; Tretyak, V.I.; Zdesenko, S.Y.; Zdesenko, Y.G.; et al. Radioactive contamination of $CaWO_4$, $ZnWO_4$, $CdWO_4$, and Gd_2SiO_5:Ce crystal scintillators. *AIP Conf. Proc.* **2005**, *785*, 87–92.
391. Danevich, F.A.; Bailiff, I.K.; Kobychev, V.V.; Kraus, H.; Laubenstein, M.; Loaiza, P.; Mikhailik, V.B.; Nagorny, S.S.; Nikolaiko, A.S.; Nisi, S.; et al. Effect of recrystallisation on the radioactive contamination of $CaWO_4$ crystal scintillators. *Nucl. Instrum. Methods Phys. Res. A* **2011**, *631*, 44–53. [CrossRef]
392. Meunier, P.; Bravin, M.; Bruckmayer, M.; Giordano, S.; Loidl, M.; Meier, O.; Pröbst, F.; Seidel, W.; Sisti, M.; Stodolsky, L.; et al. Discrimination between nuclear recoils and electron recoils by simultaneous detection of phonons and scintillation light. *Appl. Phys. Lett.* **1999**, *75*, 1335. [CrossRef]
393. Bravin, M.; Bruckmayer, M.; Frank, T.; Giordano, S.; Loidl, M.; Meier, O.; Meunier, P.; Pergolesi, D.; Pröbst, F.; Seidel, W.; et al. Simultaneous measurement of phonons and scintillation light for active background rejection in the CRESST experiment. *Nucl. Instrum. Methods Phys. Res. A* **2000**, *444*, 323–326. [CrossRef]
394. Cebrián, S.; Coron, N.; Dambier, G.; Garcia, E.; Irastorza, I.G.; Leblanc, J.; De Marcillac, P.; Morales, A.; Morales, J.; de Solórzano, A.O.; et al. The ROSEBUD experiment at Canfranc: 2001 report. *Nucl. Phys. B (Proc. Suppl.)* **2002**, *110*, 97–99.
395. Erb, A.; Lanfranchi, J.C. Growth of high-purity scintillating $CaWO_4$ single crystals for the low-temperature direct dark matter search experiments CRESST-II and EURECA. *CrystEngComm* **2013**, *15*, 2301. [CrossRef]
396. Münster, A.; Sivers, M.V.; Angloher, G.; Bento, A.; Bucci, C.; Canonica, L.; Erb, A.; Feilitzsch, F.V.; Gorla, P.; Gütlein, A.; et al. Radiopurity of $CaWO_4$ crystals for direct dark matter search with CRESST and EURECA. *J. Cosmol. Astropart. Phys.* **2014**, *5*, 018. [CrossRef]
397. Strauss, R.; Angloher, G.; Bento, A.; Bucci, C.; Canonica, L.; Erb, A.; von Feilitzsch, F.; Ferreiro, N.; Gorla, P.; Gütlein, A.; et al. A detector module with highly efficient surface-alpha event rejection operated in CRESST-II Phase 2. *Eur. Phys. J. C* **2015**, *75*, 352. [CrossRef]
398. Kiefer, M.; Angloher, G.; Bento, A.; Bucci, C.; Canonica, L.; Erb, A.; von Feilitzsch, F.; Iachellini, N.F.; Gorla, P.; Gütlein, A.; et al. In-situ study of light production and transport in phonon/light detector modules for dark matter search. *Nucl. Instrum. Methods Phys. Res. A* **2016**, *821*, 116–121. [CrossRef]
399. Strauss, R.; Angloher, G.; Bento, A.; Bucci, C.; Canonica, L.; Erb, A.; von Feilitzsch, F.; Iachellini, N.F.; Gorla, P.; Gütlein, A.; et al. Beta/gamma and alpha backgrounds in CRESST-II Phase 2. *J. Cosmol. Astropart. Phys.* **2015**, *06*, 030. [CrossRef]
400. Strauss, R.; Angloher, G.; Bento, A.; Bucci, C.; Canonica, L.; Carli, W.; Erb, A.; von Feilitzsch, F.; Gorla, P.; Gütlein, A.; et al. Energy-dependent light quenching in $CaWO_4$ crystals at mK temperatures. *Eur. Phys. J. C* **2014**, *74*, 2957. [CrossRef]
401. Danevich, F.A.; Zdesenko, Y.G.; Nikolaiko, A.S.; Tretyak, V. Search for 2β decay of ^{116}Cd with the help of a $^{116}CdWO_4$ scintillator. *JETP Lett.* **1989**, *49*, 476.
402. Danevich, F.A.; Georgadze, A.S.; Kobychev, V.V.; Kropivyansky, B.N.; Kuts, V.N.; Nikolaiko, A.S.; Tretyak, V.I.; Zdesenko, Y. The research of 2β decay of ^{116}Cd with enriched $^{116}CdWO_4$ crystal scintillators. *Phys. Lett. B* **1995**, *344*, 72. [CrossRef]
403. Danevich, F.A.; Georgadze, A.S.; Kobychev, V.V.; Kropivyansky, B.N.; Nikolaiko, A.S.; Ponkratenko, O.A.; Tretyak, V.I.; Zdesenko, S.Y.; Zdesenko, Y.G.; Bizzeti, P.G.; et al. Search for 2β decay of cadmium and tungsten isotopes: Final results of the Solotvina experiment. *Phys. Rev. C* **2003**, *68*, 035501. [CrossRef]
404. Belli, P.; Bernabei, R.; Bukilic, N.; Cappella, F.; Cerulli, R.; Dai, C.J.; Danevich, F.A.; De Laeter, J.R.; Incicchitti, A.; Kobychev, V.V.; et al. Investigation of β decay of ^{113}Cd. *Phys. Rev. C* **2007**, *76*, 064603. [CrossRef]
405. Belli, P.; Bernabei, R.; Cappella, F.; Cerulli, R.; Danevich, F.A.; d'Angelo, S.; Incicchitti, A.; Kobychev, V.V.; Nagorny, S.S.; Nozzoli, F.; et al. Search for double-β decay processes in ^{108}Cd and ^{114}Cd with the help of the low-background $CdWO_4$ crystal scintillator. *Eur. Phys. J. A* **2008**, *36*, 167–170. [CrossRef]
406. Barabash, A.S.; Belli, P.; Bernabei, R.; Boiko, R.S.; Cappella, F.; Caracciolo, V.; Chernyak, D.M.; Cerulli, R.; Danevich, F.A.; Di Vacri, M.L.; et al. Low background detector with enriched $^{116}CdWO_4$ crystal scintillators to search for double β decay of ^{116}Cd. *J. Instrum.* **2011**, *6*, P08011. [CrossRef]
407. Belli, P.; Bernabei, R.; Boiko, R.S.; Brudanin, V.B.; Cappella, F.; Caracciolo, V.; Cerulli, R.; Chernyak, D.M.; Danevich, F.A.; d'Angelo, S.; et al. Search for double-β decay processes in ^{106}Cd with the help of a $^{106}CdWO_4$ crystal scintillator. *Phys. Rev. C* **2012**, *85*, 044610. [CrossRef]
408. Belli, P.; Bernabei, R.; Brudanin, V.B.; Cappella, F.; Caracciolo, V.; Cerulli, R.; Danevich, F.A.; Incicchitti, A.; Kasperovych, D.V.; Klavdiienko, V.R.; et al. Search for 2β decay of ^{106}Cd with an enriched $^{106}CdWO_4$ crystal scintillator in coincidence with four HPGe detectors. *Phys. Rev. C* **2016**, *93*, 045502. [CrossRef]
409. Alessandrello, A.; Brofferio, C.; Camin, D.V.; Cremonesi, O.; Fiorini, E.; Giuliani, A.; de Marcillac, P.; Pavan, M.; Pessina, G.; Previtali, E.; et al. High Z Bolometers for Analysis of Internal β and α Activities. *J. Low Temp. Phys.* **1993**, *93*, 815–820. [CrossRef]
410. Helis, D.L. A low energy threshold $CdWO_4$ scintillating bolometer for g_A measurement. In Proceedings of the XXIX International (online) Conference on Neutrino Physics and Astrophysics (Neutrino 2020), Minneapolis, MI, USA, 22 June–2 July 2020.

411. Danevich, F.A.; Georgadze, A.S.; Kobychev, V.V.; Kropivyansky, B.N.; Nagorny, S.S.; Nikolaiko, A.S.; Poda, D.V.; Tretyak, V.I.; Yurchenko, S.S.; Grinyov, B.V.; et al. Application of $PbWO_4$ crystal scintillators in experiment to search for decay of ^{116}Cd. *Nucl. Instrum. Methods Phys. Res. A* **2006**, *556*, 259–265. [CrossRef]
412. Bardelli, L.; Bini, M.; Bizzeti, P.G.; Carraresi, L.; Danevich, F.A.; Fazzini, T.F.; Grinyov, B.V.; Ivannikova, N.V.; Kobychev, V.V.; Kropivyansky, B.N.; et al. Further study of $CdWO_4$ crystal scintillators as detectors for high sensitivity 2β experiments: Scintillation properties and pulse-shape discrimination. *Nucl. Instrum. Methods Phys. Res. A* **2006**, *569*, 743–753. [CrossRef]
413. Gironi, L.; Arnaboldi, C.; Capelli, S.; Cremonesi, O.; Pessina, G.; Pirro, S.; Pavan, M. $CdWO_4$ bolometers for double beta decay search. *Opt. Mat.* **2009**, *31*, 1388–1392. [CrossRef]
414. Gorla, P. Scintillating bolometers for double beta decay search. *J. Low Temp. Phys.* **2008**, *151*, 854–859. [CrossRef]
415. Schäffner, K.; Pröbst, F.; Seidel, W.; Petricca, F.; Hauff, D.; Kleindienst, R. Alternative scintillating materials for the CRESST dark matter search. *J. Low Temp. Phys.* **2012**, *167*, 1075–1080. [CrossRef]
416. Schäffner, K. Study of Backgrounds in the CRESST Dark Matter Search. Ph.D. Thesis, Technischen Universität München, Munich, Germany, 2013.
417. Helis, D.L.; Bandac, I.C.; Barabash, A.S.; Billard, J.; Chapellier, M.; de Combarieu, M.; Danevich, F.A.; Dumoulin, L.; Gascon, J.; Giuliani, A.; et al. Neutrinoless double-beta decay searches with enriched $^{116}CdWO_4$ scintillating bolometers. *J. Low Temp. Phys.* **2020**, *199*, 467. [CrossRef]
418. Galashov, E.N.; Atuchin, V.V.; Kozhukhov, A.S.; Pokrovsky, L.D.; Shlegel, V.N. Growth of $CdWO_4$ crystals by the low thermal gradient Czochralski technique and the properties of a (010) cleaved surface. *J. Cryst. Growth* **2014**, *401*, 156–159. [CrossRef]
419. Giuliani, A.; Danevich, F.A.; Tretyak, V.I. A multi-isotope $0\nu2\beta$ bolometric experiment. *Eur. Phys. J. C* **2018**, *78*, 272. [CrossRef]
420. Barinova, O.; Sadovskiy, A.; Ermochenkov, I.; Kirsanova, S.; Khomyakov, A.; Zykova, M.; Kuchuk, Z.; Avetissov, I. Solid solution Li_2MoO_4–Li_2WO_4 crystal growth and characterization. *J. Cryst. Growth* **2017**, *468*, 365–368. [CrossRef]
421. Matskevich, N.I.; Semerikova, A.N.; Shlegel, V.N.; Zaitsev, V.P.; Matskevich, M.Y.; Anyfrieva, O.I. Czochralski growth, thermodynamic analysis and luminescent properties of $Li_2Mo_{1-x}W_xO_4$ crystal material. *J. Alloys Compd.* **2021**, *850*, 156683. [CrossRef]
422. Aliane, A.; Avetissov, I.C.; Barinova, O.P.; de la Broise, X.; Danevich, F.A.; Dumoulin, L.; Dussopt, L.; Giuliani, A.; Goudon, V.; Kirsanova, S.V.; et al. First test of a Li_2WO_4(Mo) bolometric detector for the measurement of coherent neutrino-nucleus scattering. *Nucl. Instrum. Methods Phys. Res. A* **2020**, *949*, 162784. [CrossRef]
423. Mauri, B. First results from BASKET innovative bolometers for the CEνNS detection. In Proceedings of the XXIX International (online) Conference on Neutrino Physics and Astrophysics (Neutrino 2020), Minneapolis, MI, USA, 22 June–2 July 2020.
424. Bernabei, R.; Belli, P.; Cappella, F.; Cerulli, R.; Montecchia, F.; Nozzoli, F.; Incicchitti, A.; Prosperi, D.; Dai, C.J.; Kuang, H.H.; et al. Dark Matter search. *Riv. Nuovo Cim.* **2003**, *26*, 1–73. [CrossRef]
425. Bernabei, R.; Belli, P.; Cappella, F.; Caracciolo, V.; Castellano, S.; Cerulli, R.; Dai, C.J.; d'Angelo, A.; d'Angelo, S.; Di Marco, A.; et al. Final model independent result of DAMA/LIBRA-phase1. *Eur. Phys. J. C* **2013**, *73*, 2648. [CrossRef]
426. Bernabei, R.; Belli, P.; Bussolotti, A.; Cappella, F.; Caracciolo, V.; Cerulli, R.; Dai, C.J.; d'Angelo, A.; Di Marco, A.; He, H.L.; et al. First model independent results from DAMA/LIBRA-phase2. *Universe* **2018**, *4*, 116 [CrossRef]
427. Bernabei, R.; Belli, P.; Caracciolo, V.; Cerulli, R.; Merlo, V.; Cappella, F.; d'Angelo, A.; Incicchitti, A.; Di Marco, A.; Dai, C.J.; et al. DAMA/LIBRA–phase2 results and implications on several dark matter scenarios. *Int. J. Mod. Phys. A* **2020**, *35*, 2044023. [CrossRef]
428. Pandey, I.R.; Kim, H.J.; Lee, H.S.; Kim, Y.D.; Lee, M.H.; Grigorieva, V.D.; Shlegel, V.N. The $Na_2W_2O_7$ crystal: A crystal scintillator for dark matter search experiment. *Eur. Phys. J. C* **2018**, *78*, 973. [CrossRef]
429. Nagorny, S.; Rusconi, C.; Sorbino, S.; Beeman, J.W.; Bellini, F.; Cardani, L.; Grigorieva, V.D.; Pagnanini, L.; Nisi, S.; Novoselov, I.I.; et al. Na-based crystal scintillators for next-generation rare event searches. *Nucl. Instrum. Methods Phys. Res. A* **2020**, *977*, 164160. [CrossRef]
430. van Loo, W. Luminescence of Lead Molybdate and Lead Tungstate. I. Experimental. *Phys. Status Solidi A* **1979**, *27*, 565–574. [CrossRef]
431. Nagornaya, L.L.; Danevich, F.A.; Dubovik, A.M.; Grinyov, B.V.; Henry, S.; Kapustyanyk, V.; Kraus, H.; Poda, D.V.; Kudovbenko, V.M.; Mikhailik, V.B.; et al. Tungstate and Molybdate scintillators to search for Dark Matter and double beta decay. *IEEE Trans. Nucl. Sci.* **2009**, *56*, 2513–2518. [CrossRef]
432. Danevich, F.A.; Grinyov, B.V.; Henry, S.; Kosmyna, M.B.; Kraus, H.; Krutyak, N.; Kudovbenko, V.M.; Mikhailik, V.B.; Nagornaya, L.L.; Nazarenko, B.P.; et al. Feasibility study of $PbWO_4$ and $PbMoO_4$ crystal scintillators for cryogenic rare events experiments. *Nucl. Instrum. Methods Phys. Res. A* **2010**, *622*, 608–613. [CrossRef]
433. Alessandrello, A.; Arpesella, C.; Brofferio, C.; Bucci, C.; Cattadori, C.; Cremonesi, O.; Fiorini, E.; Giuliani, A.; Latorre, S.; Nucciotti, A.; et al. Measurements of internal radioactive contamination in samples of Roman lead to be used in experiments on rare events. *Nucl. Instrum. Meth. B* **1998**, *142*, 163. [CrossRef]
434. Danevich, F.A.; Kim, S.K.; Kim, H.J.; Kim, Y.D.; Kobychev, V.V.; Kostezh, A.B.; Kropivyansky, B.N.; Laubenstein, M.; Mokina, V.M.; Nagorny, S.S.; et al. Ancient Greek lead findings in Ukraine. *Nucl. Instrum. Methods Phys. Res. A* **2009**, *603*, 328–332. [CrossRef]
435. Beeman, J.W.; Bellini, F.; Cardani, L.; Casali, N.; Di Domizio, S.; Fiorini, E.; Gironi, L.; Nagorny, S.S.; Nisi, S.; Orio, F.; et al. New experimental limits on the α decays of lead isotopes. *Eur. Phys. J. A* **2013**, *49*, 50. [CrossRef]
436. Danevich, F.A.; Zdesenko, Y.G.; Nikolaiko, A.S.; Burachas, S.F.; Nagornaya, L.L.; Ryzhikov, V.D.; Batenchuk, M.M. $CdWO_4$, ZnSe and $ZnWO_4$ scintillators in studies of 2β-processes. *Instr. Exp. R.* **1989**, *32*, 1059–1064.

437. Danevich, F.A.; Kobychev, V.V.; Nagorny, S.S.; Poda, D.V.; Tretyak, V.I.; Yurchenko, S.S.; Zdesenko, Y.G. $ZnWO_4$ crystals as detectors for 2β decay and dark matter experiments. *Nucl. Instrum. Methods Phys. Res. A* **2005**, *544*, 553–564. [CrossRef]
438. Kraus, H.; Mikhailik, V.B.; Ramachers, Y.; Day, D.; Hutton, K.B.; Telfer, J. Feasibility study of a $ZnWO_4$ scintillator for exploiting materials signature in cryogenic WIMP dark matter searches. *Phys. Lett. B* **2005**, *610*, 37–44. [CrossRef]
439. Belli, P.; Bernabei, R.; Cappella, F.; Cerulli, R.; Danevich, F.A.; Dubovik, A.M.; d'Angelo, S.; Galashov, E.N.; Grinyov, B.V.; Incicchitti, A.; et al. Radioactive contamination of $ZnWO_4$ crystal scintillators. *Nucl. Instrum. Methods Phys. Res. A* **2011**, *626–627*, 31–38. [CrossRef]
440. Belli, P.; Bernabei, R.; Borovlev, Y.A.; Cappella, F.; Caracciolo, V.; Cerulli, R.; Danevich, F.A.; Incicchitti, A.; Kasperovych, D.V.; Polischuk, O.G.; et al. New development of radiopure $ZnWO_4$ crystal scintillators. *Nucl. Instrum. Methods Phys. Res. A* **2019**, *935*, 89–94. [CrossRef]
441. Bavykina, I.; Angloher, G.; Hauff, D.; Pantic, E.; Petricca, F.; Pröbst, F.; Seidel, W.; Stodolsky, L. Investigation of $ZnWO_4$ crystals as scintillating absorbers for direct dark matter search experiments. *IEEE Trans. Nucl. Sci.* **2008**, *55*, 1449–1452. [CrossRef]
442. Moszyński, M.; Syntfeld-Każuch, A.; Swiderski, L.; Grodzicka, M.; Iwanowska, J.; SSibczyński, P.; Szczęśniak, T. Energy resolution of scintillation detectors. *Nucl. Instrum. Methods Phys. Res. A* **2016**, *805*, 25–35. [CrossRef]
443. Wolszczak, W.; Dorenbos, P. Nonproportional Response of Scintillators to Alpha Particle Excitation. *IEEE Trans. Nucl. Sci.* **2017**, *64*, 1580–1591.
444. Bavykina, I.; Angloher, G.; Hauff, D.; Kiefer, M.; Petricca, F.; Pröbst, F. Development of cryogenic phonon detectors based on $CaMoO_4$ and $ZnWO_4$ scintillating crystals for direct dark matter search experiments. *Opt. Mat.* **2009**, *31*, 1382–1387. [CrossRef]
445. Belli, P.; Bernabei, R.; Cappella, F.; Caracciolo, V.; Cerulli, R.; Cherubini, N.; Danevich, F.A.; Incicchitti, A.; Kasperovych, D.V.; Merlo, V.; et al. Measurements of $ZnWO_4$ anisotropic response to nuclear recoils for the ADAMO project. *Eur. Phys. J. A* **2020**, *56*, 83. [CrossRef]
446. Jeon, J.A.; Kim, H.L.; Kim, S.R.; Kim, Y.H.; Lee, H.J.; Sekiya, H. Low temperature measurement on directional dependence of phonon-scintillation signals from a zinc tungstate crystal. In Proceedings of the 18th International Workshop on Low Temperature Detectors (LTD-18), Milan, Italy, 22–26 July 2019.
447. Belli, P.; Bernabei, R.; Cappella, F.; Cerulli, R.; Danevich, F.A.; d'Angelo, S.; Incicchitti, A.; Kobychev, V.V.; Poda, D.V.; Tretyak, V.I. Final results of an experiment to search for 2β processes in zinc and tungsten with the help of radiopure $ZnWO_4$ crystal scintillators. *J. Phys. G* **2011**, *38*, 115107. [CrossRef]
448. Casali, N.; Dubovik, A.; Nagorny, S.; Nisi, S.; Orio, F.; Pattavina, L.; Pirro, S.; Schäffner, K.; Tupitsyna, I.; Yakubovskaya, A. Cryogenic Detectors for Rare Alpha Decay Search: A New Approach. *J. Low Temp. Phys.* **2016**, *184*, 952–957. [CrossRef]
449. Khalife, H. BINGO: Bi-Isotope $0\nu2\beta$ Next Generation Observatory. In Proceedings of the GDR DUPhy (Deep Underground Physics) Online Kick-Off Meeting, Lyon, France, 31 May–2 June 2021.
450. Nones, C. (IRFU, CEA, Université Paris-Saclay, Gif-sur-Yvette, France). Private communication, 2021.
451. Belogurov, S.; Kornoukhov, V.; Annenkov, A.; Borisevich, A.; Fedorov, A.; Korzhik, M.; Ligoun, V.; Missevitch, O.; Kim, S.K.; Kim, S.C.; et al. $CaMoO_4$ scintillation crystal for the search of ^{100}Mo double beta decay. *IEEE Trans. Nucl. Sci.* **2005**, *52*, 1131–1135. [CrossRef]
452. Annenkov, A.N.; Buzanov, O.A.; Danevich, F.A.; Georgadze, A.S.; Kim, S.K.; Kim, H.J.; Kim, Y.D.; Kobychev, V.V.; Kornoukhov, V.N.; Korzhik, M.; et al. Development of $CaMoO_4$ crystal scintillators for a double beta decay experiment with ^{100}Mo. *Nucl. Instrum. Methods Phys. Res. A* **2008**, *584*, 334–345. [CrossRef]
453. Bavykina, I. Investigation of $ZnWO_4$ and $CaMoO_4$ as Target Materials for the CRESST-II Dark Matter Search. Ph.D. Thesis, Ludwig-Maximilians-Universität München, Munich, Germany, 2009.
454. Bhang, H.; Boiko, R.S.; Chernyak, D.M.; Choi, J.H.; Choi, S.; Danevich, F.A.; Efendiev, K.V.; Enss, C.; Fleischmann, A.; Gangapshev, A.M.; et al. AMoRE experiment: A search for neutrinoless double beta decay of ^{100}Mo isotope with $^{40}Ca^{100}MoO_4$ cryogenic scintillation detector. *J. Phys. Conf. Ser.* **2012**, *375*, 042023. [CrossRef]
455. Alenkov, V.V.; Buzanov, O.A.; Khanbekov, N.; Kim, S.K.; Kim, H.J.; Kornoukhov, V.N.; Kraus, H.; Mikhailik, V.B. Growth and characterization of isotopically enriched $^{40}Ca^{100}MoO_4$ single crystals for rare event search experiments. *Cryst. Res. Technol.* **2011**, *46*, 1223–1228. [CrossRef]
456. Meija, J.; Coplen, T.B.; Berglund, M.; Brand, W.A.; De Bièvre, P.; Grüning, M.; Holden, N.E.; Irrgeher, J.; Loss, R.D.; Walczyk, T.; et al. Isotopic compositions of the elements 2013 (IUPAC Technical Report). *Pure Appl. Chem.* **2016**, *88*, 293. [CrossRef]
457. Lee, J.Y.; Alenkov, V.; Ali, L.; Beyer, J.; Bibi, R.; Boiko, R.S.; Boonin, K.; Buzanov, O.; Chanthima, N.; Cheoun, M.K.; et al. A Study of Radioactive Contamination of $^{40}Ca^{100}MoO_4$ Crystals for the AMoRE Experiment. *IEEE Trans. Nucl. Sci.* **2016**, *63*, 543–547. [CrossRef]
458. Alenkov, V.V.; Buzanov, O.A.; Dosovitskii, A.E.; Kornoukhov, V.N.; Mikhlin, A.L.; Moseev, P.S.; Khanbekov, N.D. Ultrapurification of Isotopically Enriched Materials for $^{40}Ca^{100}MoO_4$ Crystal Growth. *Inorg. Mater.* **2013**, *49*, 1220–1223. [CrossRef]
459. Park, H.K. Purifications of calcium carbonate and molybdenum oxide powders for neutrinoless double beta decay experiment AMoRE. *AIP Conf. Proc.* **2015**, *1672*, 150003.
460. Kim, G.B.; Choi, S.; Danevich, F.A.; Fleischmann, A.; Kang, C.S.; Kim, H.J.; Kim, S.R.; Kim, Y.D.; Kim, Y.H.; Kornoukhov, V.A.; et al. A $CaMoO_4$ crystal low temperature detector for the AMoRE neutrinoless double beta decay search. *Adv. High Energy Phys.* **2015**, *2015*, 817530. [CrossRef]

461. Kim, G.B.; Choi, J.H.; Jo, H.S.; Kang, C.S.; Kim, H.J.; Kim, H.L.; Kim, I.W.; Kim, S.R.; Kim, Y.D.; Kim, Y.H.; et al. Heat and light measurement of a $^{40}Ca^{100}MoO_4$ crystal for the AMoRE double beta decay experiment. *IEEE Trans. Nucl. Sci.* **2016**, *63*, 539–542. [CrossRef]
462. Kim, G.B.; Choi, J.H.; Jo, H.S.; Kang, C.S.; Kim, H.L.; Kim, I.; Kim, S.R.; Kim, Y.H.; Lee, C.; Lee, H.J.; et al. Novel measurement method of heat and light detection for neutrinoless double beta decay. *Astropart. Phys.* **2017**, *91*, 105–112. [CrossRef]
463. Kang, C.S.; Jeon, J.A.; Jo, H.S.; Kim, G.B.; Kim, H.L.; Kim, I.; Kim, S.R.; Kim, Y.H.; Kwon, D.H.; Lee, C.; et al. MMC-based low-temperature detector system of the AMoRE-Pilot experiment. *Supercond. Sci. Technol.* **2017**, *30*, 084011. [CrossRef]
464. Jo, H.S.; Choi, S.; Danevich, F.A.; Fleischmann, A.; Jeon, J.A.; Kang, C.S.; Kang, W.G.; Kim, G.B.; Kim, H.J.; Kim, H.L.; et al. Status of the AMoRE Experiment Searching for Neutrinoless Double Beta Decay Using Low-Temperature Detectors. *J. Low Temp. Phys.* **2018**, *193*, 1182–1189. [CrossRef]
465. Alenkov, V.; Bae, H.W.; Beyer, J.; Boiko, R.S.; Boonin, K.; Buzanov, O.; Chanthima, N.; Cheoun, M.K.; Chernyak, D.M.; Choe, J.S.; et al. First results from the AMoRE-Pilot neutrinoless double beta decay experiment. *Eur. Phys. J. C* **2019**, *79*, 791. [CrossRef]
466. Jo, H.S. Status of the AMoRE experiment. *J. Phys. Conf. Ser.* **2017**, *888*, 012232. [CrossRef]
467. Luqman, A.; Ha, D.H.; Lee, J.J.; Jeon, E.J.; Jo, H.S.; Kim, H.J.; Kim, Y.D.; Kim, Y.H.; Kobychev, V.V.; Lee, H.S.; et al. Simulations of background sources in AMoRE-I experiment. *Nucl. Instrum. Methods Phys. Res. A* **2017**, *855*, 140–147. [CrossRef]
468. Lee, J.Y. AMoRE: A search for neutrinoless double-beta decay of ^{100}Mo using low-temperature molybdenum-containing crystal detectors. *J. Instrum.* **2020**, *15*, C08010. [CrossRef]
469. Park, H.K. The AMoRE search for neutrinoless double beta decay in ^{100}Mo. In Proceedings of the 11th International Conference MEDEX'2017, Prague, Czech Republic, 29 May–2 June 2017.
470. Pirro, S. Radiopure scintillators for Double Beta Decay searches. In Proceedings of the International Workshop on Radiopure Scintillators for EURECA (RPSCINT-2008), Kyiv, Ukraine, 9–10 September 2008.
471. Xue, M.X.; Zhang, Y.L.; Peng, H.P.; Xu, Z.Z.; Wang, X.L. Study of $CdMoO_4$ crystal for a neutrinoless double beta decay experiment with ^{116}Cd and ^{100}Mo nuclides. *Chin. Phys. C* **2017**, *41*, 046002. [CrossRef]
472. Xue, M.; Poda, D.V.; Zhang, Y.; Khalife, H.; Giuliani, A.; Peng, H.; de Marcillac, P.; Olivieri, E.; Wen, S.; Zhao, K.; et al. First test of a $CdMoO_4$ scintillating bolometer for neutrinoless double beta decay experiments with ^{116}Cd and ^{100}Mo nuclides. *Nucl. Instrum. Methods Phys. Res. A* **2019**, *943*, 162395. [CrossRef]
473. Barinova, O.P.; Cappella, F.; Cerulli, R.; Danevich, F.A.; Kirsanova, S.V.; Kobychev, V.V.; Laubenstein, M.; Nagorny, S.S.; Nozzoli, F.; Tretyak, V.I. Intrinsic radiopurity of a Li_2MoO_4 crystal. *Nucl. Instrum. Methods Phys. Res. A* **2009**, *607*, 573. [CrossRef]
474. Cardani, L.; Casali, N.; Nagorny, S.; Pattavina, L.; Piperno, G.; Barinova, O.P.; Beeman, J.W.; Bellini, F.; Danevich, F.A.; Di Domizio, S.; et al. Development of a Li_2MoO_4 scintillating bolometer for low background physics. *J. Instrum.* **2013**, *8*, P10002. [CrossRef]
475. Poda, D.V.; Bergé, L.; Boiko, R.S.; Chapellier, M.; Chernyak, D.M.; Coron, N.; Danevich, F.A.; Devoyond, L.; Drillien, A.-A.; Dumoulin, L.; et al. Molybdenum containing scintillating bolometers for double-beta decay search (LUMINEU program). In Proceedings of the 3rd French-Ukrainian workshop on the instrumentation developments for High Energy Physics, Orsay, France, 15–16 October 2015; 2015; pp. 86–94.
476. Grigorieva, V.D.; Shlegel, V.N.; Borovlev, Y.A.; Bekker, T.B.; Barabash, A.S.; Konovalov, S.I.; Umatov, V.I.; Borovkov, V.I. Li_2MoO_4 crystals grown by low thermal gradient Czochralski technique. *J. Mat. Sci. Eng. B* **2017**, *7*, 63.
477. Giuliani, A. A neutrinoless double-beta-decay search based on $ZnMoO_4$ and Li_2MoO_4 scintillating bolometers. *J. Phys. Conf. Ser.* **2017**, *888*, 012239. [CrossRef]
478. Veber, P.; Moutatouia, M.; De Marcillac, P.; Giuliani, A.; Loaiza, P.; Denux, D.; Decourt, R.; El Hafid, H.; Laubenstein, M. Exploratory growth in the Li_2MoO_4-MoO_3 system for the next crystal generation of heat-scintillation cryogenic bolometers. *Solid State Sci.* **2017**, *65*, 41.
479. Buşe, G.; Giuliani, A.; de Marcillac, P.; Marnieros, S.; Nones, C.; Novati, V.; Olivieri, E.; Poda, D.V.; Redon, T.; Sand, J.B.; et al. First scintillating bolometer tests of a CLYMENE R&D on Li_2MoO_4 scintillators towards a large-scale double-beta decay experiment. *Nucl. Instrum. Methods Phys. Res. A* **2018**, *891*, 87–91.
480. Stelian, C.; Velázquez, M.; Veber, P.; Ahmine, A.; Sand, J.B.; Buşe, G.; Cabane, H.; Duffar, T. Numerical modeling of Czochralski growth of Li_2MoO_4 crystals for heat-scintillation cryogenic bolometers. *J. Cryst. Growth* **2018**, *545*, 6–12. [CrossRef]
481. Stelian, C.; Velázquez, M.; Veber, P.; Ahmine, A.; Duffar, T.; de Marcillac, P.; Giuliani, A.; Poda, D.V.; Marnieros, S.; Nones, C.; et al. Experimental and numerical investigations of the Czochralski growth of Li_2MoO_4 crystals for heat-scintillation cryogenic bolometers. *J. Cryst. Growth* **2020**, *531*, 125385. [CrossRef]
482. Ra, S.; Lee, C.H.; Son, J.K.; Shin, K.A.; Choe, J.S.; Kim, D.Y.; Lee, M.H.; Kang, W.G.; Leonard, D.; So, J.H.; et al. Scintillation crystal growth at the CUP. *PoS* **2018**, *ICHEP2018*, 668.
483. Son, J.K.; Choe, J.; Gileva, O.; Hahn, I.S.; Kang, W.; Kim, D.; Kim, G.; Kim, H.J.; Kim, Y.D.; Lee, C.; et al. Growth and development of pure Li_2MoO_4 crystals for rare event experiment at CUP. *J. Instrum.* **2020**, *15*, C07035. [CrossRef]
484. Kim, H.L.; Jeon, J.A.; Kim, I.; Kim, S.R.; Kim, H.J.; Kim, Y.H.; Kwon, D.H.; Lee, M.K.; So, J.H. Compact phonon-scintillation detection system for rare event searches at low temperatures. *Nucl. Instrum. Methods Phys. Res. A* **2020**, *954*, 162107. [CrossRef]
485. Kim, H.L.; Kim, H.J.; Kim, I.; Kim, S.R.; Kim, Y.D.; Kim, Y.H.; Kwon, D.H.; Jeon, J.A.; Lee, M.H.; Lee, M.K.; et al. Li_2MoO_4 Phonon–Scintillation Detection Systems with MMC Readout. *J. Low Temp. Phys.* **2020**, *199*, 1082. [CrossRef]
486. Chen, P.; Jiang, L.; Chen, Y.; Chen, H.; Xue, M.; Zhang, Y.; Xu, Z. Bridgman growth and luminescence properties of Li_2MoO_4 single crystal. *Mater. Lett.* **2018**, *215*, 225–228. [CrossRef]

487. Chen, P.; Wei, R.; Jiang, L.; Yang, S.; Chen, Y.; Wang, Z.; Yu, H.; Chen, H. Crystal defects of Li_2MoO_4 scintillators grown by Bridgman method. *J. Cryst. Growth* **2018**, *500*, 80–84. [CrossRef]
488. Scintillating Bolometer Crystal Growth and Purification for NeutriNoless Double Beta Decay Experiments. Available online: https://www.sbir.gov/sbirsearch/detail/1645701 (accessed on 30 June 2021).
489. Johnston, J. Applications of Low Temperature Bolometers to Reactor Neutrinos and Neutrinoless Double Beta Decay. Ph.D. Thesis, Massachusetts Institute of Technology, Cambridge, MA, USA, 2021.
490. Hizhnyi, Y.; Borysyuk, V.; Chornii, V.; Nedilko, S.; Tesel'ko, P.O.; Dubovik, O.; Maksymchuk, P.; Tupitsyna, I.; Yakubovskaya, A.; Androulidaki, M.; et al. Role of native and impurity defects in optical absorption and luminescence of Li_2MoO_4 scintillation crystals. *J. Alloys Compd.* **2021**, *867*, 159148. [CrossRef]
491. Barinova, O.; Sadovskiy, A.; Ermochenkov, I.; Kirsanova, S.; Sukhanova, E.; Kostikov, V.; Belov, S.; Mozhevitina, E.; Khomyakov, A.; Kuchuk, Z.; et al. Li_2MoO_4 crystal growth from solution activated by low-frequency vibrations. *J. Cryst. Growth* **2017**, *457*, 151–157. [CrossRef]
492. Spassky, D.A.; Nagirnyi, V.; Savon, A.E.; Kamenskikh, I.A.; Barinova, O.P.; Kirsanova, S.V.; Grigorieva, V.D.; Ivannikova, N.V.; Shlegel, V.N.; Aleksanyan, E.; et al. Low temperature luminescence and charge carrier trapping in a cryogenic scintillator Li_2MoO_4. *J. Lumin.* **2015**, *166*, 195–202. [CrossRef]
493. Grigorieva, V.D.; Shlegel, V.N.; Borovlev, Y.A.; Ryaduna, A.A.; Bekker, T.B. Bolometric molybdate crystals grown by low-thermal-gradient Czochralski technique. *J. Cryst. Growth* **2019**, *523*, 125144. [CrossRef]
494. Grigorieva, V.D.; Shlegel, V.N.; Borovlev, Y.A.; Bekker, T.B.; Barabash, A.S.; Konovalov, S.I.; Umatov, V.I.; Borovkov, V.I.; Meshkov, O.I. $Li_2{}^{100depl}MoO_4$ crystals grown by low-thermal-gradient Czochralski technique. *J. Cryst. Growth* **2020**, *552*, 125913. [CrossRef]
495. Wang, G.; Chang, C.L.; Yefremenko, V.; Ding, J.; Novosad, V.; Bucci, C.; Canonica, L.; Gorla, P.; Nagorny, S.S.; Pagliarone, C.; et al. CUPID: CUORE (Cryogenic Underground Observatory for Rare Events) Upgrade with Particle IDentification. *arXiv* **2015**, arXiv:physics.ins-det/1504.03599.
496. Wang, G.; Chang, C.L.; Yefremenko, V.; Ding, J.; Novosad, V.; Bucci, C.; Canonica, L.; Gorla, P.; Nagorny, S.S.; Pagliarone, C.; et al. R&D towards CUPID (CUORE Upgrade with Particle IDentification). *arXiv* **2015**, arXiv:physics.ins-det/1504.03612.
497. Schmidt, B. First data from the CUPID-Mo neutrinoless double beta decay experiment. *J. Phys. Conf. Ser.* **2020**, *1468*, 012129. [CrossRef]
498. Poda, D.V. Performance of the CUPID-Mo double-beta decay bolometric experiment. In Proceedings of the XXIX International (online) Conference on Neutrino Physics and Astrophysics (Neutrino 2020), Minneapolis, MI, USA, 22 June–2 July 2020.
499. Huang, R.; Armengaud, E.; Augier, C.; Barabash, A.S.; Bellini, F.; Benato, G.; Benoît, A.; Beretta, M.; Bergé, L.; Billard, J.; et al. Pulse shape discrimination in CUPID-Mo using principal component analysis. *J. Instrum.* **2021**, *16*, P03032. [CrossRef]
500. Zolotarova, A. The CROSS experiment: Search for $0\nu2\beta$ decay with surface sensitive bolometers. *J. Phys. Conf. Ser.* **2020**, *1468*, 012147. [CrossRef]
501. Zolotarova, A. First results of CROSS underground measurements with massive bolometers. In Proceedings of the XXIX International (Online) Conference on Neutrino Physics and Astrophysics (Neutrino 2020), Minneapolis, MI, USA, 22 June–2 July 2020.
502. Belli, P.; Bernabei, R.; Cerulli, R.; Danevich, F.A.; d'Angelo, A.; Goriletsky, V.I.; Grinyov, B.V.; Incicchitti, A.; Kobychev, V.V.; Laubenstein, M.; et al. ^{7}Li solar axions: Preliminary results and feasibility studies. *Nucl. Phys. A* **2008**, *806*, 388–397. [CrossRef]
503. Belli, P.; Bernabei, R.; Cappella, F.; Cerulli, R.; Danevich, F.A.; Incicchitti, A.; Kobychev, V.V.; Laubenstein, M.; Polischuk, O.G.; Tretyak, V.I. Search for ^{7}Li solar axions using resonant absorption in LiF crystal: Final results. *Phys. Lett. B* **2012**, *711*, 41–45. [CrossRef]
504. Khalife, H. CROSS and CUPID-Mo: Future Strategies and New Results in Bolometric Search for $0\nu\beta\beta$. Ph.D. Thesis, Université Paris-Saclay, Saint-Aubin, France, 2021.
505. Huang, R.G.; Benato, G.; Caravaca, J.; Kolomensky, Y.G.; Land, B.J.; Gann, G.O.; Schmidt, B. Characterization of light production and transport in tellurium dioxide crystals. *J. Instrum.* **2019**, *14*, P10032. [CrossRef]
506. Battistelli, E.S.; Bellini, F.; Bucci, C.; Calvo, M.; Cardani, L.; Casali, N.; Castellano, M.G.; Colantoni, I.; Coppolecchia, A.; Cosmelli, C.; et al. CALDER: Neutrinoless double-beta decay identification in TeO_2 bolometers with kinetic inductance detectors. *Eur. Phys. J. C* **2015**, *75*, 353. [CrossRef]
507. Spasskii, D.A.; Kolobanov, V.N.; Mikhaĭlin, V.V.; Berezovskaya, L.Y.; Ivleva, L.I.; Voronina, I.S. Luminescence peculiarities and optical properties of $MgMoO_4$ and $MgMoO_4$:Yb crystals. *Opt. Spectrosc.* **2009**, *106*, 556–563. [CrossRef]
508. Pandey, I.R.; Kim, H.J.; Kim, Y.D. Growth and characterization of $Na_2Mo_2O_7$ crystal scintillators for rare event searches. *J. Cryst. Crowth* **2017**, *480*, 62–66. [CrossRef]
509. Minowa, M.; Itakura, K.; Moriyama, S.; Ootani, W. Measurement of the property of cooled lead molybdate as a scintillator. *Nucl. Instrum. Methods Phys. Res. A* **1992**, *320*, 500–503. [CrossRef]
510. Gonzalez-Mestres, L. Low temperature scintillation and particle detection. In Proceedings of the IV International Workshop on Low Temperature Detectors for Neutrinos and Dark Matter (LTD-4), Oxford, UK, 4–7 September 1991; Booth, N.E., Salmon, G.L., Eds.; pp. 471–479.
511. Nagorny, S.; Pattavina, L.; Kosmyna, M.B.; Nazarenko, B.P.; Nisi, S.; Pagnanini, L.; Pirro, S.; Schäffner, K.; Shekhovtsov, A.N. $^{arch}PbMoO_4$ scintillating bolometer as detector to searches for the neutrinoless double beta decay of ^{100}Mo. *J. Phys. Conf. Ser.* **2017**, *841*, 012025. [CrossRef]

512. Pattavina, L.; Nagorny, S.; Nisi, S.; Pagnanini, L.; Pessina, G.; Pirro, S.; Rusconi, C.; Schäffner, K.; Shlegel, V.N.; Zhdankov, V.N. Production and characterisation of a $PbMoO_4$ cryogenic detector from archaeological Pb. *Eur. Phys. J. A* **2020**, *56*, 38. [CrossRef]
513. Mikhailik, V.B.; Kraus, H. Development of techniques for characterisation of scintillation materials for cryogenic application. *Rad. Meas.* **2013**, *49*, 7–12. [CrossRef]
514. Beeman, J.W.; Danevich, F.A.; Degoda, V.Y.; Galashov, E.N.; Giuliani, A.; Kobychev, V.V.; Mancuso, M.; Marnieros, S.; Nones, C.; Olivieri, E.; et al. A next-generation neutrinoless double beta decay experiment based on $ZnMoO_4$ scintillating bolometers. *Phys. Lett. B* **2012**, *710*, 318. [CrossRef]
515. Tenconi, M. LUMINEU: A Pilot Scintillating Bolometer Experiment for Neutrinoless Double Beta Decay Search. *Phys. Procedia* **2015**, *61*, 782–786. [CrossRef]
516. Danevich, F.A.; Bergé, L.; Boiko, R.S.; Chapellier, M.; Chernyak, D.M.; Coron, N.; Devoyon, L.; Drillien, A.A.; Dumoulin, L.; Enss, C.; et al. Status of LUMINEU program to search for neutrinoless double beta decay of ^{100}Mo with cryogenic $ZnMoO_4$ scintillating bolometers. *AIP Conf. Proc.* **2015**, *1686*, 020007.
517. Armengaud, E.; Arnaud, Q.; Augier, C.; Benoît, A.; Benoît, A.; Bergé, L.; Boiko, B.S.; Bergmann, T.; Blümer, J.; Broniatowski, A.; et al. LUMINEU: A search for neutrinoless double beta decay based on $ZnMoO_4$ scintillating bolometers. *J. Phys. Conf. Ser.* **2016**, *718*, 062008. [CrossRef]
518. Gironi, L.; Arnaboldi, C.; Beeman, J.W.; Cremonesi, O.; Danevich, F.A.; Degoda, V.Y.; Ivleva, L.I.; Nagornaya, L.L.; Pavan, M.; Pessina, G.; et al. Performance of $ZnMoO_4$ crystal as cryogenic scintillating bolometer to search for double beta decay of molybdenum. *J. Instrum.* **2010**, *5*, P11007. [CrossRef]
519. Beeman, J.W.; Bellini, F.; Brofferio, C.; Cardani, L.; Casali, N.; Cremonesi, O.; Dafinei, I.; Di Domizio, S.; Ferroni, F.; Gorello, E.; et al. Performances of a large mass $ZnMoO_4$ scintillating bolometer for a next generation 0νDBD experiment. *Eur. Phys. J. C* **2012**, *72*, 2142. [CrossRef]
520. Mancuso, M.; Chernyak, D.M.; Danevich, F.A.; Dumoulin, L.; Giachero, A.; Giuliani, A.; Godfrin, H.; Gotti, C.; Ivanov, I.M.; Maino, M.; et al. An aboveground pulse-tube-based bolometric test facility for the validation of the LUMINEU $ZnMoO_4$ crystals. *J. Low Temp. Phys.* **2014**, *176*, 571. [CrossRef]
521. Poda, D.V. Scintillating bolometers based on $ZnMoO_4$ and $Zn^{100}MoO_4$ crystals to search for $0\nu2\beta$ decay of ^{100}Mo (LUMINEU project): first tests at the Modane Underground Laboratory. *Nucl. Part. Phys. Proc.* **2016**, *273-275*, 1801–1806. [CrossRef]
522. Armengaud, E.; Arnaud, Q.; Augier, C.; Benoît, A.; Benoît, A.; Bergé, L.; Boiko, R.S.; Bergmann, T.; Blümer, J.; Broniatowski, A.; et al. Development and underground test of radiopure $ZnMoO_4$ scintillating bolometers for the LUMINEU $0\nu2\beta$ project. *J. Instrum.* **2015**, *10*, P05007. [CrossRef]
523. Chernyak, D.M.; Danevich, F.A.; Degoda, V.Y.; Giuliani, A.; Ivanov, I.M.; Kogut, Y.P.; Kraus, H.; Kropivyansky, B.N.; Makarov, E.P.; Mancuso, M.; et al. Effect of tungsten doping on $ZnMoO_4$ scintillating bolometer performance. *Opt. Mat.* **2015**, *49*, 67. [CrossRef]
524. Poda, D.V.; Armengaud, E.; Arnaud, Q.; Augier, C.; Barabash, A.S.; Benoît, A.; Benoît, A.; Bergé, L.; Boiko, R.S.; Bergmann, T.; et al. Radiopure $ZnMoO_4$ scintillating bolometers for the LUMINEU double-beta experiment. *AIP Conf. Proc.* **2015**, *1672*, 040003.
525. Belli, P.; Cerulli, R.; Danevich, F.A.; Grinyov, B.V.; Incicchitti, A.; Kobychev, V.V.; Laubenstein, M.; Nagorny, S.S.; Tolmachev, A.V.; Tretyak, V.I.; et al. Intrinsic radioactivity of a $Li_6Eu(BO_3)_3$ crystal and α decays of Eu. *Nucl. Instrum. Methods Phys. Res. A* **2007**, *572*, 734–738. [CrossRef]
526. Belli, P.; Bernabei, R.; Cappella, F.; Cerulli, R.; Dai, C.J.; Danevich, F.A.; d'Angelo, A.; Incicchitti, A.; Kobychev, V.V.; Nagorny, S.S.; et al. Search for α decay of natural Europium. *Nucl. Phys. A* **2007**, *789*, 15–29. [CrossRef]
527. Casali, N.; Nagorny, S.S.; Orio, F.; Pattavina, L.; Beeman, J.W.; Bellini, F.; Cardani, L.; Dafinei, I.; Di Domizio, S.; Di Vacri, M.L.; et al. Discovery of the ^{151}Eu α decay. *J. Phys. G* **2014**, *41*, 075101. [CrossRef]
528. Pattavina, L. Li-containing scintillating bolometers for low background physics. *EPJ Web Conf.* **2014**, *65*, 02003. [CrossRef]
529. Czirr, J.B.; MacGillivray, G.M.; MacGillivray, R.R.; Seddon, P.J. Performance and characteristics of a new scintillator. *Nucl. Instrum. Math. A* **1999**, *424*, 15–19. [CrossRef]
530. Torres Ferrández, L.C. Bolómetros Centelleadores para Búsqueda de Materia Oscura. Ph.D. Thesis, Universidad de Zaragoza, Zaragoza, Spain, 2008.
531. Cerdeño, D.G.; Cuesta, C.; Fornasa, M.; García, E.; Ginestra, C.; Huh, J.H.; Martínez, M.; Ortigoza, Y.; Peiró, M.; Puimedón, J.; et al. Complementarity of dark matter direct detection: The role of bolometric targets. *J. Cosmol. Astropart. Phys.* **2013**, *7*, 028.
532. de Bellefon, A.; Berkes, I.; Bobin, C.; Broszkiewicz, D.; Chambon, B.; Chapellier, M.; Chardin, G.; Charvin, P.; Chazal, V.; Coron, N.; et al. Dark matter search with a low temperature sapphire bolometer. *Astropart. Phys.* **1996**, *6*, 35–43. [CrossRef]
533. Cebrián, S.; Coron, N.; Dambier, G.; García, E.; González, D.; Irastorza, I.G.; Leblanc, J.; de Marcillac, P.; Morales, A.; Morales, J.; et al. Performances and prospects of the "ROSEBUD" dark matter search experiment. *Astropart. Phys.* **1999**, *10*, 361–368. [CrossRef]
534. Cebrián, S.; Coron, N.; Dambier, G.; García, E.; González, D.; Irastorza, I.G.; Leblanc, J.; de Marcillac, P.; Morales, A.; Morales, J.; et al. Status of the ROSEBUD Dark Matter search experiment. *Nucl. Instrum. Methods Phys. Res. A* **2000**, *444*, 315–318. [CrossRef]
535. Cebrián, S.; Coron, N.; Dambier, G.; García, E.; González, D.; Irastorza, I.G.; Leblanc, J.; de Marcillac, P.; Morales, A.; Morales, J.; et al. Performances and prospects of the "ROSEBUD" dark matter search experiment. In Proceedings of the Third International Workshop on The Identification of Dark Matter, York, UK, 18–22 September 2000.
536. Bravin, M.; Bruckmayer, M.; Bucci, C.; Cooper, S.; Giordano, S.; Von Feilitzsch, F.; Höhne, J.; Jochum, J.; Jörgens, V.; Keeling, R.; et al. The CRESST dark matter search. *Astropart. Phys.* **1999**, *12*, 107–114. [CrossRef]

537. Angloher, G.; Bruckmayer, M.; Bucci, C.; Bühler, M.; Cooper, S.; Cozzini, C.; DiStefano, P.; Von Feilitzsch, F.; Frank, T.; Hauff, D.; et al. Limits on WIMP dark matter using sapphire cryogenic detectors. *Astropart. Phys.* **2002**, *18*, 43–55. [CrossRef]
538. Amaré, J.; Beltrán, B.; Cebrián, S.; García, E.; Gómez, H.; Irastorza, I.G.; Luzón, G.; Martínez, M.; Morales, J.; de Solórzano, A.O.; et al. Light yield of undoped sapphire at low temperature under particle excitation. *Appl. Phys. Lett.* **2005**, *87*, 264102. [CrossRef]
539. Amaré, J.; Beltrán, B.; Carmona, J.M.; Cebrián, S.; Coron, N.; Dambier, G.; García, E.; Irastorza, I.G.; Gómez, H.; Leblanc, J.; et al. Recent developments on scintillating bolometers for WIMP searches: ROSEBUD status. *J. Phys. Conf. Ser.* **2006**, *39*, 133–135. [CrossRef]
540. Ortigoza, Y.; Coron, N.; Cuesta, C.; García, E.; Ginestra, C.; Gironnet, J.; De Marcillac, P.; Martínez, M.; Pobes, C.; Puimedón, J.; et al. Energy partition in sapphire and BGO scintillating bolometers. *Astropart. Phys.* **2011**, *34*, 603–607. [CrossRef]
541. Ortigoza, Y.; Torres, L.; Coron, N.; Cuesta, C.; García, E.; Ginestra, C.; Gironnet, J.; de Marcillac, P.; Martínez, M.; de Solórzano, A.O.; et al. Light Relative Efficiency Factors for ions in BGO and Al_2O_3 at 20 mK. *Astropart. Phys.* **2013**, *50-52*, 11–17. [CrossRef]
542. Di Stefano, P.C.F.; Coron, N.; De Marcillac, P.; Dujardin, C.; Luca, M.; Petricca, F.; Proebst, F.; Vanzetto, S.; Verdier, M.A. The SciCryo Project and Cryogenic Scintillation of Al_2O_3 for Dark Matter. *J. Low Temp. Phys.* **2008**, *151*, 902–907. [CrossRef]
543. Luca, M. Sapphire Scintilation Tests for Cryogenic Detectors in the EDELWEISS Dark Matter Search. Ph.D. Thesis, Université Claude Bernard Lyon-I, Lyon, France, 2007.
544. Coron, N.; García, E.; Gironnet, J.; Leblanc, J.; de Marcillac, P.; Martínez, M.; Ortigoza, Y.; de Solórzano, A.O.; Pobes, C.; Puimedón, J.; et al. A BGO scintillating bolometer as dark matter detector prototype. *Opt. Mat.* **2009**, *31*, 1393–1397. [CrossRef]
545. Coron, N.; Gironnet, J.; Leblanc, J.; de Marcillac, P.; Redon, T.; García, E.; Martínez, M.; Ortigoza, Y.; de Solórzano, A.O.; Pobes, C.; et al. Sapphire, BGO and LiF scintillating bolometers developed for dark matter experiments. *PoS* **2009**, *idm2008*, 007.
546. Coron, N.; Cuesta, C.; García, E.; Gironnet, J.; Leblanc, J.; de Marcillac, P.; Martínez, M.; Ortigoza, Y.; de Solórzano, A.O.; Pobes, C.; et al. BGO scintillating bolometer: Its application in dark matter experiments. *J. Phys. Conf. Ser.* **2010**, *203*, 012038. [CrossRef]
547. Coron, N.; García, E.; Gironnet, J.; Leblanc, J.; de Marcillac, P.; Martínez, M.; Ortigoza, Y.; de Solórzano, A.O.; Pobes, C.; Puimedón, J.; et al. Our short experience at IAS and within ROSEBUD with radioactive contaminations in scintillating bolometers: Uses and needs. In Proceedings of the 1st International Workshop on Radiopure Scintillators for EURECA (RPSCINT-2008), Kyiv, Ukraine, 9–10 September 2008.
548. Cardani, L.; Di Domizio, S.; Gironi, L. A BGO scintillating bolometer for γ and α spectroscopy. *J. Instrum.* **2012**, *7*, P10022. [CrossRef]
549. Coron, N.; Cuesta, C.; García, E.; Ginestra, C.; Gironnet, J.; de Marcillac, P.; Martínez, M.; Ortigoza, Y.; Pobes, C.; Puimedón, J.; et al. Measurement of the L/K electron capture ratio of the ^{207}Bi decay to the 1633 keV level of ^{207}Pb with a BGO scintillating bolometer. *Eur. Phys. J. A* **2012**, *48*, 89. [CrossRef]
550. Derbin, A.V.; Gironi, L.; Nagorny, S.S.; Pattavina, L.; Beeman, J.W.; Bellini, F.; Biassoni, M.; Capelli, S.; Clemenza, M.; Drachnev, I.S.; et al. Search for axioelectric effect of solar axions using BGO scintillating bolometer. *Eur. Phys. J. C* **2014**, *74*, 3035. [CrossRef]
551. Borovlev, Y.A.; Ivannikova, N.V.; Shlegel, V.N.; Vasiliev, Y.V.; Gusev, V.A. Progress in growth of large sized BGO crystals by the low-thermal-gradient Czochralski technique. *J. Cryst. Growth* **2001**, *229*, 305. [CrossRef]
552. Abdelhameed, A.H.; Angloher, G.; Bauer, P.; Bento, A.; Bertoldo, E.; Breier, R.; Bucci, C.; Canonica, L.; D'Addabbo, A.; Di Lorenzo, S.; et al. Cryogenic characterization of a $LiAlO_2$ crystal and new results on spin-dependent dark matter interactions with ordinary matter. *Eur. Phys. J. C* **2020**, *80*, 834. [CrossRef]
553. Dafinei, I.; Diemoz, M.; Longo, E.; Peter, A.; Földvári, I. Growth of pure and doped TeO_2 crystals for scintillating bolometers. *Nucl. Instrum. Methods Phys. Res. A* **2005**, *554*, 195–200. [CrossRef]
554. Coron, N.; Dambier, G.; Leblanc, J.; de Marcillac, P.; Moalic, J.P.; Leblanc, E. Study of the low temperature properties of some scintillating crystals with high performance optical bolometers. In Proceedings of the 10th International Workshop on Low Temperature Detectors (LTD-10), Genoa, Italy, 7–11 July 2003.
555. Casali, N.; Vignati, M.; Beeman, J.W.; Bellini, F.; Cardani, L.; Dafinei, I.; Di Domizio, S.; Ferroni, F.; Gironi, L.; Nagorny, S.; et al. TeO_2 bolometers with Cherenkov signal tagging: Towards next-generation neutrinoless double-beta decay experiments. *Eur. Phys. J. C* **2015**, *75*, 12. [CrossRef] [PubMed]
556. Pattavina, L.; Casali, N.; Dumoulin, L.; Giuliani, A.; Mancuso, M.; de Marcillac, P.; Marnieros, S.; Nagorny, S.S.; Nones, C.; Olivieri, E.; et al. Background Suppression in Massive TeO_2 Bolometers with Neganov-Luke Amplified Light Detectors. *J. Low Temp. Phys.* **2016**, *184*, 286–291. [CrossRef]
557. Pattavina, L.; Laubenstein, M.; Nagorny, S.S.; Nisi, S.; Pagnanini, L.; Pirro, S.; Rusconi, C.; Schäffner, K. An innovative technique for the investigation of the 4-fold forbidden beta-decay of ^{50}V. *Eur. Phys. J. A* **2018**, *54*, 79. [CrossRef]
558. Fujimoto, Y.; Yanagida, T.; Yokota, Y.; Chani, V.; Kochurikhin, V.V.; Yoshikawa, A. Comparative study of optical and scintillation properties of YVO_4, $(Lu_{0.5}Y_{0.5})VO_4$, and $LuVO_4$ single crystals. *Nucl. Instrum. Methods Phys. Res. A* **2011**, *635*, 53–56. [CrossRef]
559. Voloshina, O.V.; Baumer, V.N.; Bondar, V.G.; Kurtsev, D.A.; Gorbacheva, T.E.; Zenya, I.M.; Zhukov, A.V.; Sidletskiy, O.T. Growth and scintillation properties of gadolinium and yttrium orthovanadate crystals. *Nucl. Instrum. Methods Phys. Res. A* **2012**, *664*, 299–303. [CrossRef]
560. Danevich, F.A.; Hult, M.; Kasperovych, D.V.; Klavdiienko, V.R.; Lutter, G.; Marissens, G.; Polischuk, O.G.; Tretyak, V.I. Decay scheme of ^{50}V. *Phys. Rev. C* **2020**, *102*, 024319. [CrossRef]
561. Arnold, R.; Augier, C.; Baker, J.; Barabash, A.; Blum, D.; Brudanin, V.; Caffrey, A.J.; Campagne, J.E.; Caurier, E.; Dassie, D.; et al. Double beta decay of ^{96}Zr. *Nucl. Phys. A* **1999**, *658*, 299–312. [CrossRef]

562. Argyriades, J.; Arnold, R.; Augier, C.; Baker, J.; Barabash, A.S.; Basharina-Freshville, A.; Bongrand, M.; Broudin-Bay, G.; Brudanin, V.; Caffrey, A.J.; et al. Measurement of the two neutrino double beta decay half-life of Zr-96 with the NEMO-3 detector. *Nucl. Phys. A.* **2010**, *847*, 168–179. [CrossRef]
563. Tretyak, V.I. Beta decays in investigations and searches for rare effects. In Proceedings of the International Workshop MEDEX 2017, Prague, Czech Republic, 29 May–2 July 2017.
564. Leder, A.; Danevich, F.; Tretyak, V.I.; Giuliani, A.; de Marcillac, P.; Novati, V.; Olivieri, E.; Poda, D.; Nones, C.; Zolotarova, A.; et al. Measurement of Quenched Axial Vector Coupling Constant in In-115 Beta Decay and its Impact on Future $0\nu\beta\beta$ Searches. In Proceedings of the XXVIII International Conference on Neutrino Physics and Astrophysics (Neutrino 2018), Heidelberg, Germany, 4–9 June 2018.
565. Beeman, J.W.; Bellini, F.; Cardani, L.; Casali, N.; Dafinei, I.; Di Domizio, S.; Ferroni, F.; Gironi, L.; Giuliani, A.; Nagorny, S.; et al. Performances of a large mass ZnSe bolometer to search for rare events. *J. Instrum.* **2013**, *8*, P05021. [CrossRef]
566. Dafinei, I. The LUCIFER project and production issues for crystals needed in rare events physics experiments. *J. Cryst. Growth* **2014**, *393*, 13–17. [CrossRef]
567. Cardani, L. ZnSe and $ZnMoO_4$ Scintillating Bolometers to Search for 0νDBD. Ph.D. Thesis, University of Rome, Rome, Italy, 2014.
568. Azzolini, O.; Barrera, M.T.; Beeman, J.W.; Bellini, F.; Beretta, M.; Biassoni, M.; Brofferio, C.; Bucci, C.; Canonica, L.; Capelli, S.; et al. First result on the neutrinoless double-β decay of ^{82}Se with CUPID-0. *Phys. Rev. Lett.* **2018**, *120*, 232502. [CrossRef]
569. Azzolini, O.; Barrera, M.T.; Beeman, J.W.; Bellini, F.; Beretta, M.; Biassoni, M.; Bossio, E.; Brofferio, C.; Bucci, C.; Canonica, L.; et al. Analysis of cryogenic calorimeters with light and heat read-out for double beta decay searches. *Eur. Phys. J. C* **2018**, *78*, 734. [CrossRef]
570. Beretta, M.; Cardani, L.; Casali, N.; Gironi, L.; Pagnanini, L.; Bellini, F.; Brofferio, C.; Chiesa, D.; Capelli, S.; Di Domizio, S.; et al. Resolution enhancement with light/heat decorrelation in CUPID-0 bolometric detector. *J. Instrum.* **2019**, *14*, P08017. [CrossRef]
571. Azzolini, O.; Beeman, J.W.; Bellini, F.; Beretta, M.; Biassoni, M.; Brofferio, C.; Bucci, C.; Capelli, S.; Cardani, L.; Carniti, P.; et al. Background model of the CUPID-0 experiment. *Eur. Phys. J. C* **2019**, *79*, 583. [CrossRef]
572. Azzolini, O.; Beeman, J.W.; Bellini, F.; Beretta, M.; Biassoni, M.; Brofferio, C.; Bucci, C.; Capelli, S.; Cardani, L.; Celi, E.; et al. Search for Neutrino-less Double Beta Decay of ^{64}Zn and ^{70}Zn with CUPID-0. *Eur. Phys. J. C* **2020**, *80*, 702. [CrossRef]
573. Beeman, J.W.; Bellini, F.; Benetti, P.; Cardani, L.; Casali, N.; Chiesa, D.; Clemenza, M.; Dafinei, I.; Di Domizio, S.; Ferroni, F.; et al. Current Status and Future Perspectives of the LUCIFER Experiment. *Adv. High Energy Phys.* **2013**, *2013*, 237973. [CrossRef]
574. Azzolini, O.; Barrera, M.T.; Beeman, J.W.; Bellini, F.; Beretta, M.; Biassoni, M.; Bossio, E.; Brofferio, C.; Bucci, C.; Canonica, L.; et al. Search of the neutrino-less double beta decay of ^{82}Se into the excited states of ^{82}Kr with CUPID-0. *Eur. Phys. J. C* **2018**, *78*, 888. [CrossRef]
575. Nagorny, S.; Cardani, L.; Casali, N.; Dafinei, I.; Pagnanini, L.; Pattavina, L.; Pirro, S.; Schäffner, K. Quenching factor for alpha particles in ZnSe scintillating bolometers. *IOP Conf. Ser. Mat. Sci. Eng.* **2017**, *169*, 012011. [CrossRef]
576. Silva, B.C.; de Oliveira, R.; Ribeiro, G.M.; Cury, L.A.; Leal, A.S.; Nagorny, S.; Krambrock, K. Characterization of high-purity ^{82}Se-enriched ZnSe for double-beta decay bolometer/scintillation detectors. *J. Appl. Phys.* **2018**, *123*, 085704. [CrossRef]
577. der Mateosian, E.; Goldhaber, M. Limits for lepton-conserving and lepton-nonconserving double beta decay in Ca^{48}. *Phys. Rev.* **1966**, *146*, 810–815. [CrossRef]
578. You, K.; Zhu, Y.; Lu, J.; Sun, H.; Tian, W.; Zhao, W.; Zheng, Z.; Ye, M.; Ching, C.; Ho, T.; et al. A search for neutrinoless double β decay of ^{48}Ca. *Phys. Lett. B* **1991**, *265*, 53–56. [CrossRef]
579. Belli, P.; Bernabei, R.; Dai, C.J.; Grianti, F.; He, H.L.; Ignesti, G.; Incicchitti, A.; Kuang, H.H.; Ma, J.M.; Montecchia, F.; et al. New limits on spin-dependent coupled WIMP and on 2β processes in ^{40}Ca and ^{46}Ca by using low radioactive CaF_2(Eu) crystal scintillators. *Nucl. Phys. B* **1999**, *563*, 97–106. [CrossRef]
580. Ogawa, I.; Hazama, R.; Miyawaki, H.; Shiomi, S.; Suzuki, N.; Ishikawa, Y.; Kunitomi, G.; Tanaka, Y.; Itamura, M.; Matsuoka, K.; et al. Search for neutrino-less double beta decay of ^{48}Ca by CaF_2 scintillator. *Nucl. Phys. A* **2004**, *730*, 215–223. [CrossRef]
581. Umehara, S.; Kishimoto, T.; Ogawa, I.; Miyawaki, H.; Matsuoka, K.; Kishimoto, K.; Katsuki, A.; Sakai, H.; Yokoyama, D.; Mukaida, K.; et al. Neutrino-less double-β decay of ^{48}Ca studied by CaF_2(Eu) scintillators. *Phys. Rev. C* **2008**, *78*, 058501. [CrossRef]
582. Umehara, S.; Kishimoto, T.; Nomachi, M.; Ajimura, S.; Takemoto, Y.; Chan, W.M.; Takihira, K.; Matsuoka, K.; Nakatani, N.; Trang, V.T.T.; et al. Neutrino-less double beta decay of ^{48}Ca studied by CaF_2(pure) scintillators. *J. Phys. Conf. Ser.* **2020**, *1342*, 012049. [CrossRef]
583. Ajimura, S.; Chan, W.M.; Ichimura, K.; Ishikawa, T.; Kanagawa, K.; Khai, B.T.; Kishimoto, T.; Kino, H.; Maeda, T.; Matsuoka, K.; et al. Low background measurement in CANDLES-III for studying the neutrinoless double beta decay of ^{48}Ca. *Phys. Rev. D* **2021**, *103*, 092008. [CrossRef]
584. Bacci, C.; Belli, P.; Bernabei, R.; Dai, C.J.; Di Nicolantonio, W.; Ding, L.K.; Gaillard-Lecanu, E.; Gerbier, G.; Giraud-Heraud, Y.; Kuang, H.H.; et al. Dark matter search with calcium fluoride crystals. *Astropart. Phys.* **1994**, *2*, 117–125. [CrossRef]
585. Cerdeño, D.G.; Marcos, C.; Peiró, M.; Fornasa, M.; Cuesta, C.; García, E.; Ginestra, C.; Martínez, M.; Ortigoza, Y.; Puimedón, J.; et al. Scintillating bolometers: A key for determining WIMP parameters. *Int. J. Mod. Phys. A* **2014**, *29*, 1443009. [CrossRef]
586. Tetsuno, K.; Ajimura, S.; Akutagawa, K.; Batpurev, T.; Chan, W.M.; Fushimi, K.; Hazama, R.; Iida, T.; Ikeyama, Y.; Khai, B.T.; et al. Status of ^{48}Ca double beta decay search and its future prospect in CANDLES. *J. Phys. Conf. Ser.* **2020**, *1468*, 012132. [CrossRef]
587. Li, X.; Kwon, D.H.; Tetsuno, K.; Kim, I.; Kim, H.L.; Lee, H.J.; Yoshida, S.; Kim, Y.H.; Lee, M.K.; Umehara, S.; et al. Study of a large CaF_2(Eu) scintillating bolometer for neutrinoless double beta decay. *J. Phys. Conf. Ser.* **2020**, *1468*, 012116. [CrossRef]

588. Li, X.; Tetsuno, K.; Kim, H.L.; Kim, I.; Kim, Y.H.; Kishimoto, T.; Kwon, D.H.; Lee, H.J.; Lee, M.K.; Umehara, S.; et al. Development of scintillating bolometer with large undoped and Eu-doped CaF_2 crystals for neutrino less double beta decay of ^{48}Ca. In Proceedings of the XXIX International (Online) Conference on Neutrino Physics and Astrophysics (Neutrino 2020), Minneapolis, MI, USA, 22 June–2 July 2020.
589. Smith, P.F.; Homer, G.J.; Read, S.F.J.; White, D.J.; Lewin, J.D. Tests on low temperature calorimetric detectors for dark matter experiments. *Phys. Lett. B* **1990**, *245*, 265. [CrossRef]
590. Minowa, M.; Sakamoto, M.; Ito, Y.; Watanabe, T.; Ootani, W.; Ootuka, Y. Cryogenic thermal detector with LiF absorber for direct dark matter search experiment. *Nucl. Instrum. Methods Phys. Res. A* **1993**, *327*, 612–614. [CrossRef]
591. De Marcillac, P.; Coron, N.; Leblanc, J.; Bobin, C.; Berkes, I.; De Jesus, M.; Hadjout, J.P.; Gonzalez-Mestres, L.; Zhou, J.W. Characterization of a 2 g LiF bolometer. *Nucl. Instrum. Methods Phys. Res. A* **1993**, *337*, 95–100. [CrossRef]
592. Calleja, A.; Coron, N.; García, E.; Gironnet, J.; Leblanc, J.; de Marcillac, P.; Martínez, M.; Ortigoza, Y.; de Solórzano, A.O.; Pobes, C.; et al. Recent performance of scintillating bolometers developed for dark matter searches. *J. Low Temp. Phys.* **2008**, *151*, 848–853. [CrossRef]
593. Ginestra, C.; Coron, N.; García, E.; de Marcillac, P.; Martínez, M.; Ortigoza, Y.; Redon, T.; Torres, L. Characterization of a SrF_2 scintillating bolometer. *J. Low Temp. Phys.* **2012**, *167*, 973–978. [CrossRef]
594. Wang, M.Z.; Yue, Q.; Deng, J.R.; Lai, W.P.; Li, H.B.; Li, J.; Liu, Y.; Qi, B.J.; Ruan, X.C.; Tang, C.H.; et al. Nuclear recoil measurement in CsI(Tl) crystal for Cold Dark Matter detection. *Phys. Lett. B* **2002**, *536*, 203–208. [CrossRef]
595. Kim, T.Y.; Cho, I.S.; Choi, D.H.; Choi, J.M.; Hahn, I.S.; Hwang, M.J.; Jang, H.K.; Jain, R.K.; Kang, U.K.; Kim, H.J.; et al. Study of the internal background of CsI(Tl) crystal detectors for dark matter search. *Nucl. Instrum. Methods Phys. Res. A* **2003**, *500*, 337–344. [CrossRef]
596. Lee, H.S.; Bhang, H.; Choi, J.H.; Hahn, I.S.; He, D.; Hwang, M.J.; Kim, H.J.; Kim, S.C.; Kim, S.K.; Kim, S.Y.; et al. First limit on WIMP cross section with low background CsI(Tl) crystal detector. *Phys. Lett. B* **2006**, *633*, 201–208. [CrossRef]
597. Lee, H.S.; Bhang, H.C.; Choi, J.H.; Dao, H.; Hahn, I.S.; Hwang, M.J.; Jung, S.W.; Kang, W.G.; Kim, D.W.; Kim, H.J.; et al. Limits on interactions between weakly interactingmMassive particles and nucleons obtained with CsI(Tl) crystal detectors. *Phys. Rev. Lett.* **2007**, *99*, 091301. [CrossRef] [PubMed]
598. Lee, H.S.; Bhang, H.; Hahn, I.S.; Hwang, M.J.; Kim, H.J.; Kim, S.C.; Kim, S.K.; Kim, S.Y.; Kim, T.Y.; Kim, Y.D.; et al. Development of low-background CsI(Tl) crystals for WIMP search. *Nucl. Instrum. Methods Phys. Res. A* **2007**, *571*, 644–650. [CrossRef]
599. Kim, H.J.; Lee, H.S.; Bhang, H.C.; Choi, J.H.; Dao, H.; Hahn, I.S.; Hwang, M.J.; Jung, S.W.; Kang, W.G.; Kim, D.W.; et al. Development of low background CsI(Tl) crystals and search for WIMP. *IEEE Trans. Nucl. Sci.* **2008**, *55*, 1420–1424. [CrossRef]
600. Kim, S.C.; Bhang, H.; Choi, J.H.; Kang, W.G.; Kim, B.H.; Kim, H.J.; Kim, K.W.; Kim, S.K.; Kim, Y.D.; Lee, J.; et al. New limits on interactions between weakly interacting massive particles and nucleons obtained with CsI(Tl) crystal detectors. *Phys. Rev. D* **2012**, *108*, 181301. [CrossRef]
601. Lee, H.S.; Bhang, H.; Choi, J.H.; Choi, S.; Hahn, I.S.; Jeon, E.J.; Joo, H.W.; Kang, W.G.; Kim, B.H.; Kim, G.B.; et al. Search for low-mass dark matter with CsI(Tl) crystal detectors. *Phys. Rev. D* **2014**, *90*, 052006. [CrossRef]
602. Lee, J.H.; Kim, G.B.; Seong, I.S.; Kim, B.H.; Kim, J.H.; Li, J.; Park, J.W.; Lee, J.K.; Kim, K.W.; Bhang, H.; et al. Measurement of the quenching and channeling effects in a CsI crystal used for a WIMP search. *Nucl. Instrum. Methods Phys. Res. A* **2015**, *782*, 133–142. [CrossRef]
603. Yoon, Y.S.; Park, H.K.; Bhang, H.; Choi, J.H.; Choi, S.; Hahn, I.S.; Jeon, E.J.; Joo, H.W.; Kang, W.G.; Kim, B.H.; et al. Search for solar axions with CsI(Tl) crystal detectors. *J. High Energy Phys.* **2016**, *2016*, 11. [CrossRef]
604. Angloher, G.; Dafinei, I.; Gektin, A.; Gironi, L.; Gotti, C.; Gütlein, A.; Hauff, D.; Maino, M.; Nagorny, S.S.; Nisi, S.; et al. A CsI low-temperature detector for dark matter search. *Astropart. Phys.* **2016**, *84*, 70–77. [CrossRef]
605. Derenzo, S.; Essig, R.; Massari, A.; Soto, A.; Yu, T.T. Direct detection of sub-GeV dark matter with scintillating targets. *Phys. Rev. D* **2017**, *96*, 016026. [CrossRef]
606. Nadeau, P.; Clark, M.; Di Stefano, P.C.F.; Lanfranchi, J.C.; Roth, S.; von Sivers, M.; Yavin, I. Sensitivity of alkali halide scintillating calorimeters with particle identification to investigate the DAMA dark matter detection claim. *Astropart. Phys.* **2015**, *67*, 62–69. [CrossRef]
607. Saint-Gobain Scintillation Crystal Materials. Available online: https://www.crystals.saint-gobain.com/products/crystal-scintillation-materials (accessed on 30 June 2021).
608. Clark, M.; Nadeau, P.; Hills, S.; Dujardin, C.; Di Stefano, P.C.F. Particle detection at cryogenic temperatures with undoped CsI. *Nucl. Instrum. Methods Phys. Res. A* **2018**, *901*, 6–13. [CrossRef]
609. Clark, M.; Nadeau, P.; Di Stefano, P.C.F.; Lanfranchi, J.C.; Roth, S.; Von Sivers, M.; Yavin, I. Sensitivity of sodium iodide cryogenic scintillation-phonon detectors to WIMP signals. *J. Phys. Conf. Ser.* **2016**, *718*, 042015. [CrossRef]
610. Coron, N.; Cuesta, C.; García, E.; Ginestra, C.; Girard, T.A.; de Marcillac, P.; Martínez, M.; Ortigoza, Y.; de Solórzano, A.O.; Pobes, C.; et al. Study of parylene-coated NaI(Tl) at low temperatures for bolometric applications. *Astropart. Phys.* **2013**, *47*, 31–37. [CrossRef]
611. Angloher, G.; Carniti, P.; Cassina, L.; Gironi, L.; Gotti, C.; Gütlein, A.; Hauff, D.; Maino, M.; Nagorny, S.S.; Pagnanini, L.; et al. The COSINUS project: Perspectives of a NaI scintillating calorimeter for dark matter search. *Eur. Phys. J. C* **2016**, *76*, 441. [CrossRef]
612. Angloher, G.; Carniti, P.; Cassina, L.; Gironi, L.; Gotti, C.; Gütlein, A.; Maino, M.; Mancuso, M.; Pagnanini, L.; Pessina, G.; et al. Results from the first cryogenic NaI detector for the COSINUS project. *J. Instrum.* **2017**, *12*, P11007. [CrossRef]